Fisheries and Environment Canada

Pêches et Environnement Canada

Service de la protection de l'environnement

Probable Behaviour and Fate of a Winter Oil Spill in the Beaufort Sea

Technology Development Report
Report EPS-4-EC-77-5

Environmental Impact Control Directorate
August, 1977

Behaviour and Fate of a Winter Oil Spill in the Beaufort Sea

ENVIRONMENTAL PROTECTION SERVICE REPORT SERIES

Technology Development Reports describe technical apparatus and procedures, and results of laboratory, pilot plant, demonstration or equipment evaluation studies. They provide a central source of information on the development and demonstration activities of the Environmental Protection Service.

Other categories in the EPS series include such groups as Regulations, Codes, and Protocols; Policy and Planning; Economic and Technical Review; Surveillance; Briefs and Submissions to Public Inquiries; and Environmental Impact and Assessment.

Inquiries pertaining to Environmental Protection Service Reports should be directed to the Environmental Protection Service, Department of Fisheries and the Environment, Ottawa, Ontario, K1A 1C8, Canada.

Cat. No.: En 46-4/77-5

ISBN 0-662-01029-9

PROBABLE BEHAVIOUR AND FATE OF A WINTER OIL SPILL IN THE BEAUFORT SEA

NORCOR Engineering and Research Limited
Yellowknife, Northwest Territories

A Report Submitted to:

Research and Development Division
Environmental Emergency Branch
Environmental Impact Control Directorate
Environmental Protection Service
Department of Fisheries and the Environment

EPS 4-EC-77-5

August, 1977

REVIEW NOTICE

This report has been reviewed by the Environmental Impact Control Directorate, Environmental Protection Service, and approved for publication. Approval does not necessarily signify that the contents reflect the views and policies of the Environmental Protection Service. Mention of trade names and commercial products does not constitute endorsement for use.

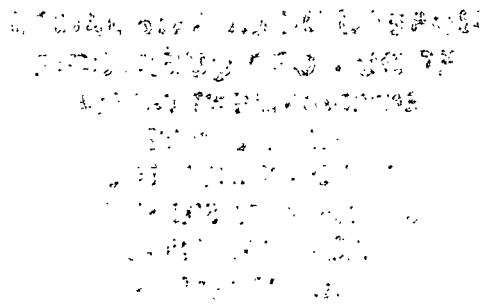

TYPOGRAPHICAL ERRATA

In most compound units (e.g. km day^{-1}) a slash (/) has been inserted in error between the two component units.

P.4, L.14 "over an area of up to 50 km" should read "up to 50 km away"

P.23, Eq.3 $L(V_1, V_2)$ should read $L_t(V_1, V_2)$

P.24, L.25-26 "The ratio, Total Distance travelled/Net Displacement, provides an indication of the type of buoys and the camp" should read "The ratio, Total Distance travelled/Net Displacement, provides an indication of the type of movement. This ratio has been tabulated for the AIDJEX buoys and the camp"

P.29, L.1 "soil" should read "oil"

P.29, Eq.6 &
P.33, Eq.13 Should read $D=1.7\, z \left(\frac{Q_t}{z + 10.36} \right)^{1/3}$

P.33, Eq.14 $W_s L_s)$ should read $W_s L_s$, and C_o should read $\bar{C}_o$

P.33, Eq.15 $(W_s L_s$ should read $W_s L_s$

P.35, L.19 "usually" should read "unusually"

P.43, L.25 "unpredicatble" should read "unpredictable"

P.47, L.3 "According to the model used here, by September 15 between 30..." should read "According to the model used here, between 30..."

P.47, L.5-6 "on the ice surface in a weathered state in the water..." should read "on the ice surface, in a weathered state in the water..."

FOREWORD

NORCOR Engineering and Research Limited carried out this study under contract to the Environmental Emergency Branch, Fisheries and Environment Canada. The scientific authority for this work was Dr. D.E. Thornton, Environmental Emergency Branch, Edmonton, Alberta.

Ocean and Aquatic Sciences (OAS) of Fisheries and Environment Canada contributed a large portion of the funds for this study. The support and advice of Mr. A. Milne of OAS in this work is gratefully acknowledged.

ABSTRACT

With increasing levels of offshore petroleum exploration in the Beaufort Sea, there is an urgent need to be able to define the behaviour and fate of a major winter oil spill. Much of the drilling activity centers on the area of dynamic ice called the transition zone, between the 20 and 100-m water contours. This report combines data from a 4-month winter field study of ice conditions, with other sources such as AIDJEX and satellite photography. The resulting statistical description of ice conditions in the Beaufort Sea is then used to generate a model of oil disposition under a moving ice sheet in the event of an oil blowout. Major areas for future study are identified as oil migration in multi-year ice, the effects of gas on oil behaviour and hourly ice drift rates.

Realistic spring oil migration rates through the ice sheet are applied to a typical set of ice conditions and a rough mass balance estimate is made of oil remaining at the end of the first summer. Oil films are generally thin (<0.5 cm). Based on available ice drift information, less than 15% of the contaminated area could be partially cleaned by burning. Evaporation would account for between 35 and 55% of the oil. By September it is estimated that about 30 to 50% of the original oil volume would remain on the water, ice or shore.

RÉSUMÉ

Le nombre accru de forages d'exploration dans la mer de Beaufort entraîne la nécessité de connaître rapidement le comportement et le devenir d'un important déversement d'hydrocarbures en hiver. La plupart de ces forages font dans la région des ''glaces dynamiques'', appelée zone de transition, entre les isobathes de 20 et de 100 m. Le présent rapport rassemble les données provenant d'une étude sur place des conditions de la glace pendant quatre mois d'hiver, avec celles d'autres sources telles que l'AIDJEX et la photographie par satellite. La description statistique ainsi obtenue des conditions des glaces sert alors à modéliser la répartition des hydrocarbures sous un inlandsis en mouvement lors d'une éruption d'hydrocarbures. Les principaux domaines d'études futures comme le déplacement des hydrocarbures dans la glace de plusieurs années, l'effet du gaz sur le comportement des hydrocarbures et la vitesse horaire de dérive de la glace, sont identifiés.

On applique des vitesses réalistes de déplacement des hydrocarbures au printemps à un ensemble type de conditions de la glace et on évalue approximativement ce qui resterait d'hydrocarbures à la fin du premier été. Les couches d'hydrocarbures sont généralement (<0,5 cm). D'après les renseignements disponibles sur la dérive des glaces, moins de 15% du volume total d'hydrocarbures pourrait être brûlé. L'évaporation en éliminerait entre 35 et 55%. On calcule qu'en septembre il resterait entre 30 et 50% du volume initial d'hydrocarbures dan l'eau et la glace ou sur la côte.

TABLE OF CONTENTS

LIST OF FIGURES

NOTE: In the Figure B series a typical reconnaissance flight would extend from 2100 hours one day to 0130 hours the next.

LIST OF TABLES

LIST OF PLATES

1 INTRODUCTION

A comprehensive understanding of ice conditions is essential for predicting the behaviour and fate of an oil spill in the Beaufort Sea. For 9 to 10 months of the year, Mackenzie Bay and the southern Beaufort Sea are ice covered or ice infested. Conditions vary greatly with the time and location. Since all the sites being proposed for offshore drilling lie in an area which in winter becomes a transition zone between the fast ice and the permanent polar pack, oil could be deposited in a wide variety of ice types and configurations in the event of a blowout.

Fig. 1 – LOCATION MAP

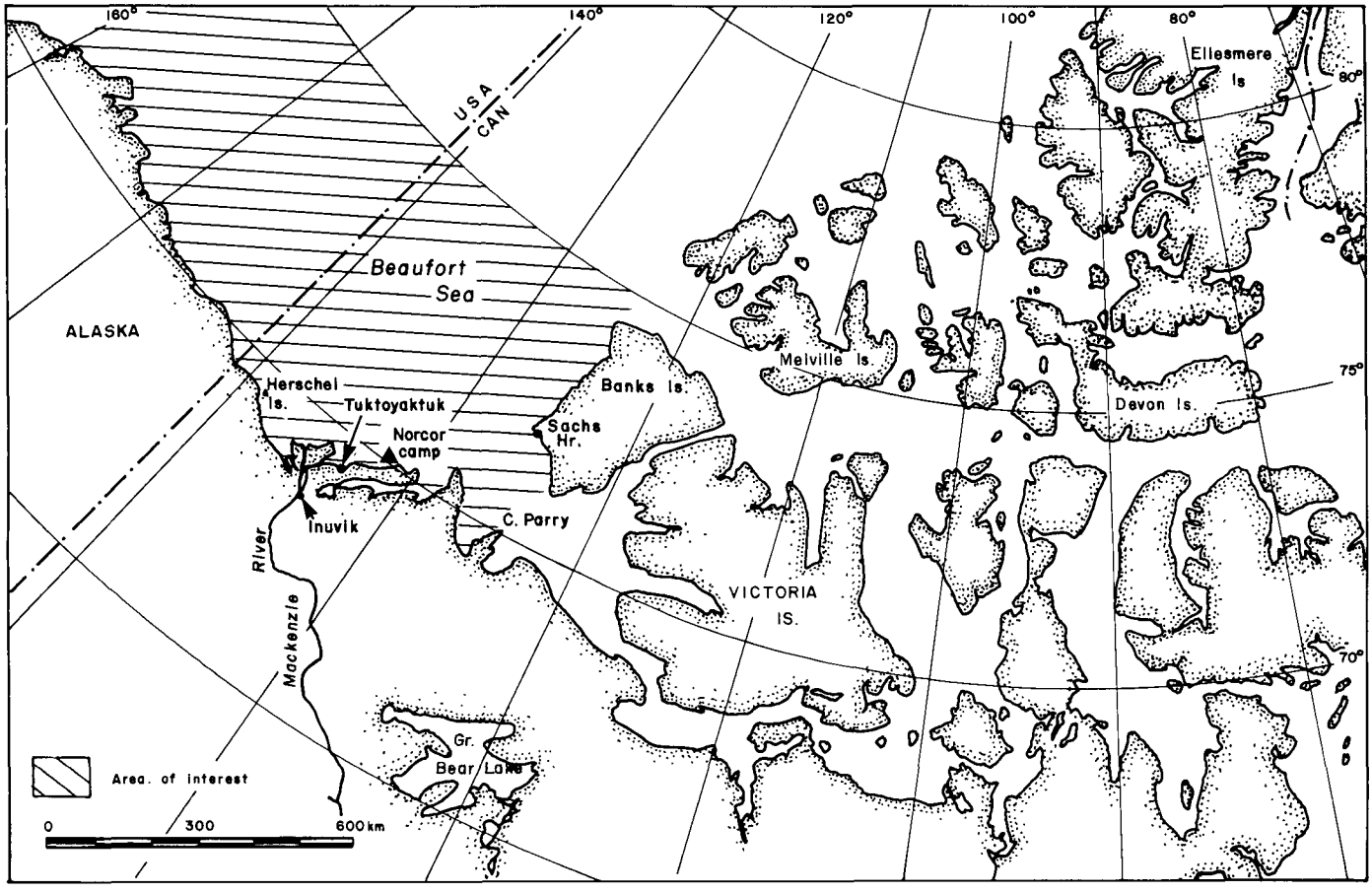

As initially conceived, one of the prime components of this program was a series of controlled discharges in selected ice conditions in the shear zone. All previous field work had been focused on the fast ice zone where conditions are relatively stable. The tests were designed to provide information on the rate of spreading, method of incorporation and nature of migration of oil in broken and multi-year ice.

Just prior to the scheduled starting date, the tests involving offshore oil discharges were postponed indefinitely in response to concerns expressed by local groups. Subsequently, the emphasis was placed on documenting ice conditions. To meet the new objectives a joint field program was developed by the Environmental Protection Service and Ocean and Aquatic Sciences of the Department of Fisheries and the Environment. This program was carried out from a manned camp in the transition zone, occupied for a total of 73 days between November 16, 1975 and March 30, 1976 (Appendix A).

In addition to surface weather and oceanographic investigations, detailed ice studies were conducted along a band approximately 20 km wide and extending from the edge of the fast ice zone to the permanent polar pack. Conditions were continuously monitored, and movements determined by means of high-frequency beacons placed on the ice. Six reconnaissance flights were undertaken along the length of the transition zone for the purpose of extending the detailed studies to July. AIDJEX buoy data was analyzed and used in conjunction with NORCOR drift values to provide a large-scale view of ice movement from January to August, 1976.

The interactions between oil and different potential ice conditions are discussed qualitatively to demonstrate the physical complexity involved. Actual ice conditions encountered in the Beaufort Sea are then detailed. Utilizing all available field data and satellite imagery, ice characteristics most relevant to oil behaviour are presented, with both spatial and time trends where possible. Ranges are placed on the significant mathematical variables and a model is constructed describing a standard blowout, with particular emphasis on oil film thicknesses under the ice and the implications for cleanup operations. Finally, observed crude oil spring migration and evaporation rates are applied to projected winter oil distributions. The probable summer fate of oil discharged during the winter is discussed and ranges are placed on oil volumes remaining by September.

2 OIL IN ICE

2.1 Oil Under a Solid Ice Cover

The behaviour of oil under solid ice covers has been the subject of a variety of field and laboratory studies, the largest of which took place at Balaena Bay, N.W.T. (NORCOR 1976).

From this and other investigations in the Beaufort Sea, a distinct variation in sea ice thickness has been observed on a horizontal scale of tens of meters or less. The irregularities tend to be sinusoidal and of a depth approximately equal to 20% of the mean ice thickness. Oil released into the water column under a solid ice cover will rise and gather in pools or lenses at the bottom of the ice sheet. The effect of gas can only be postulated because no experimentation to date has examined the behaviour of oil and gas under an ice sheet. It is expected that the gas would fill the cavities in the ice, allowing only a thin film of oil to build up before spreading would occur. If the gas is vented or not present, this saturation is very unlikely to occur in the transition zone due to the ice drift. At projected discharge rates for a blowout in the Beaufort Sea, first-year ice would have to remain almost stationary for over a week to completely fill the natural depressions with oil alone in an area 100 m square (based on typical ice thickness for December).

During the ice growth season a new layer of ice will form beneath the oil in a matter of days (NORCOR 1975). With the presence of gas, the final disposition of oil within the under-ice pools is difficult to predict. The gas might remain trapped under the ice while new ice grows beneath the oil, or it may dissipate slowly through natural cracks in the sheet. Some oil may surface through cracks almost immediately, but the accompanying oil volume would probably not be significant unless the gas pressure actually ruptured the sheet locally. Current knowledge of ice strength properties does not allow for a

reliable prediction of rupturing. However, at this stage it appears reasonable to expect significant gas venting through thin first-year ice and relatively little through multi-year ice. Once entrapped within the ice, the oil experiences practically zero weathering until the sheet begins to warm in the spring (Section 2.3).

The general behaviour of oil under a solid ice cover may be summarized as follows. In the absence of comprehensive observations, the roughness of the ice under-surface can be approximated for both first and multi-year ice by a simple sinusoidal model. Depending on the ice thickness and velocity, oil-gas volume flow rate, and the physical properties of the ice, the sheet may fracture due to the forces created by the gas pockets. If there is no significant gas venting, the thin oil films will be trapped by a new layer of ice within 48 hours. With violent gas venting, much thicker oil films are possible, and the area of contamination will be reduced to the minimum (equal to the plume diameter at the ice under-surface).

2.2 Oil in Broken Ice

In broken ice conditions, most of the oil and gas is likely to be contained by all but the smaller floes. Even if the floes should fracture after becoming contaminated, only the oil immediately adjacent to the crack would be released (NORCOR 1975). In the case of a first-year floe, the bulk of the oil will migrate to the surface of the ice during the first summer. With a multi-year floe, it could take a number of years for all the oil to be released. Each summer some oil is likely to escape around the edges of the floe and up melt-holes and cracks.

There has been considerable speculation as to the fate of oil released in leads and cracks. The principal factors which will influence the behaviour of the oil are the quantity and physical properties of the oil and gas, the size and condition of the lead or crack, and atmospheric conditions. Although there are numerous possible combinations, the dominant considerations are whether the oil is fresh or aged, the lead is clear or congested and the temperature is above or below freezing.

The spreading of oil is likely to be limited during the depth of winter, regardless of the size or condition of the lead. A new layer of ice begins to form on most leads in less than a day. The combined effect of the oil and gas will depress the freezing point and the surrounding uncontaminated ice will grow much faster, creating a natural barrier to spreading. The turbulent action of the gas will likely maintain a hole directly above the plume and cause some oil to overrun on the surface. Because the gas is vented, the area of contamination would be greatly reduced. The presence of small floes will tend to further restrict the movement of the oil.

With the temperature above freezing in the summer, the areal extent of contamination will depend on the condition of the lead or crack, and surface weather. If the lead is relatively free of ice, the oil will move in a similar manner to a slick on open water. The principal difference will occur at the edges. If the edge is well defined and relatively solid, the oil will tend to flow along the edge, gathering in sheltered depressions and eddies. The oil will remain herded against the edge until there is a change in wind direction. If the edge is badly broken or consists of a large number of loosely packed floes, the oil will be driven into the interstices between the floes. Once sheltered from the wind, it will tend to move

in response to the ice. As the floes compress, the oil will be progressively pumped along channels. If a channel is restricted and the film is sufficiently thick, the oil will be forced onto the surface of the ice. As the oil weathers and emulsifies, a substantial quantity will adhere to the sides of floes. This effect should be most pronounced late in the summer when the edges of floes are terraced and the ice is porous.

If the oil is driven by either wind or wave action into broken ice, the surface contamination of the ice is likely to be limited. However, if a broken ice field passes over a plume, some thin floes will likely be fractured and small ones even overturned by the violent action of the gas. The surface of some floes may be heavily oiled and any oil which pooled on the bottom of first-year ice will quickly migrate to the surface. Any quantitative treatment of the pack edge zone as it passed over a blowout site would be extremely complex. In this transient area between open water and the relatively solid polar pack, conditions vary from brash ice several meters across, to floes over 2 km in diameter (Plate 9).

On a small scale these floes are in a constant state of relative motion. A sudden wind shift could drive this ice south in a matter of hours and disperse the floes over an area of up to 50 km. If oil is injected into such a diverse set of conditions, the number of variables becomes unmanageable. Oil may be locked in by the floes in relatively heavy concentrations or swept over a large area by wind action either as a slick on open water (velocity - 1.5% to 3% of the windspeed) or in the form of contaminated floes moving at velocities averaging 10 km/day^{-1}. In either situation cleanup becomes extremely difficult from both technical and operational considerations.

2.3 Oil on the Ice Surface

As first-year sea ice warms in the spring, brine drainage occurs. The resulting clear channels provide a passage for any oil entrained in the ice to surface. This process of vertical oil movement in columnar first-year sea ice has been documented in detail at Balaena Bay (NORCOR 1975). Depending on sea state and freezing rate, the top 10 cm or more of a sea ice sheet may be composed of ice with a random crystal structure, as opposed to columnar ice which is made up of vertically oriented parallel platelets of ice. Consequently, to obtain estimates of oil pooling on the ice surface in the spring, it is necessary to confirm that oil migration can easily occur in ice with a random structure. Laboratory tests have provided a positive answer to this question (Martin 1976).

Initially, in early May the migration of oil is slow. However, once the surface of the snow becomes discoloured, the surface albedo is greatly reduced. The increased solar radiation absorbed then accelerates the process. The contaminated snow quickly melts, causing a depression in which the oil and melt-water pools. The oil film on the water causes a greenhouse effect and the temperature of the pool rises. At Balaena Bay water temperatures over $+8°C$ were recorded immediately below an oil film in a pool 10 cm deep. The ambient air temperature at the time was $+2.5°C$. The pool progressively deepens and increases in area as oil is splashed on the surrounding snow by wind and wave action, and the process continues until the melt-pool drains. Most oils, even badly weathered, are less dense than ice or seawater and will remain on the surface. The intense and continuous radiation causes the oil to weather rapidly. Evaporation rates of over 40% in 10 days have been measured (NORCOR 1975). However,

because all the oil is not released until the melt actually reaches the initial level of the lens, the pool is continuously replenished with new oil. Deep trenches and melt-holes form beneath the oil. The end result of the greatly reduced surface albedo is an accelerated ice deterioration. At Balaena Bay for instance, the contaminated areas were free of ice between two and three weeks before breakup of the surrounding sheet.

There have been no tests with crude oil in multi-year ice and consequently, it is only possible to hypothesize as to the impact of oil on the surface heat exchange. Brine channels do not exist in the upper layers of multi-year ice to the same extent as in first-year ice. Some oil might migrate to the surface through worm holes and thermal cracks. Although easily explained for first-year ice as an enlargement of the main brine channels, the concept of a worm or melt-hole in multi-year ice is not well understood.

The actual oil drainage capability of any one hole is quite limited in areal extent. This, combined with the fact that the oil will be present under the ice in discrete oil lenses, would make it unlikely for large quantities of oil to reach the surface of multi-year ice through worm holes or thermal cracks.

An oil film, even entrapped several meters below the surface of the ice, serves as an effective barrier to solar radiation, and once the snow melts, the oil should substantially increase the energy level of the multi-year sheet. The net effect of the oil will depend on the extent of surface contamination, and the location, thickness and size of entrapped lenses. It is difficult to predict when all the oil will surface. In multi-year ice it could range from the first-year ice migration rate to the natural ablation rate of multi-year ice, which is estimated to be between four and eleven years. Because of its low salinity, multi-year ice will take several weeks longer in the spring to reach the melting temperature at a particular depth. Once this temperature is reached, some oil will probably start to rise. However, predictions of rates and quantities are not possible without actual full-scale trials alongside first-year ice as a control.

Eventually much of the first-year ice in the transition zone will melt completely and break up into fine fragments, thus releasing any oil still entrapped or on the ice surface. With mixing by wind and wave action, some emulsification will occur, but it is not known whether an appreciable volume of oil would sink. Some oil will be splashed back onto other ice floes. By September much of the oil will have evaporated. Section 5.0 places possible limits on weathering and attempts to quantify oil migration and evaporation.

At freeze-up, a new layer of ice will form beneath any slicks that remain and snow will quickly cover the oil. By October most of the oil will be incorporated into a granular layer of snow-ice. During subsequent years the entire process is likely to be repeated on a progressively decreasing scale.

3 ICE CONDITIONS IN THE BEAUFORT SEA

3.1 Principal Ice Zones

During a typical summer, the permanent polar pack resides between 200 and 400 km offshore. In the fall, driven by onshore winds, the pack advances to about the 100-m seabed contour. Simultaneously, a band of new first-year ice begins to form along the shore. The width of this landfast ice zone is very much dependent on the sequence of events at freeze-up. For example, in the fall of 1970 the pack was driven onshore by a violent storm and many large multi-year floes were locked into the landfast ice. The width of the landfast ice zone was reduced in this storm by several kilometers on the west side of Mackenzie Bay. More typically, the landfast ice grows out to meet the permanent polar pack.

Because the landfast ice is stationary while the permanent polar pack is continuously in motion, a transition zone exists between the two ice zones. During the fall the pressure of the pack against the thin first-year ice causes considerable deformation and the limits of the transition zone are quite pronounced. The most active area is a band between 5 and 10 km wide, immediately adjacent to the landfast ice, known as the shear zone. In general, the floe sizes are smaller and the frequency of leads, cracks, and first-year ridges are much greater than in the surrounding ice. There is a progressive decrease in the concentration of first-year ice across the transition zone, reaching a low of about 30% in the permanent polar pack. As the pack consolidates and the first-year ice thickens, variations across the transition zone become more subtle, making it difficult to delineate the edge of the permanent polar pack.

During the depth of winter the permanent polar pack consists of between 60 and 70% multi-year ice and 1 to 5% open water, with the remainder being first-year ice. The landfast ice zone is predominantly first-year ice, with the exception of the occasional isolated floe that was locked in at freeze-up. The transition zone, or seasonal polar pack, varies from a high concentration of first-year ice in the shear zone to 50 to 60% per multi-year ice near the permanent polar pack. During breakup the major changes occur in the seasonal polar pack. The progression can best be demonstrated by examining the sequence of events for a typical year. Figures B2 through B11 in Appendix B show ice concentrations between March 10 and October 2, 1975.

In the spring the pack begins to recede, creating a lead between it and the fast ice. The loose and broken ice of the shear and transition zone tends to be driven against the pack. The width and ice concentrations in the lead vary considerably depending on surface weather. With strong offshore winds, the pack and broken ice are driven out causing the lead to open. Initially, the entire shoreline is protected by a band of fast ice. As breakup progresses, floes break free from the outer edge, while the outflow from the Mackenzie and other rivers along the coast erodes the inner side. The landfast ice is generally breached in late June or early July on the west side of the Mackenzie Delta and at the Horton River in Franklin Bay. The remaining fast ice breaks out shortly thereafter.

Detailed summer ice conditions for a typical year (1975) and an extreme year (1974) are presented in Appendix B.

3.2 Winter Ice Conditions - 1976

Although conditions are reasonably well documented in the landfast zone and permanent polar pack, there are no statistical data on ice parameters in the transition zone during the winter. The overflights undertaken on January 20, March 6 and April 29 provide some indication as to the nature and range of ice conditions during winter and immediately prior to breakup. Data from these flights are presented in graphical form in Figures B18 through B26 in Appendix B. By comparing mutual areas shared by these three flights, an attempt was made to gain some insight into the change of ice conditions with time. Mean summaries covering three major parameters, floe size, cracks and leads, and ridges, are presented for each flight in Table 1.

TABLE 1 SUMMARY OF DATA FROM COMPARATIVE AREAS ON FLIGHTLINES - MEAN ± STANDARD DEVIATION (see Figures B18 - B26)

Date	Floe Size (km)	Frequency/km
Jan. 20	1.4 ± 1.5	.17 ± 0.06
March 6	0.64 ± 0.42	.85 ± 0.57
April 29	0.65 ± 0.52	.25 ± 0.26
	# Cracks & Leads/km	Orientation
Jan. 20	0.32 ± 0.2	322° ± 35°
March 6	0.19 ± 0.23	288° ± 61°
April 29	0.27 ± 0.27	307° ± 50°
	# Ridges/km	Orientation
Jan. 20	0.13 ± 0.14	286° ± 51°
March 6	3.43 ± 1.15	315° ± 26°
April 29	6.94 ± 5	302° ± 47°

Mean values are a useful way of quantifying changes with time, but it should be emphasized that in the transition zone there can be a wide variety of ice conditions over a very short distance. In a matter of 5 km, multi-year floes may range in size from several hundred meters to several kilometers. These floes may be smooth or ridged. Between the multi-year ice, the first-year ice may be smooth or heavily ridged with ice pile-ups of 5 m or more. In flying north from the landfast ice to a point about 100 km offshore (80 m water) there is no distinct edge marking the polar pack, only a gradual change in the concentration of multi-year floes from 1/10 to 2/10 to 6/10. Plates 1 and 2 show some typical

ice features observed on reconnaissance flights near the camp in February and April. The difficulty involved in specifically quantifying any aspect of the surface relief and ice type is readily apparent in these views.

Several trends are evident from these mean values. From freeze-up until March, multi-year floes within the transition zone appear to become smaller and more frequent. At all times there is an increase in floe size progressing out from the coast (eg. March 6, 0.2 km at the landfast edge to 1 or 2 km at the 100-m water depth). During the winter of 1976, cracks and refrozen leads were oriented predominantly in a northwesterly direction (see also Marko, 1976). During the overflights a very limited amount of open water was visible in leads due to rapid refreezing. New ice cover formed on several leads adjacent to the camp within 12 hours. Rafting was very common. In some of the larger leads three or four terraces could be observed. In general, the paths of both leads and cracks tended to be more erratic in the late fall and early winter, while the first-year ice was thin. The features would zigzag to skirt multi-year floes. As the sheet consolidated, the orientation of features became more pronounced and an increasing number of multi-year floes were fractured. In some cases a single lead could be followed for over 30 km. Shear movements of several hundred meters could be observed across cracks. Due to snow cover, the frequency of leads and cracks is not an additive function. In many cases a feature could not be detected for longer than one week.

A series of four photographs taken of different crack conditions at different times will serve to show the progression in the appearance of open water and subsequent refreezing. Plate 3 shows a typical severe crack pattern just prior to breakup. Plate 4 shows what such a fractured area could look like a few days later. If the time is April,as in the photograph, the ice may continue to open up. However, in the winter period the crack will refreeze almost immediately. Plate 5 shows new ice less than 10 cm thick (24 hrs. old), rafting in multiple layers as the ice moves. Finally, after a week or more, the crack may look like Plate 6. Note that a first-year ridge has been divided and displaced slightly by the lead.

The ridge orientation between January and May was also NW i.e. roughly perpendicular to the direction of gross ice movements. Since the refrozen cracks and leads are the weakest points in the ice sheet, it is reasonable for the ridges to assume a similar mean orientation. Later in the fall more ridges tended to parallel the shore lead, with the end result being a distinct rectilinear ridge pattern (also observed by Marko in NOAA imagery). Ridge frequency increased by a factor of 60 between January 20 and April 29, while the multi-year floe size was cut in half during the same period.

3.3 Spring Ice Conditions - 1976

The first evidence of a major ice movement in 1976 was the March 8 appearance of a distinct NS lead several kilometers wide between Cape Kellet on Banks Island and the Bathurst Peninsula (NOAA satellite photograph). No other useful imagery is available until April 14, when NOAA imagery shows a similar lead continuing up the west coast of Banks Island.

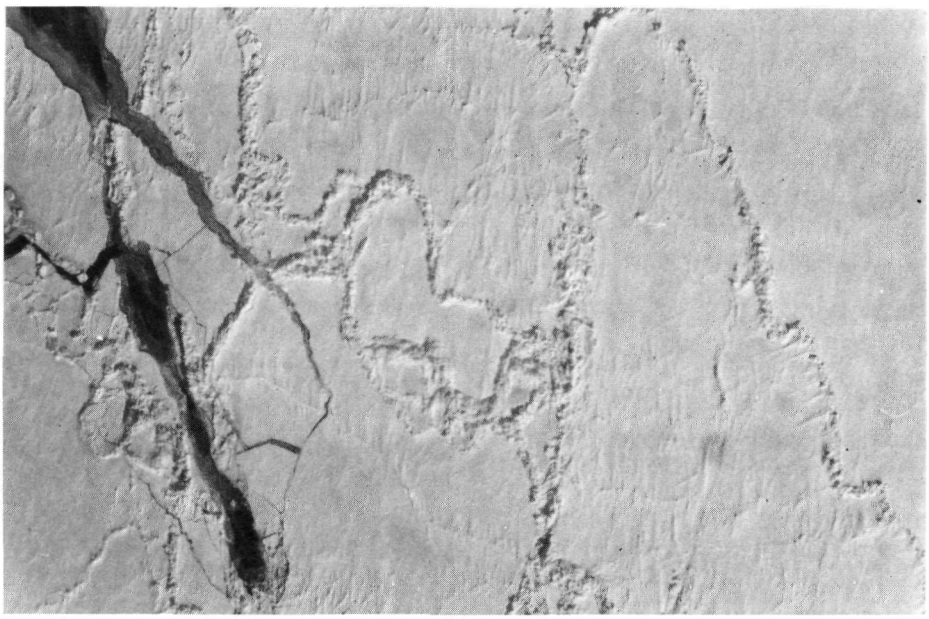

Plate 1 Typical Winter Ice Conditions
Transition Zone April, 1976
Scale 1 cm = 120 m

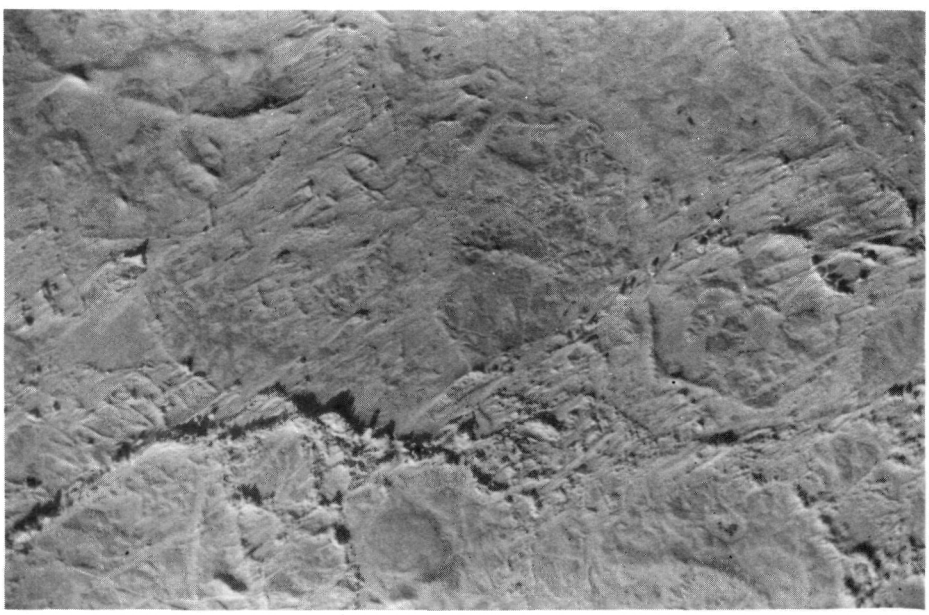

Plate 2 Typical Winter Ice Conditions
Transition Zone February, 1976
Scale 1 cm = 120 m

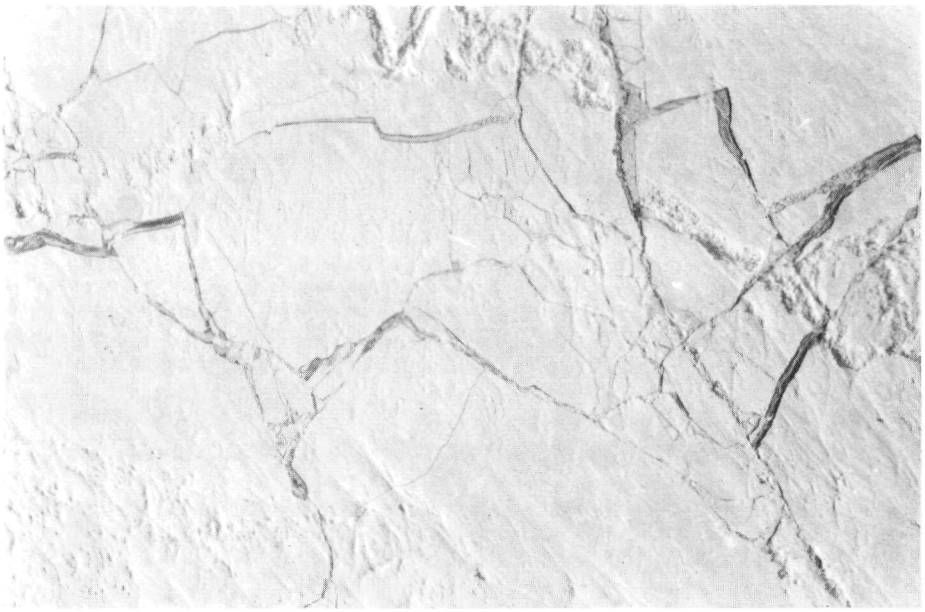

Plate 3 Severe Crack Pattern Typical of Ice Sheet Just Prior to Breakup April 29, 1976 Scale 1 cm = 120 m

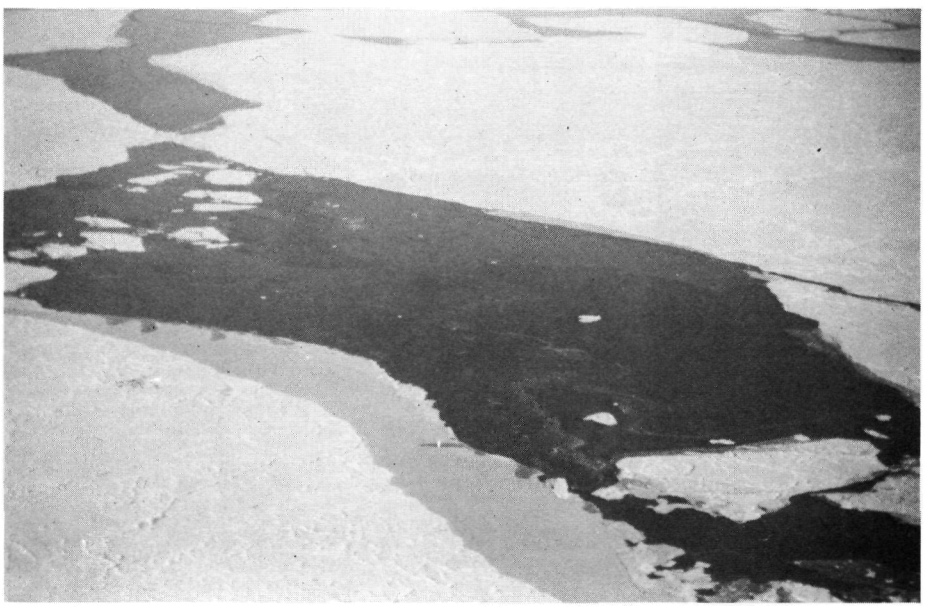

Plate 4 Open Crack Representing Next Stage in Deterioration From Conditions Above (Plate 3) Scale (picture centre) Approx. 1 cm = 80 m

Plate 5 Fresh Crack Near Camp March, 1976
Showing Rafted Ice < 10 cm Thick
Scale Approx. 1 cm = 25 m

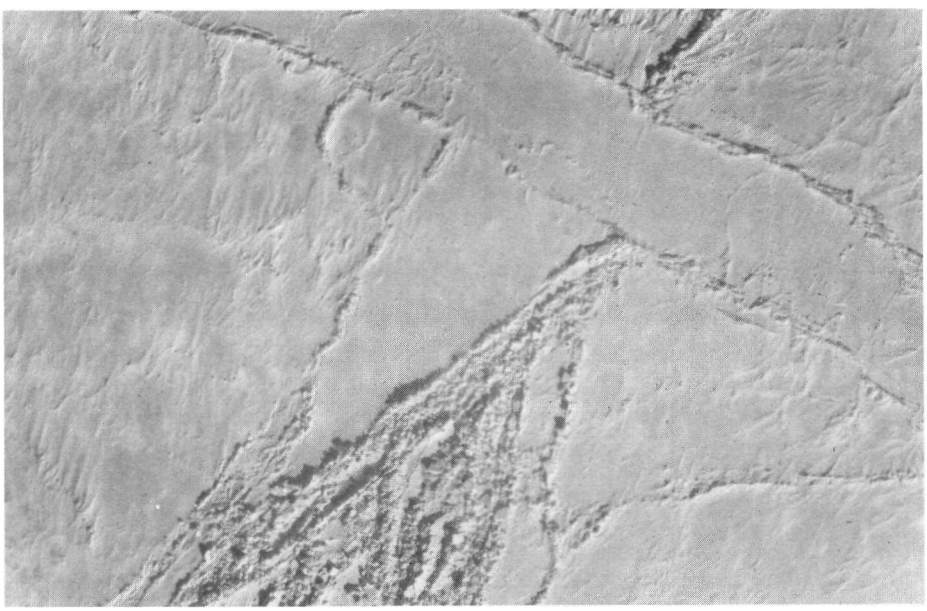

Plate 6 Refrozen Crack February, 1976
Scale 1 cm = 120 m

An overflight on April 29 observed conditions just prior to breakup. The sheet was generally fractured all along the flight line. In many areas large floes were floating free with patches of open water up to a kilometer in width.

There was some evidence of new ice forming at the floe edges. The ice surface itself was still completely snow covered with only hummocked multi-year floes beginning to show bare patches.

Five days later on May 4, the NOAA image shows breakup well advanced with 30 to 50 km of open water stretching from Cape Kellet to Herschel Island. Off Cape Bathurst major NS lead patterns stretched for over 600 km, and the pack was considerably broken up off the west coast of Banks Island to a distance of 150 km.

Unfortunately, no useful 1976 imagery is available for the rest of May. By June 8 the pack had moved west to leave an open-water area 10 to 30 km wide, stretching east from Herschel Island to Cape Bathurst and then north off Banks Island to 75°N. In the area of Storkerson Bay, open water stretched west from the coast of Banks Island for a distance of 100 km. To have accomplished this the pack would have had to have averaged about 1 to 2 km/day westerly movement for the previous 35 days. The NORCOR overflight on June 2-3 flew along the northern boundary of the EW lead, which had much the same extent as the NOAA satellite photograph of June 9.

Before presenting a summary of the spring overflight data, some discussion of the term lead edge will be very relevant in terms of oil behaviour and cleanup techniques. The northern boundary of the EW lead is not a well-defined edge, such as the south side which borders on the landfast ice. Instead, there is no real edge, just a transition over a distance of 5 to 10 km between primarily open water and the predominantly solid 9/10 + polar pack. It is the southern part of this broken "edge" that was flown in an attempt to define the conditions most difficult from a summer oil cleanup point of view.

The true nature of this northern lead boundary is best demonstrated by comparing photography of the same area from three different sources: overflights (1 mm = 15 m), LANDSAT (1mm = 1km) and NOAA (1mm = 12km). The only time during 1976 in which such a comparison proved possible was June 12-13. Plate 7 shows a NOAA image of June 12, 1976 with the corresponding LANDSAT image area superimposed. A shore lead 5 to 20 km wide stretched from Herschel Island to Point Barrow. In the Beaufort Sea the landfast ice was still intact and the polar pack badly fractured.

Plate 8 shows two LANDSAT images of the transition zone north of Tuktoyaktuk 23 hours later. On this scale the pack edge is seen to contain loose floes of 6/10 concentration extending for over 100 km. NORCOR flight tracks covered 14 hours earlier are shown with two selected blocks of aerial coverage superimposed over the actual ice photographed. The ice movement between 0100 hours and 1400 hours on June 13 is shown by the displacement of the photo block relative to the aircraft track. The pack edge has moved north 10 km in this period. It is interesting to see how closely the landfast ice edge follows the 20-m water depth contour. Plates 9 and 10 show the two aerial photo blocks referred to on the LANDSAT image. Immediately striking is the tremendous diversity of conditions visible only at this large scale. Floes range in size from 10 m to 5 km. The significant area of open water actually present is not evident from either satellite photograph. On LANDSAT, and especially NOAA, the ice in the edge

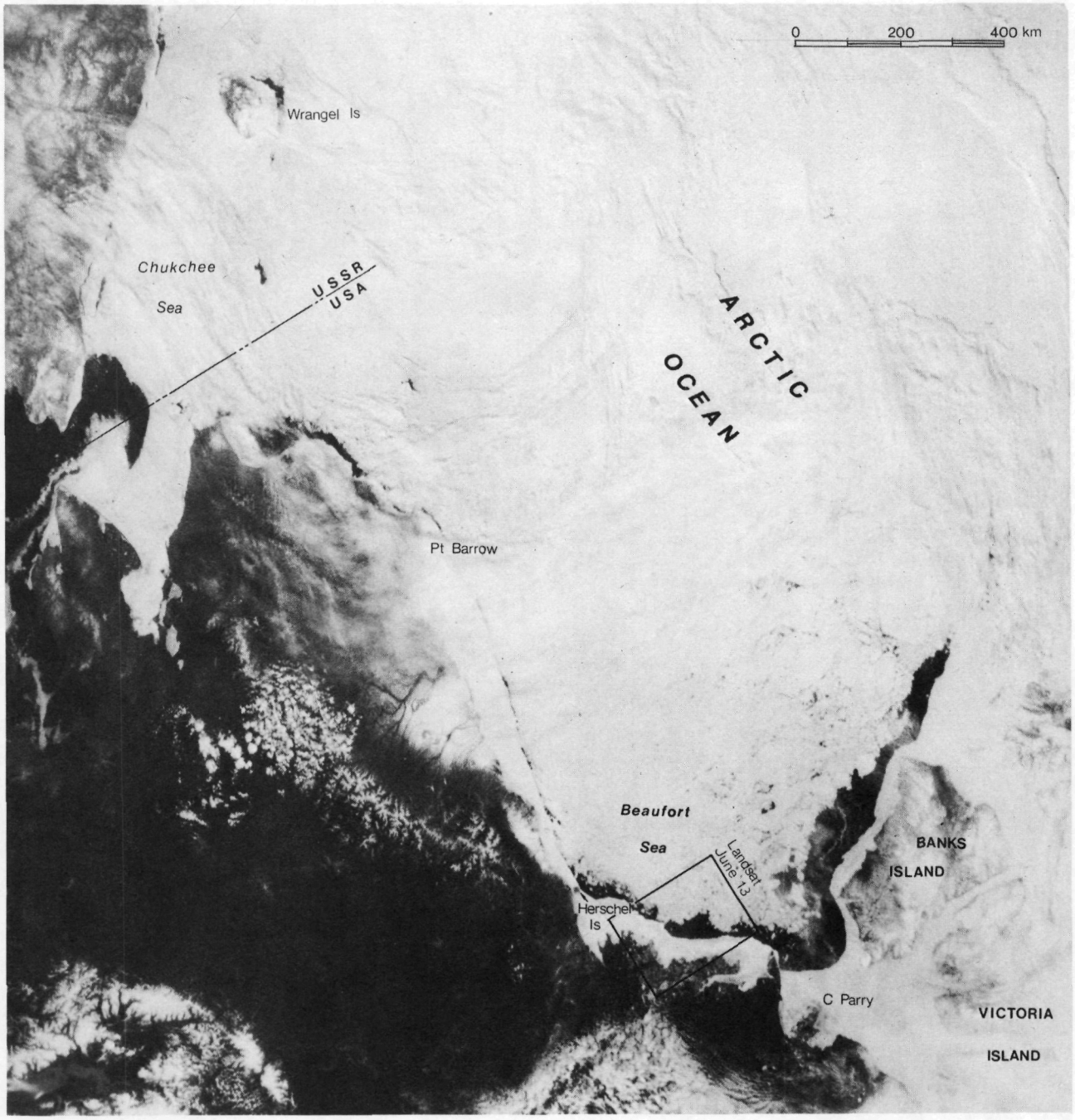

Plate 7 NOAA Image 12/06/76 5:17
For Corresponding Landsat Frame
See Plate 8

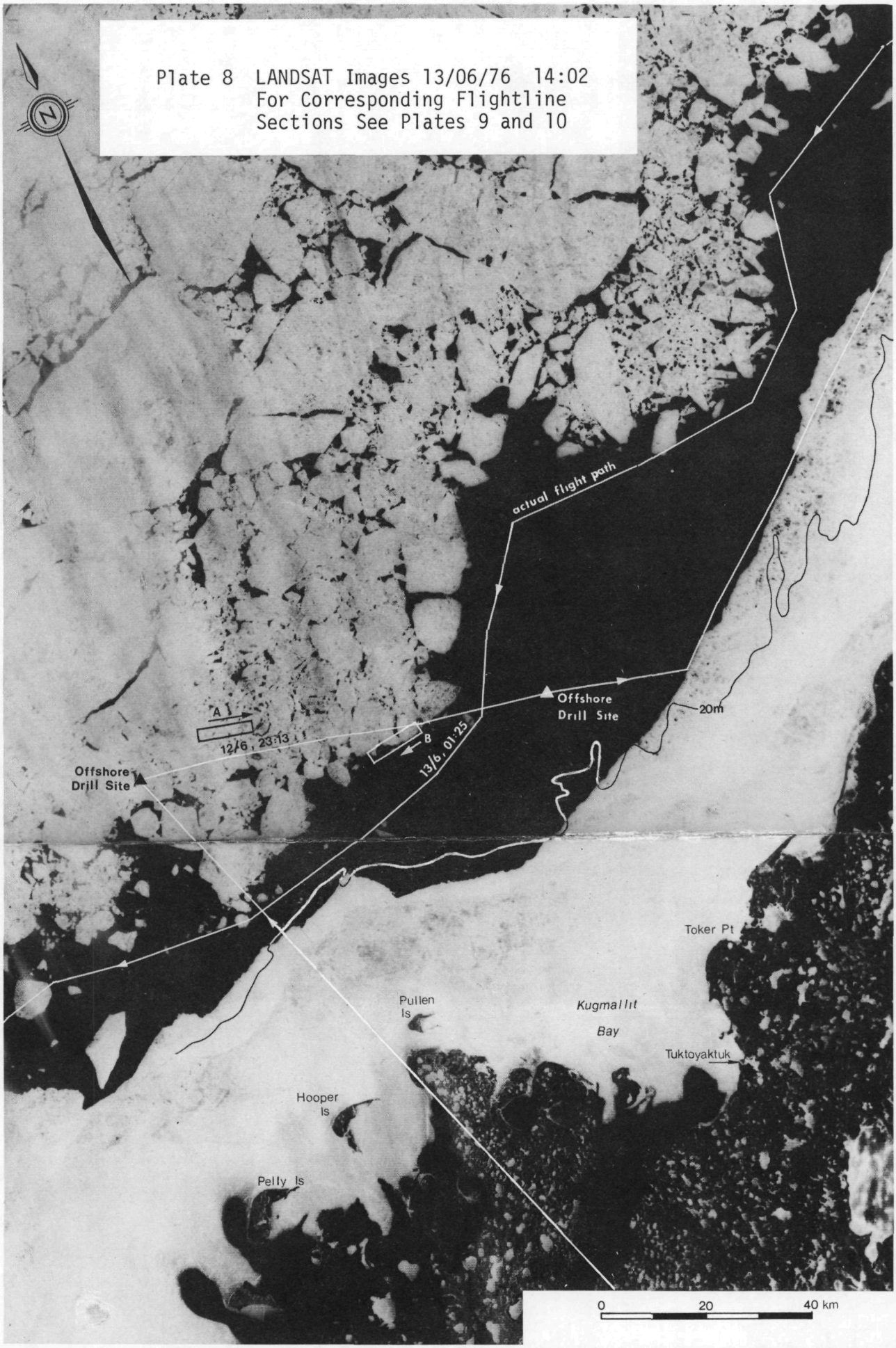
Plate 8 LANDSAT Images 13/06/76 14:02
For Corresponding Flightline
Sections See Plates 9 and 10
N
actual flight path
Offshore
Drill Site
20m
A
12/6, 23:13
B
13/6, 01:25
Offshore
Drill Site
Toker Pt
Pullen
Is
Kugmallit
Bay
Tuktoyaktuk
Hooper
Is
Pelly Is
0
20
40 km

zone appears relatively intact, although ragged in appearance. Only an overflight picks up the details necessary to estimate the nature of oil contamination in this area. The behaviour of oil in floating ice conditions similar to those in Plates 9 and 10 was discussed in Section 2.2.

Table 2 summarizes conditions within the lead edge zone observed on overflights in June and July (see Figures B27 to B35). It can be seen that although this time period covers substantial changes in the amount of open water between the landfast ice on shore and the polar pack, the per cent area of open water along the edge itself remained substantially constant (43% to 56%). Per cent area of small floes (<1 km) varied between 8% and 13%, while the area attributed to larger floes varied from 31% to 46%. The mean size of these large floes varied from 3 to 5 km.

Conditions at the most northerly drill site (Kopanoar D-14) never exceeded 10% of open water between June 2 and July 15.

On June 2 there appeared to be one massive floe some 34 km across covering the drilling location. At the more southerly location (Tingmiark K-91) ice concentrations went from 9/10 to completely open water in the 10-day period June 2 to June 12, and were 2/10 on July 15.

LANDSAT photography from the period June 21 to July 2 shows the landfast ice still intact and slightly closer inshore than on June 12. Between July 9 and July 16 most of the landfast ice broke away, leaving the shoreline ice free. Figure B35 shows the large expanse of open water on July 15, with the pack now over 70 km offshore. Between shore and the pack edge there were frequent areas of loose floes to a concentration of 1/10 to 2/10. The pack edge had a similar broken nature as in Plate 9, with about 56% of open water along the edge (up to 10% from June 12). Mean large floe size was 2.9 km down from a mean of 5.3 km observed a month earlier. From this date on the pack continued to retreat until it reached a position 270 km north of Tuktoyaktuk on September 24.

3.4 Ice Movement - Transition Zone and Polar Pack

Summer Beaufort Sea ice movements related to the overall dynamics of the polar pack are thoroughly covered within the limitations of available data by J. Marko (Beaufort Sea Technical Report 34). However, the lack of LANDSAT imagery during winter months means that present treatments of ice movement are limited to the March through October period. To date, no large-scale winter ice movement studies have utilized the infrared coverage provided year round by NOAA.

Until more advanced low light-level coverage becomes available, the only methods suitable for measuring winter ice movement from October to March involve remote data buoys, manned camps and low-altitude overflights.

By examining available imagery for the three winters 1973 - 1975, Marko was able to describe a recurring pattern in lead development whereby a systematic eastward progression of north-south leads was seen to be an early step in the spring breakup process. Changes in wind fields can inhibit coast-paralleling lead development, as occurred in 1974.

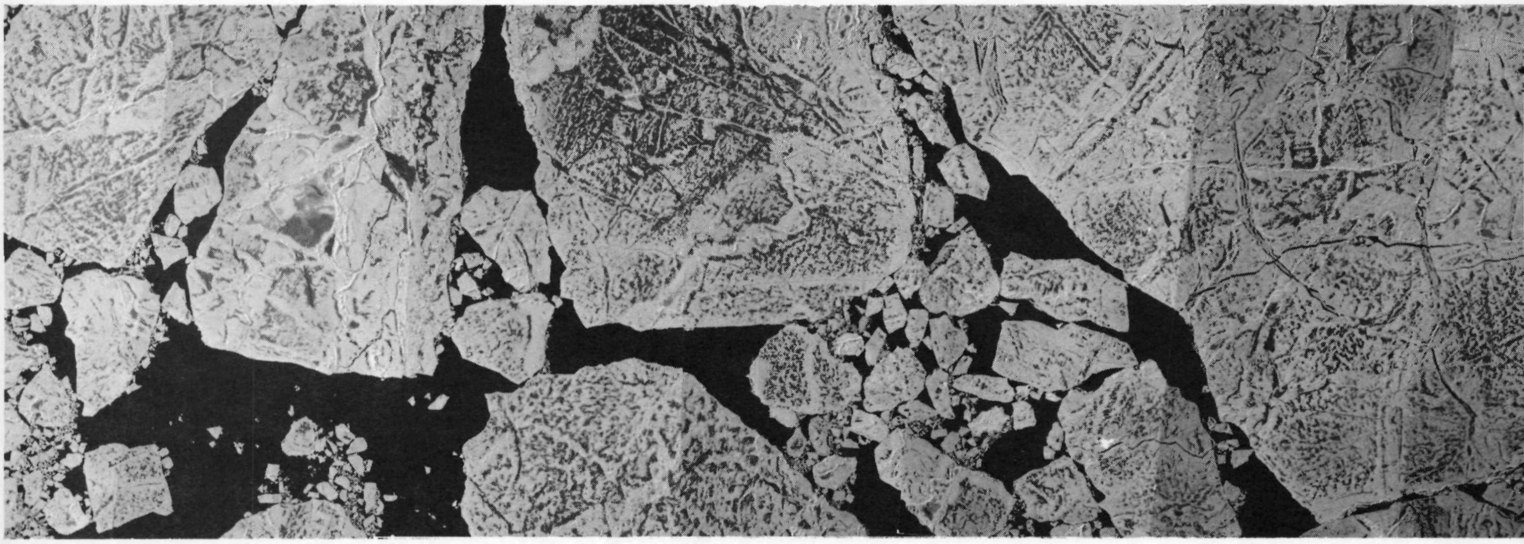

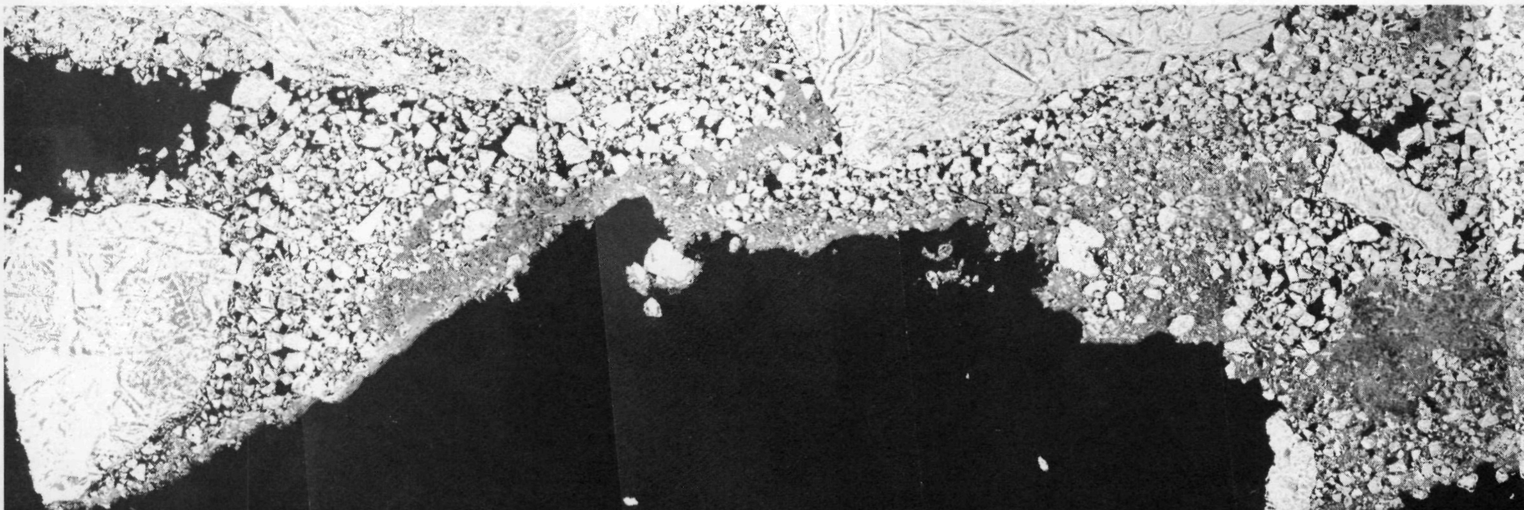

Plate 9 FLIGHTLINE SECTION A
12/06/76, 23:11·5 – 23:14·5

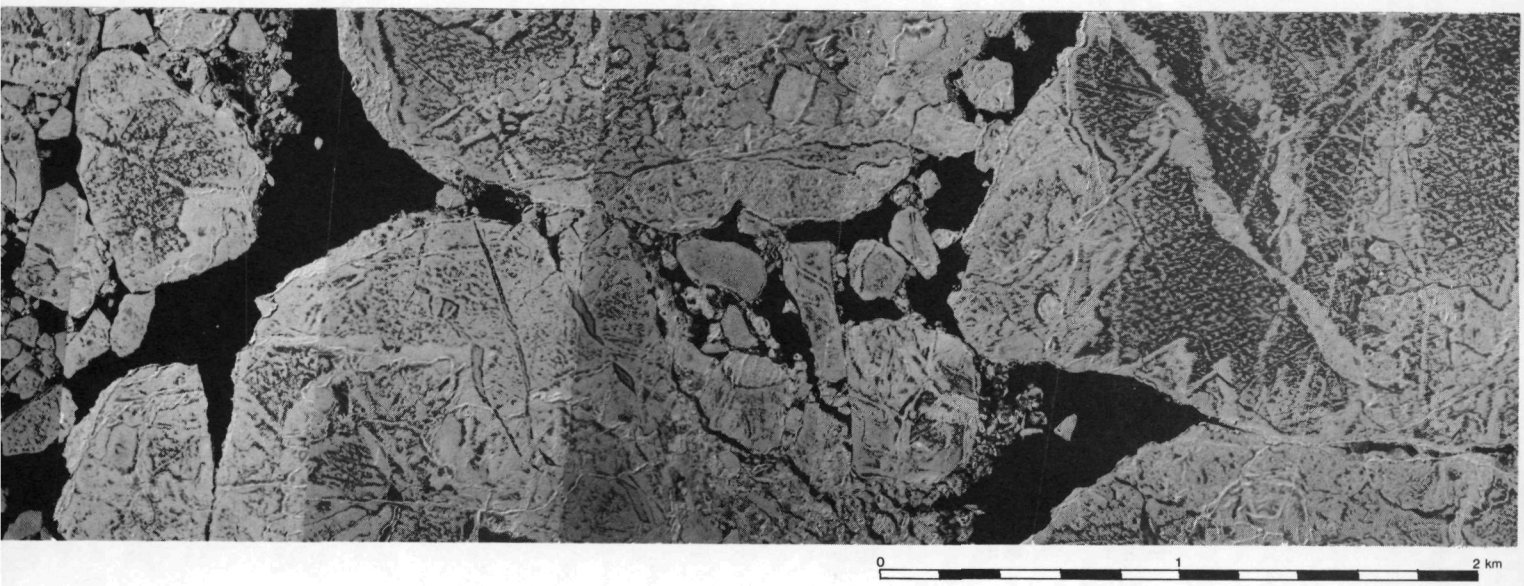

0 1 2 km

Plate 10 FLIGHTLINE SECTION B
13/06/76, 01:24 – 01:27

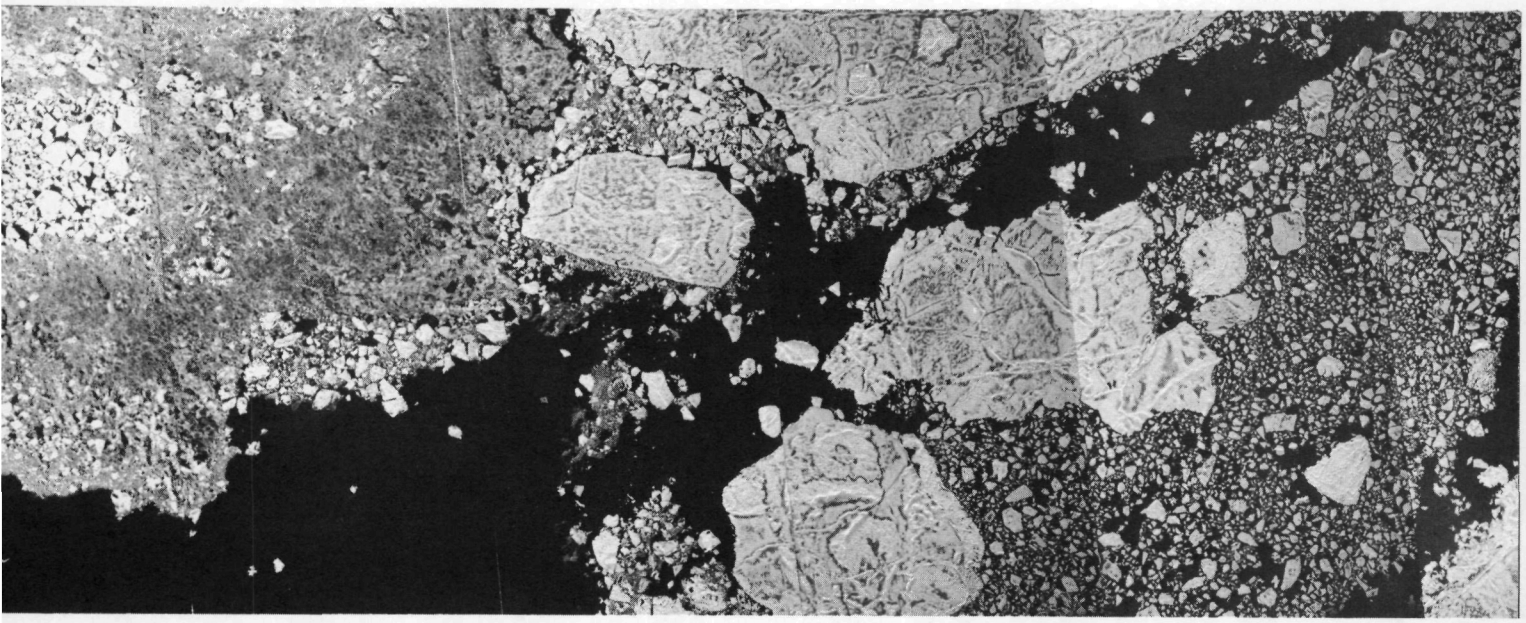

0 1 2 km

TABLE 2 SUMMARY OF ICE CONDITIONS ALONG THE PACK EDGE AND AT OFFSHORE DRILL SITES - FROM OVERFLIGHTS JUNE 2, JUNE 12 AND JULY 15, 1976 (FIGURES B27-B35)

Condition	Date	Mean value (Herschel Island to C. Bathurst)	Drill site D-14	Drill site K-91
Per Cent Area	02/6	43%	2%	13%
Open Water	12/6	46	10	100
	15/7	56	4	80
Per Cent Area	02/6	13%	0	10%
Small Floes	12/6	8	9	0
(<1 km)	15/7	13	10	10
Per Cent Area	02/6	44%	0	77%
Large Floes	12/6	46	80	0
(>1 km)	15/7	31	0	10
Mean Floe Size	02/6	2.9 km	34 km*	3.5 km
(>1 km)	12/6	5.3	7	-
	15/7	2.9	1.5 to 8	1.5

* single isolated floe

In reviewing available LANDSAT imagery it became quite clear that any given configuration of leads and polynyi is a transient condition and can easily be unrecognizable within a few days. Marko refers to a close correspondence between the production of major lead and polynya systems, and significant easterly wind components.

Marko has tabulated ice displacement vectors in the Canada Basin between 72° and 76° N for the period of March 29 to September 6, 1975 in 5-to-8-day intervals. During this period the mean daily displacement was 4.5 ± 3.2 km. Major displacements (75 km) were invariably to the west. In late June and July there was a distinct seasonal shift in ice drift noted, from southwest to northeast, in the vicinity of the Canmar drill sites. At this time major north-south leads in the polar pack reached all the way to the landfast ice boundary. Summer ice movements in the southern Beaufort Sea appear to more or less follow local winds in direction if not in velocity. It should be noted that summer ice drift south of the pack has far fewer constraints during the winter months when there are limited, discrete open-water areas available to accommodate ice movement. Markham has noted a consistent leftward rotation of the

ice displacement vectors relative to average wind vectors. However, too little information is available on short-term ice response to accurately determine the time period over which a wind should be applied. An attempt to relate NORCOR winter beacon movements with wind and current measurements only served to prove the complexity of any kind of ice modelling process and emphasized the fact that not enough is known about internal pack forces. In March 1975 drift data near Canmar Site 2 computed from net 13-day displacement showed an average movement of 7 km/day^{-1}. Daily displacements during this period were in excess of 15 km/day^{-1}, peaking at 25 km/day^{-1} near Cape Dalhousie on March 26-29. In April and May individual floes have been observed to move as much as 55 km/day^{-1}. Generally, from May until September the average daily drift in the Beaufort Sea transition zone has been considered to be about 10 km/day^{-1}.

The largest source of comprehensive long-term ice movement data is the AIDJEX buoy program covering the period December 26, 1975 to August 22, 1976, at 13 locations in the polar pack (not all buoys were operational at the end - one is still operating (December 1976)). Figure 2 shows the positions of the five buoys relevant to our study area. Drift data from these buoys has been reduced and plotted on a daily basis and incorporated with NORCOR's movement study in the transition zone. The AIDJEX data serves as a confirmation of general trends observed in the transition zone and provides a complete picture of large-scale ice movement varying from zero at the landfast edge to a maximum in the polar pack. Satellite fixes for the buoys used here are considered accurate to ± 1 to 2 km (Brown, Polar Research Laboratory).

NORCOR's ice movement data in the vicinity of 131°W, 70°30'N covers the period November 16 to December 7, 1975 and February 10 to March 30, 1976. Ice movement was recorded by obtaining radar fixes over known points. This range and bearing data was then translated into co-ordinates from which displacement vectors are tabulated. The error in these fixes varies slightly with range, but is estimated to be no greater than ± 1 km within the area of interest. Errors are not cumulative and should tend to balance out over the long term.

Daily position checks were obtained at the station. The data is tabulated in terms of daily displacement vectors, net long-term movement and drift velocities in Tables C1 to C4, Appendix C. During early winter, drift was predominantly to the west within the transition zone, with an average velocity of only 1 km/day^{-1}. The most active periods for ice displacement were from November 16 to December 7 (1.0 km/day^{-1} generally west) and January 20 to February 10 (0.8 km/day^{-1} in a random direction). The maximum displacement during any 24-hour period was 11.9 km. During February and March the station experienced a net displacement of only 2.2 km, reflecting the overall ice consolidation during this time. Throughout February there was no evidence of open water within an 80-km radius of camp. A manifestation of internal stress was the development of a substantial 8-to-10m-high ridge along the perimeter of the multi-year floe where the camp was situated. The ridge developed during a storm which lasted from February 6 to February 9 (Plate 11).

The total distance travelled by the ice (sum of daily movements) is generally much larger than net displacements over long time intervals. For example, between November 16 and December 7 the ice moved a total of 67 km in a predominantly westward direction, while the net displacement was

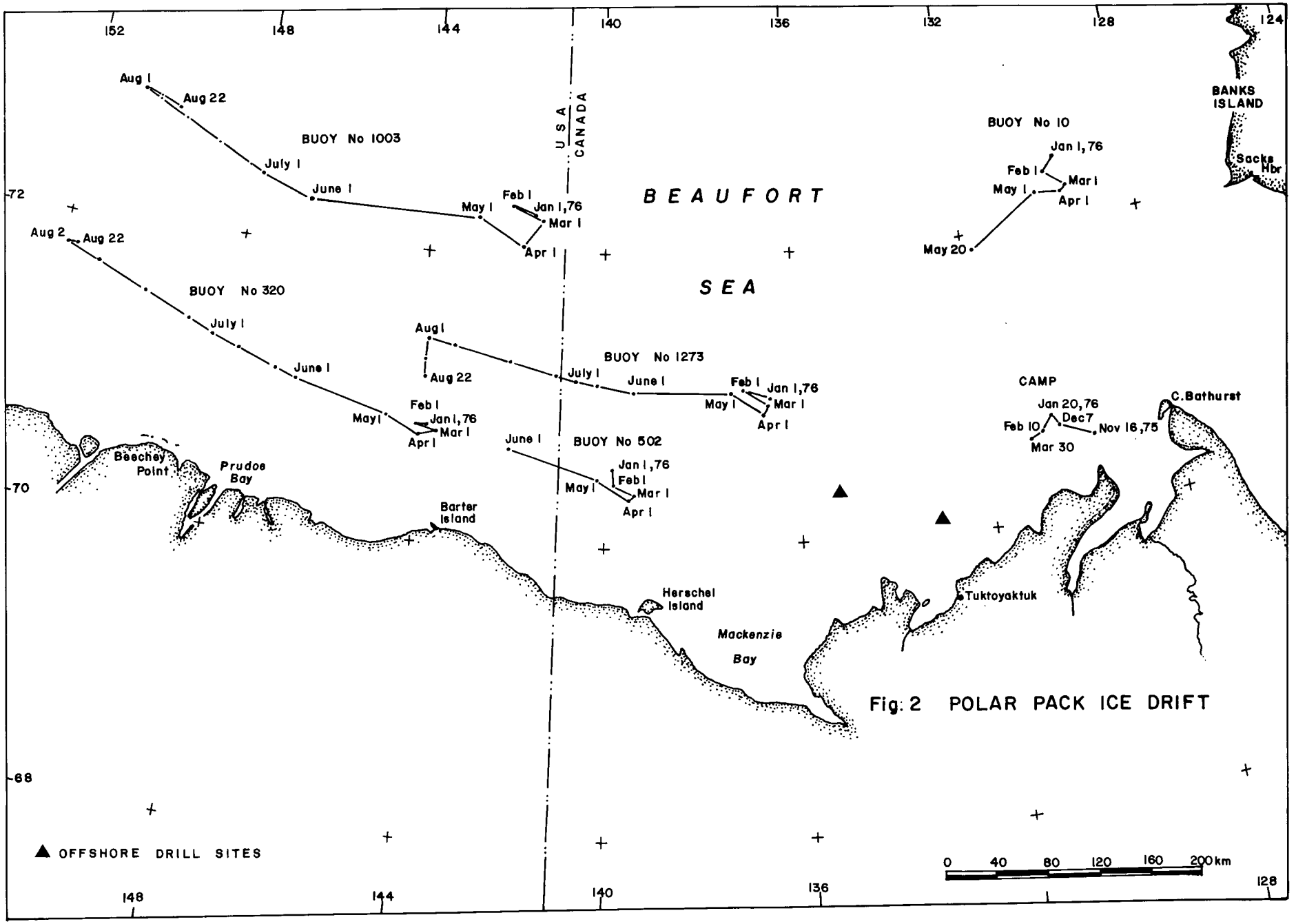

Fig. 2 POLAR PACK ICE DRIFT

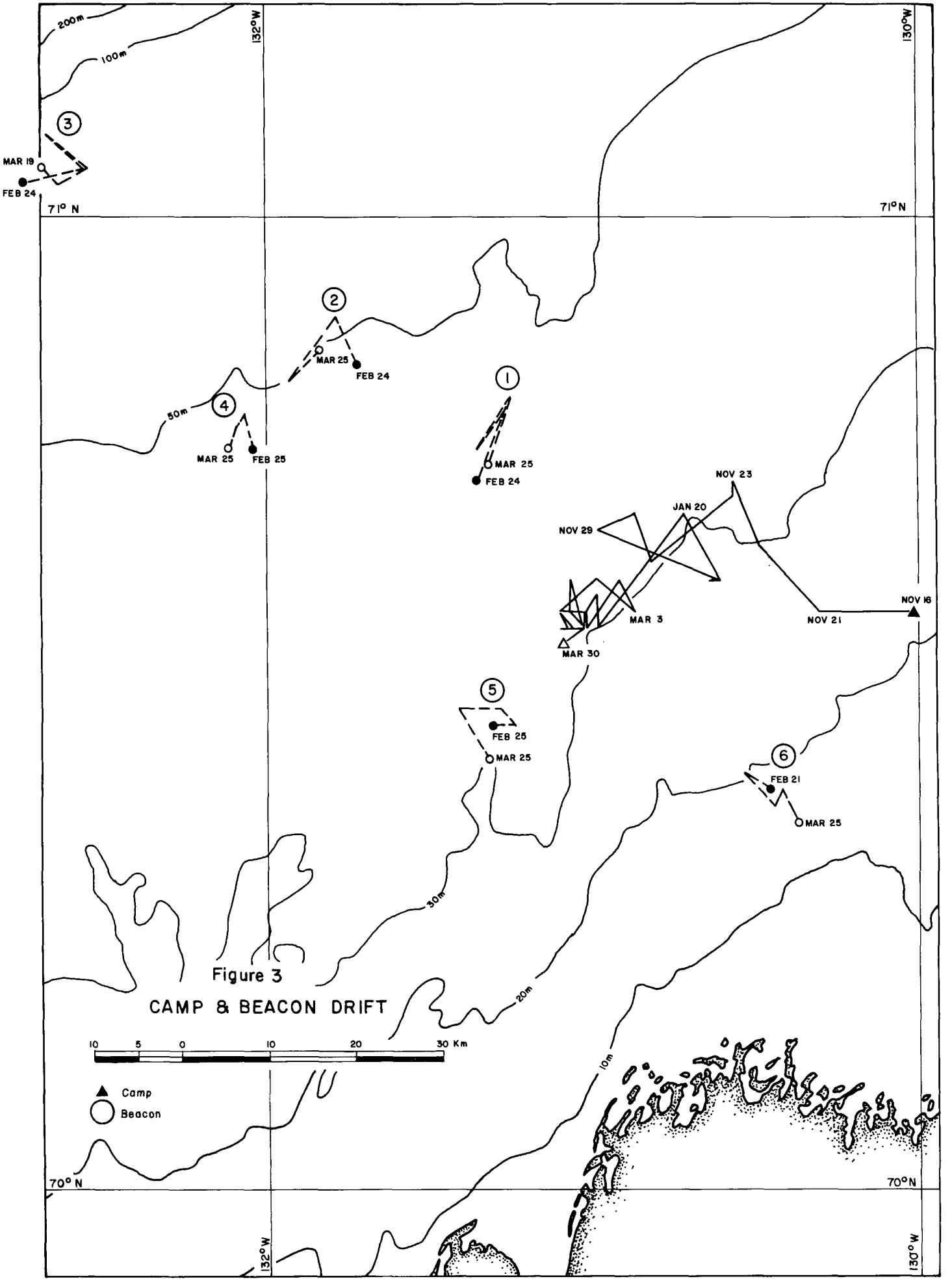

Figure 3

CAMP & BEACON DRIFT

Plate 11 Aerial View of Ridge Near Norcor Ice Station

only 21.8 km. During the ''static'' period between February 10 and March 30 the net displacement was only 2.2 km, while the actual sum of daily displacements was over 60 km (Table C3).

Between February 21 and March 21 position checks were made on seven radio beacons laid out in two parallel lines running from the fast ice to permanent polar pack (Figure 2, Table C2). The beacons spanned the width of the transition zone, covering water depths from 20 m to 70 m along a NW line. At the edges of the transition zone the net displacement between February 24 and March 19 was about 5 km in a SE direction, while the beacons and camp between the 20 and 50-m contours moved in a general westerly direction, with net displacements ranging from 2.2 km to 5.6 km. During this period of beacon checks the ice sheet was intact all the way from shore to the polar pack. The local movements measured by the beacons were manifested in the pattern of decreasing floe size and increasing ridge frequency observed between January 20 and March 6. The only visual indications of movement at that time were the development of several leads roughly parallel to the 20-m contour between the base camp and shore. However, the maximum lead width did not exceed 300 m and refroze within 24 hours (Plates 5, 6).

It is difficult to draw general conclusions about winter ice movement in the transition zone due to the limited data base. The drift rate experienced by the NORCOR station was almost half that previously assumed for the winter period in the transition zone ($\simeq$ 4 km/day^{-1}).

The 67 daily displacement values collected by this program constitute the only detailed displacement data currently available for the transition zone during the winter period. A statistical analysis

of the data was conducted in order to yield distributions for two parameters:

P(V) - the probability of ice drift below a velocity V (or proportion of time spent travelling at a velocity below V)

L(V) - the proportion of distance travelled below velocity V

The data contained in Table C1 was grouped in 1 km/day^{-1} intervals, and the frequency of occurrence determined for each group (Table C5). A number of regressions were run on the probability of velocities less than a given velocity. A best fit was provided by a standard probability distribution function:

$$P(V) = 1 - e^{-\lambda v} \qquad [1]$$

the negative exponential distribution

where $\lambda = 0.45$ (V km/day^{-1})
or 0.65 (V m/min^{-1})

For this distribution the mean is $1/\lambda$ (2.16 km/day^{-1}), and the variance is $1/\lambda^2$.

Figure 4 is a plot of equation [1] along with actual probabilities calculated from the data (Table C6). In calculating possible oil film thicknesses and areas of contamination, it is also necessary to know the proportion of the distance, L(V), travelled below a given velocity, V.

If we let Lt (V_1, V_2) be the distance moved in time (t), while travelling at velocities between V_1 and V_2, then:

$$L(V) = \frac{Lt\ (0, V)}{Lt\ (0, \infty)} \qquad [2]$$

Using the probability density function $p(V) = -dP(V)/dV$ we have:

$$L(V_1, V_2) = t\int_{V_1}^{V_2} Vp(V)dV \qquad [3]$$

$$= t\int_{V_1}^{V_2} V\lambda e^{-\lambda V}\, dV \qquad [a]$$

$$\therefore L(V) = 1 - (1 + \lambda V)e^{-\lambda V} \qquad [4]$$

or $$1 - (1 + 0.45V)e^{-0.45V} \qquad [5]$$

with V expressed in km/day^{-1}

Figure 4 contains a plot of [5] together with data from Table C6. Note that the empirical curve is a good fit and tends to L = 1 at large V. It can be seen from the velocity and distance curves in Figure 4 that the ice will move at less than the mean velocity for 62% of the time while covering only

25% of the total distance. The importance of these facts will be discussed in the treatment of various hypothetical blowout cases in Section 4.2.

The AIDJEX buoy data was evaluated initially by plotting the monthly movements from January to August, 1976 to gain an understanding of how the drift varied with location and time (Figure 5, Table 3).

All five buoys displayed a generally increasing monthly drift from winter to summer with the exception of a decrease in March and June. Maximum monthly drift was 130 km. Monthly directions were very consistent with standard deviations in the monthly mean of five buoys averaging 7%. With the exception of February when the buoys moved SE, all the net movement was westerly in the range of 236° to 297°. There is a general trend evident, progressing from high velocities in the order of 4 to 6 km/day^{-1} in January to slower movement in March, and rising sharply to peak velocities of up to 7.5 km/day^{-1} in May and June. As there are only a few data points that can be used for comparison, it is difficult to establish a quantitative difference between movement in the transition zone and polar pack. From December to February the camp appeared to move slower than the pack by a factor of about two. Data from March shows the camp velocity rapidly approaching. 70-80% of the pack velocity. Extrapolating past March, the ice velocity in the transition zone would be expected to level off throughout April at about 2 to 3 km/day^{-1}. As breakup commenced in May, ice velocities would be expected to increase sharply in the transition zone. By late May the open-water conditions would allow individual daily floe velocities in this zone to far exceed the pack movement. However, strong offshore winds often force large quantities of ice against the pack during the summer months and this ice could then be expected to move at a rate similar to the pack itself for short periods.

When considering ice movement patterns, quite different results can be obtained depending on the time scale chosen. A large fluctuation in individual daily vectors can result in a very small net displacement at the end of a month, even though the actual distance travelled may be up to 30 times greater. The ratio, Total Distance travelled/Net Displacement, provides an indication of the type of buoys and the camp (Table C9). With February and March ratios of 6.5, the camp movement is similar to the pack at that time (mean ratio of 7.4). As the pack moves more consistently to the west, the ratio drops to a low of 1.5 in July. This is reflected in the extremely large net displacements measured at that time.

In order to provide a specific comparison between movement in the transition zone and the pack, the period February 10 to March 30 has been examined in detail. Daily camp velocities are available for this time frame to coincide with the AIDJEX data. In all cases the standard deviation in velocity was between 60 and 100% of the mean value. Mean daily velocities in the pack for this period varied from 2.1 to 4 km/day^{-1}. All data for the period February 10 to March 30 was tabulated in terms of frequency, for different velocity intervals, in a similar manner to Table C5. Figure 6 presents the resulting probability curves.

Fig. 4 PROPORTION OF TIME AND DISTANCE TRAVELLED BELOW A GIVEN VELOCITY

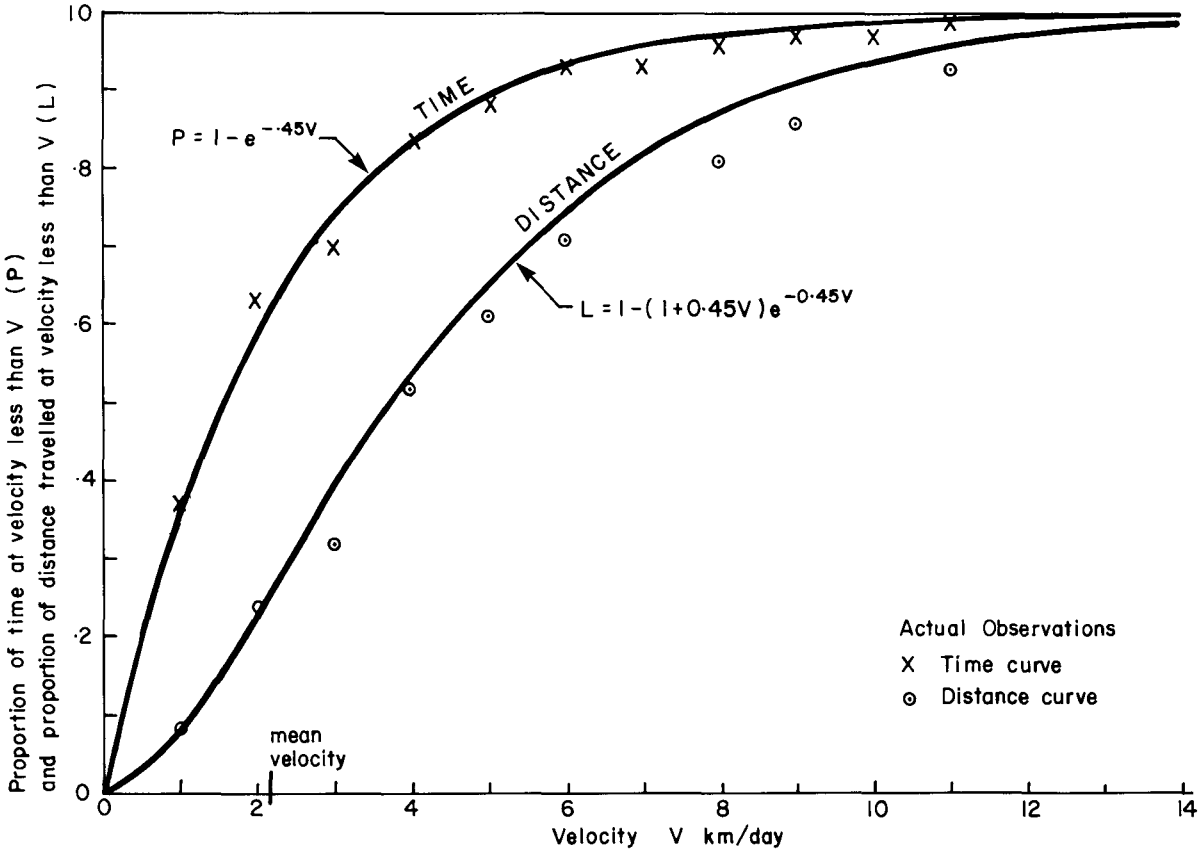

Fig. 5 MEAN DAILY ICE DRIFT VELOCITIES
January to July 1976

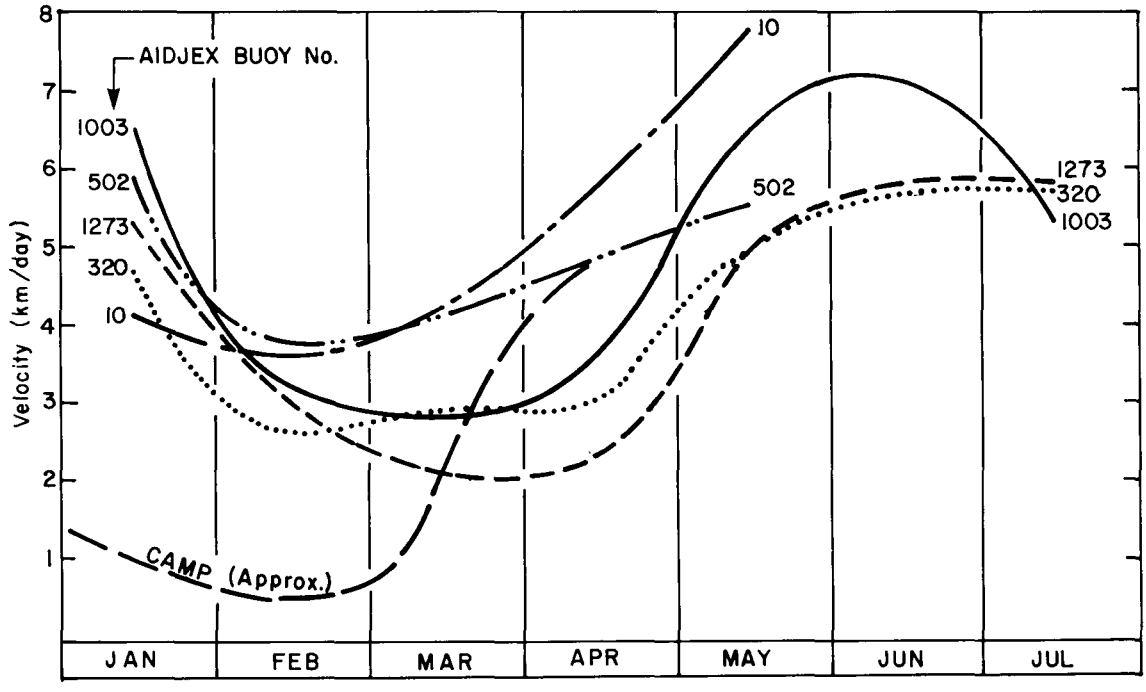

Fig. 6 COMPARISON OF ICE VELOCITY PROBABILITIES
TRANSITION ZONE vs POLAR PACK Feb 10 to Mar 30, 76

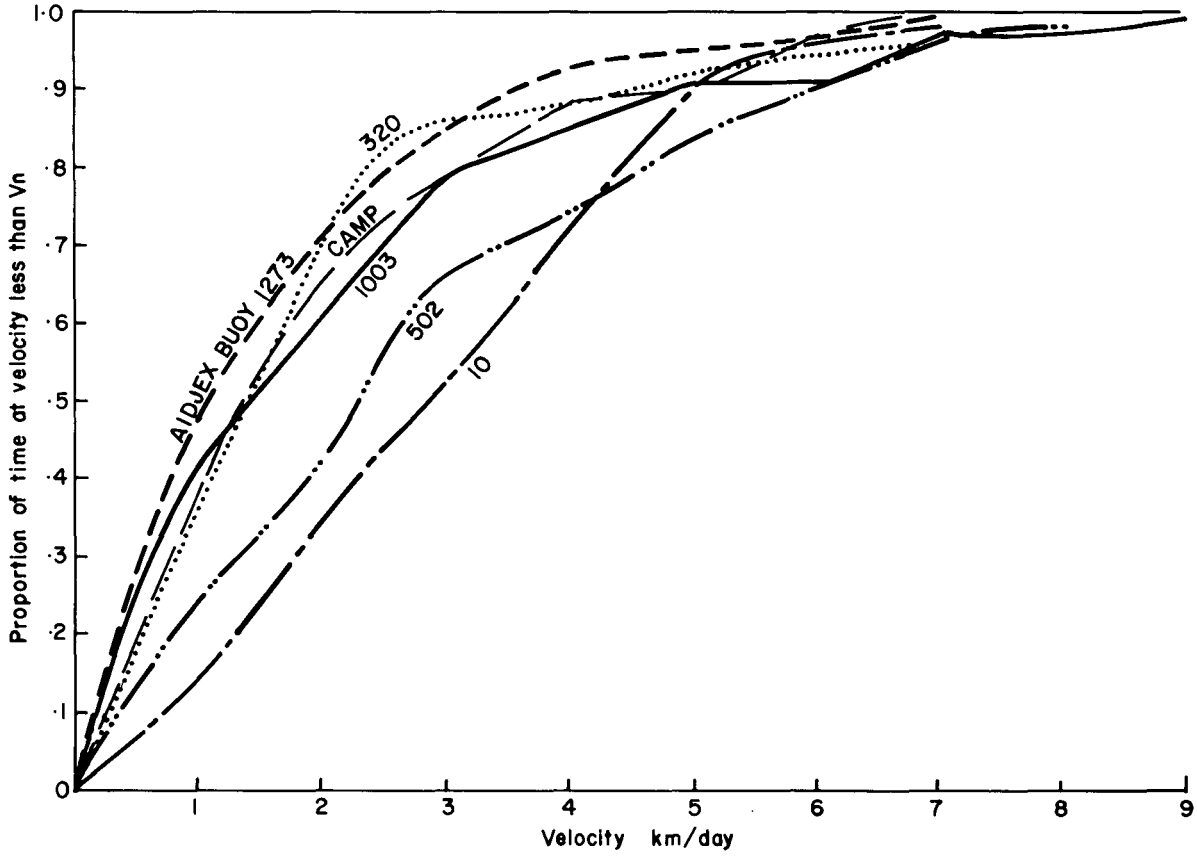

TABLE 3 MEAN MONTHLY ICE DRIFT - POLAR PACK (5 AIDJEX BUOYS)

Month	Displacement (km)	Direction (°True)
January	13 ± 6.5	254° ± 22
February	23 ± 4.3	117° ± 8
March	12 ± 7.5	236° ± 40
April	32 ± 7.3	297° ± 9
May	82 ± 28	271° ± 9
June	48 ± 12	293° ± 0 (3 buoys)
July	117 ± 12	297° ± 3 (3 buoys)

The camp data and all buoys except # 10 follow a similar exponential curve to that already observed for the camp's November to March movement. The different behaviour of buoy # 10 is reflected in its movement plot for this period (Figure C2). Daily movements have been plotted for all buoys and the camp in Figures C1 to C6. On a daily basis it is impossible to see any consistent pattern to the buoy movements. However, when the long-term tracks are compared a distinct trend is evident. All buoys except # 10 and the camp remained roughly static (within error bounds) from February 10 to February 29, moved NW for 2 or 3 days, west from March 1 to March 12, SE for about 6 days and then in a random pattern with little net movement for the remainder of the month. Net displacements at the end of the 50-day period were all within the range 9 to 24 km in a westerly direction (240 to 276°). The fact that such patterns are visible not only confirms the validity of measured buoy positions, but also indicates the different movement of ice in the transition zone. Although the camp during this period experienced a net movement in a similar direction to the pack, the track has no systematic pattern and appears to be composed of almost random daily movements. Possibly in April the movements would smooth out as they did in the pack in 1976.

In viewing the drift data presented here, the accuracy limitations must be considered. As stated earlier, camp positions are considered to be ± 1 km, while AIDJEX buoys are accurate to ± 1 to 2 km. While not significant from May to July when net movements are large, these errors could change the appearance of a February-to-March track.

Spring and summer motions of individual floes have been measured off satellite imagery by a number of people. Marko (1976) states that finely divided ice during April and May moves to the southwest with speeds averaging 10 km/day^{-1}, and rising to at least 55 km/day^{-1} on occasion. Measurements off LANDSAT images for June 6 and June 14 north of Herschel Island show a SW movement of between 25 and 30 km. Between June 12 and June 13, LANDSAT images north of Tuktoyaktuk show 14-hour movements to the north of between 7 and 10 km (Plate 8). At these drift rates an individual floe is unlikely to remain stationary over a blowout long enough to collect any significant volume of oil. The importance of summer floe drift velocities is to provide an indication of just how far contaminated ice could move after breakup. The divergence of floes is impossible to predict accurately. If the concentration is reasonably heavy (6/10 +), ice appears from LANDSAT photography to move as roughly one body over periods up to 10 days. That is, large floes remain in approximately the same spatial position relative to one another. Rotations of the large floes can easily occur and smaller floes in the order of 0.5 km can redistribute themselves completely. With a possible range in summer ice movements of 4 to 50 km/day^{-1}, and the dominant effect of wind, it would be extremely difficult to estimate the disposition of previously contaminated ice during the summer period.

It is obvious from this discussion that the data base for ice movement in the transition zone is extremely limited. However, as a result of the AIDJEX program there is now a far better understanding of long-term pack movement. NORCOR data provides an indication of the movement scale likely to be encountered during the winter period in the transition zone. Summer ice motion in the transition zone is much more difficult to quantify or predict and experiences tremendous variation from year to year. Much more work needs to be done to obtain accurate drift data for the area of interest during the period April to August.

4 WINTER OIL DISTRIBUTION IN THE BEAUFORT SEA

The primary objective of this report is to determine the fate of oil discharged during the winter months in the Beaufort Sea. To do this, it is necessary to quantify the probable winter oil distribution before looking at the spring and summer conditions. There are three potential sources of a major winter oil spill in the Beaufort Sea: rupture of a tanker, rupture of a pipeline and an oil well blowout.

The first case would likely result in a very localized concentration of a large quantity of oil, either on the ice surface or within a sunken hull. Of these two possibilities, a surface spill would be much

easier to cope with. Even if not burned immediately by cleanup crew, any soil that became trapped in the ice would be available in thick films for burning the following spring. The other option of a sunken hull still containing large quantities of oil would be far more serious. Rate of discharge would vary with the degree of structural damage and oil type. Winter recovery operations would be complicated by the ice movement and a leak may not be brought under control until the following summer.

The cases of a pipeline, oil well blowout or ruptured submerged hull all constitute a point source under an ice canopy and can be modelled in a similar fashion.

Of these three possible sources of a major winter oil spill in the Beaufort Sea, only the wellhead blowout is of immediate interest. Consequently, the mathematical simulation presented here will treat a blowout running at realistic flow rates in the transition zone from October 1 to June 1. This would result in a total oil volume of about 10 million gallons, compared with 40 million gallons for a 200,000 DWT tanker. Many of the conclusions presented following the analysis will apply in a general fashion to other types of accidents, but the film thickness analysis in particular would have to be modified as necessary for future scenarios.

4.1 General Mathematical Model - Point Oil Source

The release of oil and gas beneath a moving ice field is considered similar to a liquid being discharged on a moving conveyor belt which has a textured surface. At slow drift rates the oil and gas will fill the depressions along the underside of the ice and spread to contaminate an area larger than the diameter of the plume.

At higher drift rates the oil will be limited to a band approximately equal to the width of the plume, but the depressions will not be completely filled. The distribution of oil and gas is shown schematically in Figure 7.

The minimum width of the contaminated band is the diameter of the plume. From open-water studies by Topham, the diameter of the plume can be approximated by:

$$D = 1.7\, Z \left(\frac{Qt}{Z + 10.36} \right)^{1/3} \text{ m} \qquad [6]$$

where Qt = total flow (m^3/min^{-1}) - oil and gas
Z = water depth

This formula applies over the experimental range examined by Topham -Qt = 4 to 40 m^3/min^{-1}; Z = 30 to 60 m. (Nb. The Beaufort Sea initial blowout flow estimated at about 40 m^3/min^{-1}).

Fig. 7 SCHEMATIC OF OIL DISTRIBUTION (Plan view)

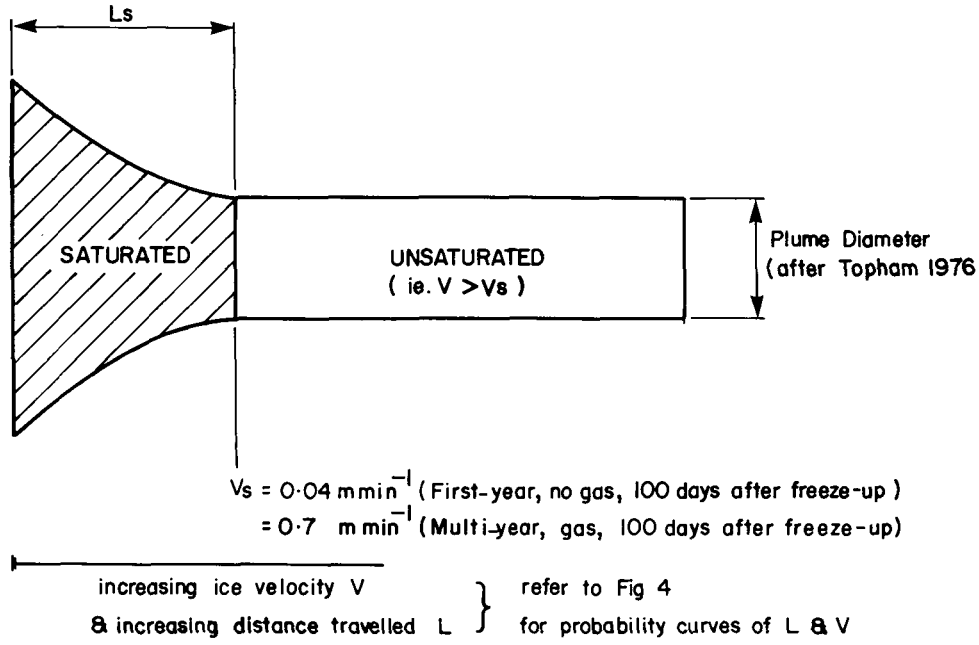

"It was not practical to perform the experiment under ice or to provide a solid sea cover over a large enough area, but it is believed that the broad features of the resulting flow patterns will be similar and can be derived from the open water case." (Topham 1975).

From work at Balaena Bay (NORCOR 1976) and other studies in the Beaufort Sea, the total variation in ice thickness is approximately 20% of the mean ice thickness. With a sinusoidal irregularity in ice thickness, an average oil-gas film thickness of 10% of the mean ice thickness could occur before spreading could take place. With a growth rate of about 1 cm per day and an initial multi-year ice thickness of 3 m, the respective saturated film thicknesses (gas and oil) for multi-year ice (C_m) and first-year ice (C_f) are:

$$C_m = (300 + n)\ 10^{-3}\ m \qquad [7]$$

$$C_f = n\ 10^{-3}\ m \qquad [8]$$

where n = number of days after freeze-up

Note that these formulae are not intended as accurate ice growth predictions, but simply a convenient method of estimating ice roughness. To calculate saturated oil film thickness with gas present [7], [8] must be divided by the product K_1K_2

where K_1 = ratio total flow/oil flow (max. 150)

K_2 = fractional proportion of total flow retained under the ice (0 to 100%)

A realistic assumption for modelling purposes is that for first-year ice, 100% of the gas is vented due to fracturing. In fact, fracturing of the sheet would allow some oil to surface and, of course, some gas would still remain trapped in undamaged pockets beneath the ice. With a first-year ice thickness of about 1 m, 100 days after freeze-up, an average, saturated oil-pool thickness of 10 cm could develop with no gas present. If the gas is 100% retained, then the maximum possible oil film thickness could be reduced by a factor as high as 150 (gas/oil ratio commonly cited as typical for the Beaufort Sea). A corresponding assumption has been made for thicker multi-year ice (n = 100 day) would be 0.26 cm. An existing theory describes gas venting criteria for different ice thicknesses, but is limited in practical value due to the present unreliability in ice strength values (Topham, 1976). The ice roughness model with two extreme cases for gas venting is shown in Figure 8.

Fig. 8 ICE ROUGHNESS MODEL (not to scale)

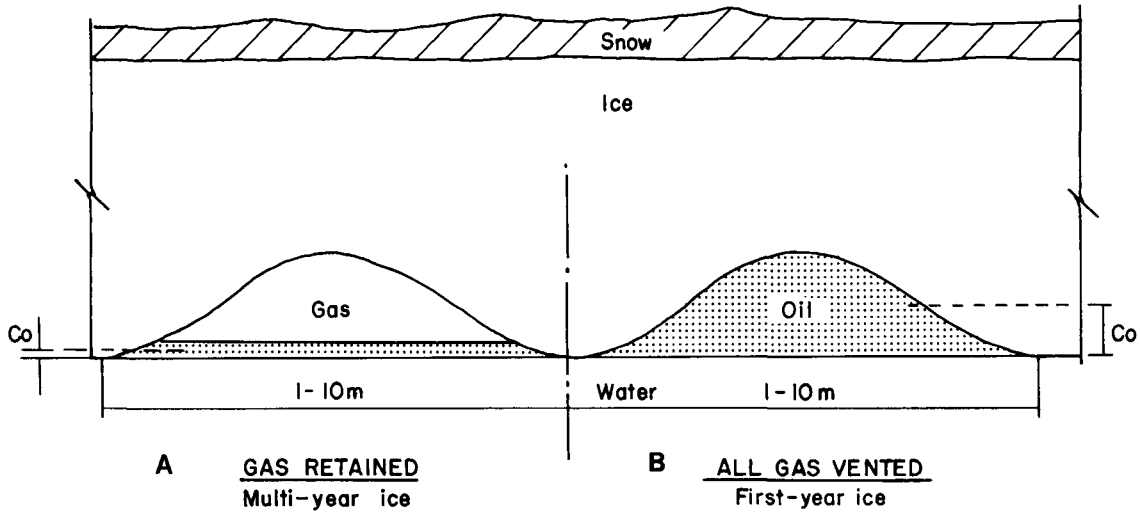

Knowing the average oil film thickness at saturation (C_o), the velocity V_s below which the depressions in the ice are completely filled, can be expressed as:

$$V_s = \frac{Q_o}{DC_o} \text{ m/min}^{-1} \qquad [9]$$

where Q_o = rate of discharge of oil (m^3/min^{-1})
C_o = average saturated oil film thickness (m)

For the two extremes of gas venting shown in Figure 8, the ice velocity for saturation can range from 0.04 m/min^{-1} in Case B to 0.7 m/min^{-1} in Case A.

From observed drift rates in the Beaufort Sea over the period November 16 to March 30, 1976 (Section 3.2) the probability of ice movement slower than a given velocity V will take the form:

$$P = 1 - e^{-0.65V} \qquad [10]$$

where V = ice velocity (m/min^{-1})

Similarly, the proportion of distance travelled below a given velocity V can be presented as:

$$L = 1 - (1 + 0.65V)e^{-0.65V} \qquad [11]$$

See Section 3.4 for a derivation of [10], [11]. These detailed distributions will likely change with time and location. However, the same general exponential dependence applies to AIDJEX buoys, as well as to the ice station movement over different time intervals (Figure 6). Consequently, if the expressions [10] and [11] are assumed to prevail throughout the winter, a number of mean characteristics of the contaminated band can be expressed as functions of the discharge rate, water depth and time.

Since the principal topic of interest is oil contamination, the following formulae rates of discharge are expressed in terms of the volume of oil per unit time (Q_o).

4.1.1 Nomenclature

Q_o = rate of discharge of oil (m^3/min^{-1})
Q_t = total flow of oil and gas (m^3/min^{-1}) ($Q_t = Q_oK_1$)
V_s = ice velocity necessary to achieve saturation (m/min^{-1})
P_s = probability of ice velocities less than V_s
L_s = probability of distance travelled by the ice at velocities less than V_s
$\bar{V}$ = mean ice velocity (1.5 m/min^{-1} from NORCOR camp movement) (m/min^{-1})
$C_{m,f}$ = average combined oil and gas film thickness at saturation (governed for different ice types by formulae [8], [9]) (m)
C_o = average saturated oil film thickness (m)
Z = water depth (m)

4.1.2 Derived Formulae

A. *Mean Width of Saturated Area – W_s*

$$W_s = \frac{Q_oP_s}{L_s\bar{V}\,C_o} \qquad [12]$$

B. *Minimum Width of Contaminated Area = Plume Width D*

$$D = 1.7\,Z\,\frac{Q_t}{Z + 10.36}^{1/3} \qquad [13]$$

Topham, 1975

C. *Mean Thickness of Oil Film* $\bar{C}_o$

$$C_o = \frac{Q_o}{[W_s L_s) + D(1 - L_s)]\bar{V}} \qquad [14]$$

D. *Per Cent Area Below a Given Average Oil Thickness d*

$$\%\ A(C < d) = \frac{\bar{C}_o\, D(1 - L)\bar{V}}{Q_o} \times 100\% \qquad [15]$$

or

$$\frac{D\,(1 - L)}{[(W_s L_s + D(1 - L_s)]} \times 100\%$$

hence, L = proportion of distance travelled by the ice sheet below velocity V

where $V = Q_o/dD\ m/min^{-1}$

E. *Per Cent Volume Below a Given Oil Thickness d*

$$\%\ Vol\ (C<d) = e^{-0.6Q_o/dD} \qquad [16]$$

NOTE: Equation [16] only applies when the average thickness of oil, d, is less than that required for saturation (see Figure 7).

The model represented by the these formulae provides a reasonable framework for calculating important oil distribution parameters for an under-ice spill from pipelines or wellheads. The limitations in the model are due to a distinct lack of detailed information in a number of important areas: under-ice roughness, gas venting with its effects on oil disposition and incorporation, and ice conditions. Assumptions inherent in developing the model will be dealt with here. Subsequently, a sensitivity analysis will show, fortunately, that even major errors in all but two specific areas should not markedly affect the final results.

Very little is known about the shape distribution or size of under-ice roughness. (See Rosenegger, 1975 for a theoretical treatment of slope angle versus oil movement). It is clear from numerous detailed coring studies and sonar measurements that there are substantial variations in ice thickness within a very local area. From the point of view of oil pooling, it would be totally unrepresentative to assume a flat sheet for the ice under-surface. Snow drifts on the surface tend to form in a preferred wave distribution. Consequently, a sinusoidal variation in the ice under-surface has been used (Figure 8). Using this approximation effectively doubles the maximum possible oil thickness calculated on the basis of a flat sheet ($d = Q_o/DV$ [17], where $V > V_s$). Depending on the degree of

uniformity in the type of under-ice roughness, there will be localized areas where the oil may collect and pool to thicknesses much greater than predicted by any such averaging formulae as [17]. However, at ice velocities commonly encountered in the transition zone, the total volume of oil trapped in these deep pockets will be extremely small.

The presence of gas with its effects on oil film thickness and contaminated area is probably the most important controlling factor in the mathematical model used here. Unfortunately, there is really no relevant experimental data on this subject. Topham has conducted an extensive mathematical evaluation of the gas-ice interaction, but until the reliability of ice strength measurements improves, his theory cannot define venting criteria. The gas-oil interaction under the ice can only be hypothesized. With the present state of knowledge on this subject, contamination parameters must be calculated for the two possible extremes of zero venting (probably multi-year ice) and 100% venting (probably first-year ice).

Only four months of winter movement data are available for the Beaufort Sea transition zone where offshore drilling activities are concentrated. AIDJEX buoys provided a complementary picture of polar pack movements in 1976 and confirmed both the general magnitude and distribution of ice velocities. There could be considerable annual variations in ice movement patterns. However, the ice velocity necessary for oil saturation of the first-year ice under-surface is so low (0.25 km/day^{-1}) that even large variations in the ice velocity probability distribution could not significantly increase the likelihood of saturation.

Perhaps a more important question in terms of oil contamination is the ice movement on an hourly basis. All existing data is limited to a minimum time period of one day due to positioning errors. AIDJEX buoy data is available approximately every two hours, but is not usable on this time scale due to errors of up to ± 2 km between consecutive fixes. Hourly movements are invariably the same order of magnitude as the error, making interpretation extremely difficult. It is quite probable that for substantial portions of many days the ice is almost stationary. This could enable more oil to collect in thicker films than predicted on the basis of mean daily velocities used here.

In considering ice type and morphology, the major components are per cent multi-year floes and their size, ridges, cracks and leads. From the mean values observed on NORCOR's overflights and reported in the literature (Table 1, Topham, 1976; Wadhams, 1975), ridges, cracks and leads would constitute less than 10% of the area of any contaminated track. Consequently, within the overall error bounds, a refinement of the model at this stage to take these features into account does not appear worthwhile. The distribution of ice types is a much more important parameter. In the area of exploration interest the proportion of multi-year ice could easily vary between 10 and 60% in different years, with a proportional effect on the volume of oil available in thick films. It is generally considered that the spring migration of oil to the ice surface will be slower in multi-year ice than in first-year ice. With the retention of more gas under thicker ice, oil films under multi-year ice will likely be orders of magnitude thinner than under first-year ice. Consequently, the presence of substantial quantities of multi-year ice could leave a large proportion of the oil almost irrecoverable.

4.2 Application of the Distribution Model to Some Typical Cases in the Beaufort Sea

Oil flow rates stated by industry and government to apply in the Beaufort Sea are 2,500 b/day^{-1} (398 m^3/day^{-1}) initially, decreasing to 1,000 b/day^{-1} (159 m^3/day^{-1}) after 30 days. It should be noted that these figures are not universally accepted and various sources quote long-term flow rates larger by a factor of two or more. From industry experience, 22.7 m^3 of free gas is produced per barrel of oil, resulting in a gas-to-oil ratio of 150. These values will be considered as a ''standard blowout''. This term is a useful means of understanding the relative importance of the variables affecting oil contamination. Table 4 shows the model results for a typical case. Here the water depth is 60 m or about the centre of the transition zone. First-year ice is considered fractured by the gas, while multi-year ice stays intact. Calculations are based on velocities distributed according to NORCOR ice station movements.

To determine the model sensitivity the following variable ranges were used:

- Double oil flow rate;
- Vary water depth from 10 to 100 m;
- Assume 50% gas vented for both ice types.

These typical extremes likely to be encountered in the Beaufort Sea drilling activities allow upper and lower bounds to be set on the important oil distribution parameters.

Table 5 summarizes the variation of oil distribution parameters as conditions are changed from the typical case. Only with very shallow water or usually high-flow situations (5,000 barrels/day) will more than 35% of the oil collect in films thicker than 0.5 cm on the average. In every case these ''thick'' oil films cover less than 15% of the total contaminated area.

4.3 Hypothetical Winter Distribution of Oil Along a Known Ice Drift Track

From measurements of the camp movement it is obvious that the ice in the transition zone during winter is quasi-stationary for a considerable proportion of the time ($\pm$0.5 km within position error). For the period February 10 to March 30 the camp experienced 19 zero-movement days. This constitutes 40% of the time, and if applied to ice moving across a blowout, could substantially change the oil film thickness and contamination area at specific points along the track. In an effort to provide a more realistic picture of the behaviour and fate of oil, actual station ice-movement data for the period February 10 to March 30 was used in the expressions developed in Section 4.1. The dependence of oil film thickness on ice velocity for this time of year has been plotted in Figure 9. (The maximum film thickness used here is double that referred to previously).

It can be seen that for velocites in excess of 0.5 km/day^{-1}, oil will not collect in films greater than 1 cm. This calculation is based on the sinusoidal roughness model shown in Figure 8. In actual fact, there could be isolated pockets of much thicker oil. Under multi-year ice the presence of gas would limit the maximum model oil film to about 0.6 cm regardless of velocity.

TABLE 4 THE "STANDARD BLOWOUT"

	Initial Flow		Stable (30 days after)	
	First-Year	Multi-Year	First-Year	Multi-Year
Oil flow (m^3/min^{-1})	0.28	0.28	0.11	0.1
Gas-to-oil ratio	150	150	150	150
Water depth (m)	60	60	60	60
Per cent gas retained (%)	0	100%	0	100%
Plume diameter ie. minimum band width (m)	86	86	63	63
Mean width of saturated area (m)	-	202	-	139
Average saturated oil film thickness (cm)	10	0.26	10	0.26
Mean oil film thickness (cm)	0.21	0.17	0.12	0.11
% Oiled area less than mean oil film thickness	74%	52%	74%	66%
% Volume in films less than mean oil film thickness	38%	29%	38%	35%
% Oiled area less than film thickness of 0.5 cm (avg.)	93%	100%	98%	100%
% Volume in films less than 0.5 cm (avg.)	65%	100%	80%	100%

TABLE 5 POSSIBLE RANGES OF OIL DISTRIBUTION PARAMETERS

Variations on "Standard" Case	Oil Distribution Parameters					
	Mean Oil Film Thickness (cm)		% Volume < 0.5 cm		% Area < 0.5 cm	
	First	Multi	First	Multi	First	Multi
Oil flow, 0.55 m^3/min^{-1}	0.34	0.22	52	100	85	100
Water depth, 20 m	0.26	0.19	60	100	93	100
Water depth, 100 m	0.08	0.08	79	100	98	100
Venting, 50%	0.09	0.11	100	80	100	92

The actual net daily path travelled by the camp between February 10 and March 30 is shown at a scale of 1 cm = 500 m in Figure 10, with the basic plume width for a 60-m water depth superimposed on the track centreline. The two large-dotted circles delineate the extent of contamination that could occur if multi-year floes remained stationary over the blowout for a 7 and 8-day period (maximum diameter 720 m). The smaller circles show the extent of contamination under multi-year ice during one day of zero movement (255 m diameter). With first-year ice and no gas, it would take over six days of zero movement to just saturate the ice. Only then would the contamination area extend past the basic plume diameter. In fact, this may take even longer since a considerable portion of oil would likely flow onto the ice surface through fractures in the sheet.

Figure 11 is a linear plot of theoretical oil film thickness along the track from 0 to 75 km. The oil only occurs in significant film thicknesses while the ice is stationary. Consequently, the area receiving heavy oil concentration is very small.

In reality, due to natural variations in the ice cover and different gas venting situations, some oil will be present under both ice types in films thicker than those suggested by the model (Section 4.1). However, the two extremes of all multi-year ice with no venting, and all first-year ice with total venting, offer a reasonable estimate of the upper and lower bounds of under-ice oil contamination likely to be encountered.

These two extremes have been plotted in Figure 12 as per cent oil in films greater than a given thickness versus film thickness. As a best case (upper curve) 37% of the oil will occur in films greater than 1.0 cm. These thick films cover an area of only 0.03 km^2 out of a total contaminated area of 5.6 km^2.

Fig. 9 OIL FILM THICKNESS vs ICE VELOCITY
(Feb 10 — Mar 30 period) assume freeze-up on Oct 10

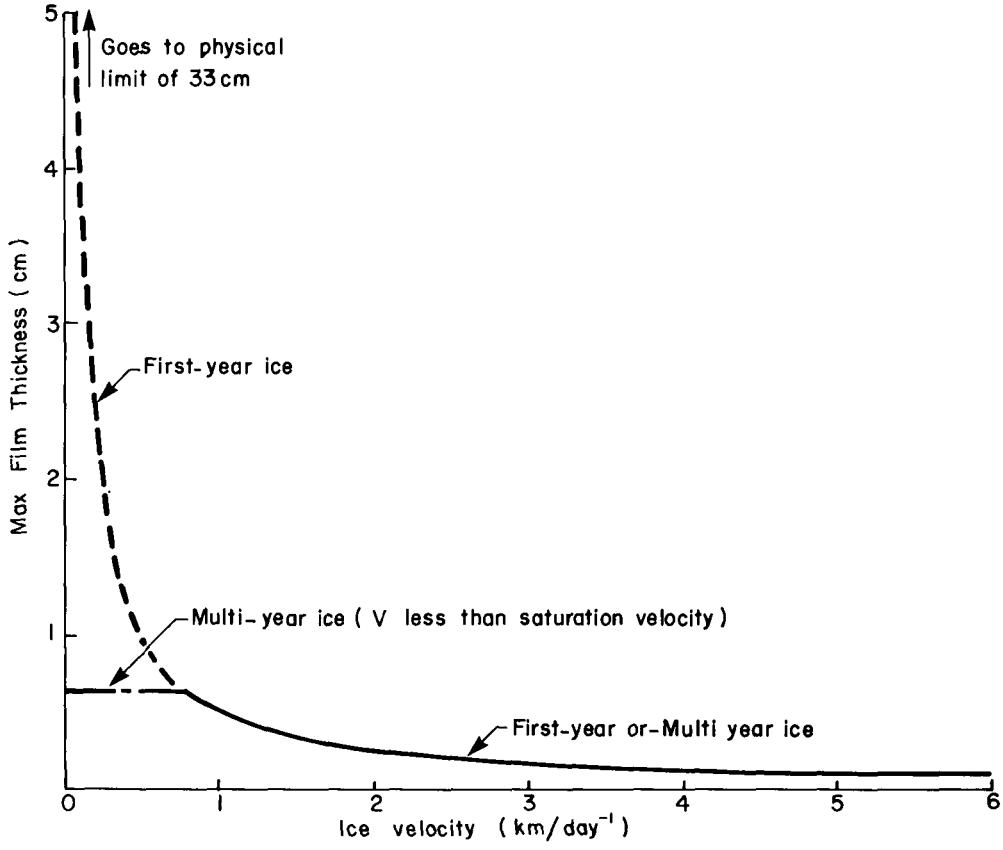

Fig.10 DETAILED CAMP MOVEMENT, Feb 10 - Mar 30, 1976

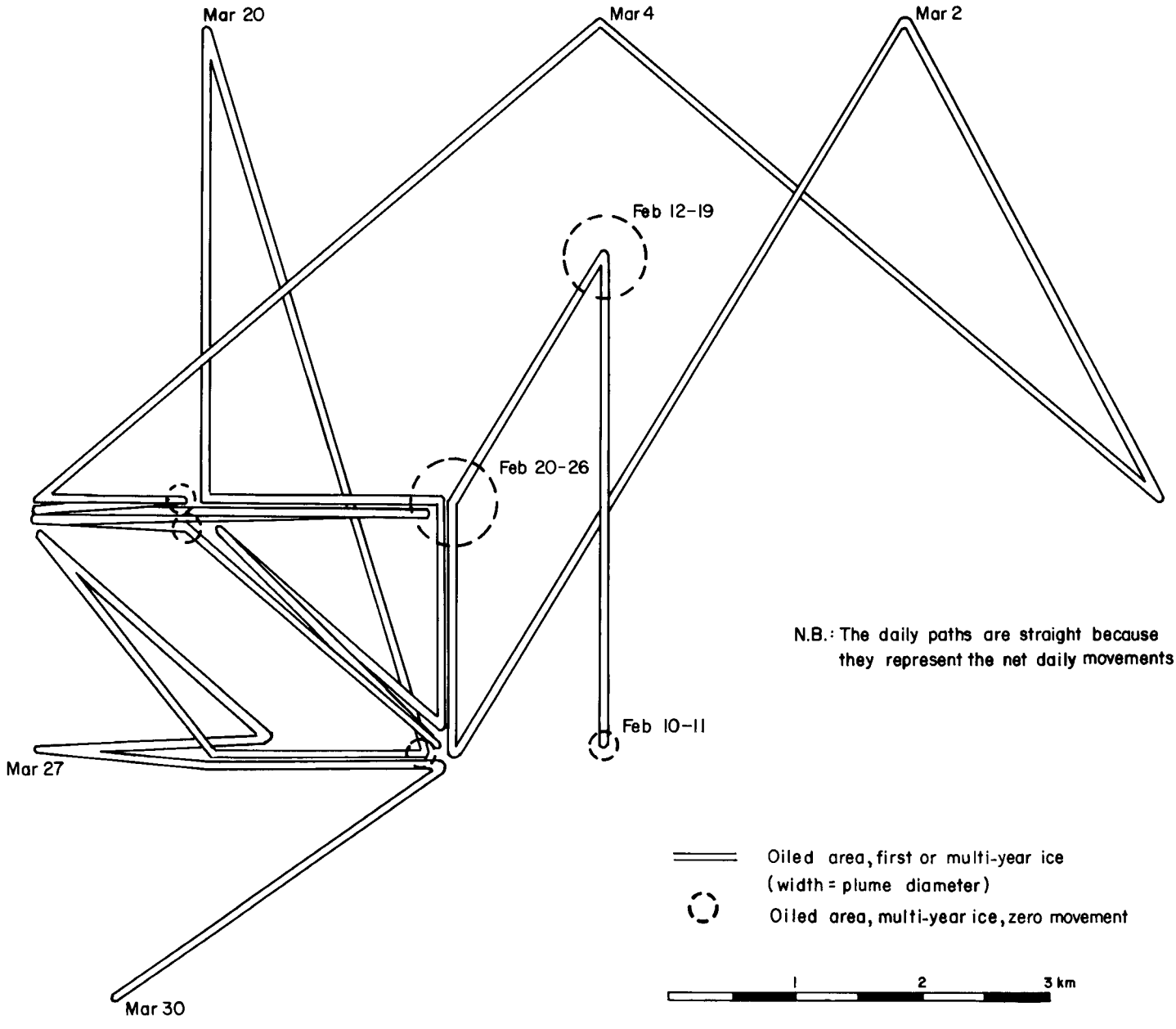

Fig. 11 VARIATION IN OIL FILM THICKNESS ALONG A TYPICAL ICE DRIFT TRACK

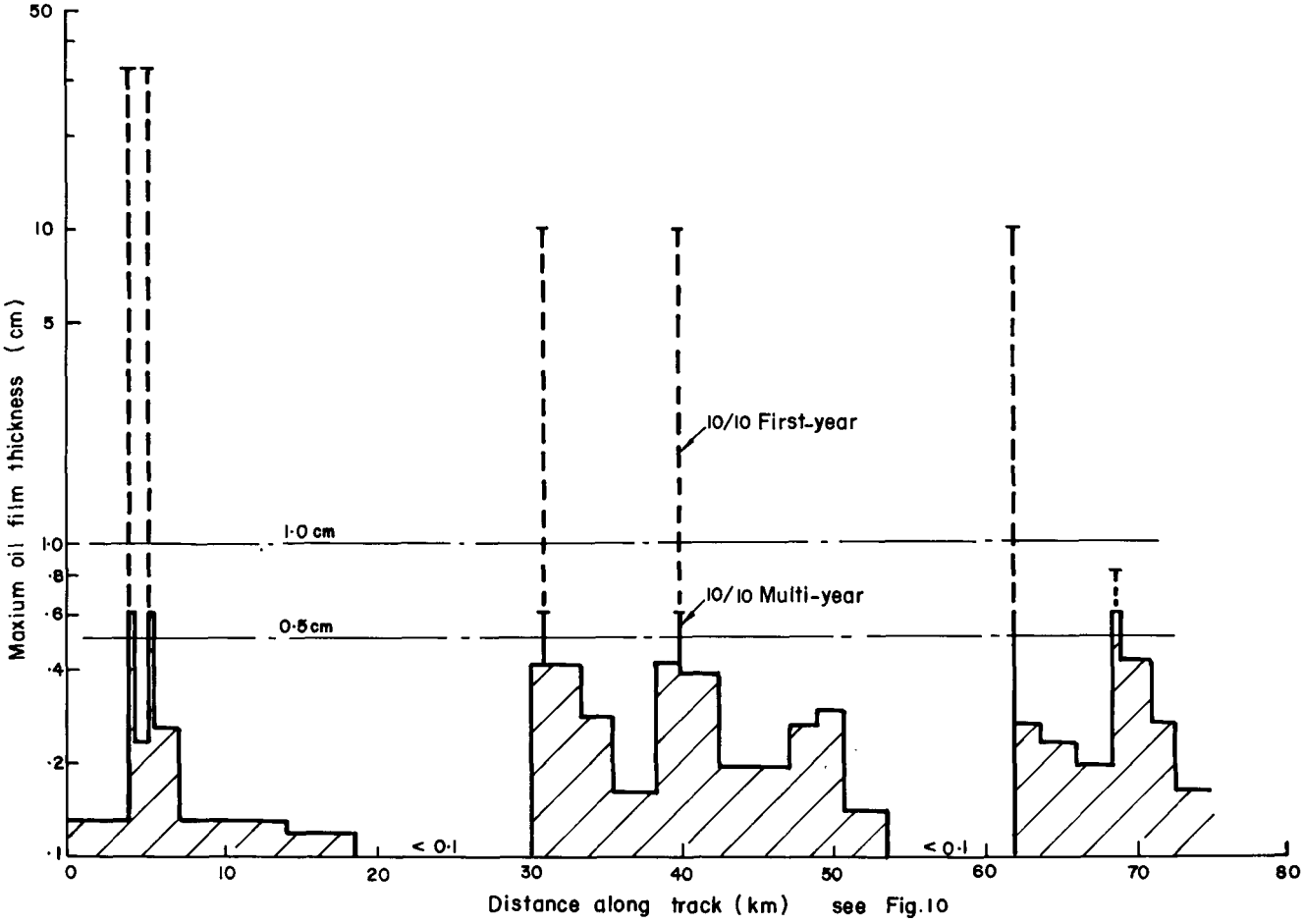

Fig. 12 PERCENT of OIL PRESENT in FILMS GREATER THAN GIVEN THICKNESS

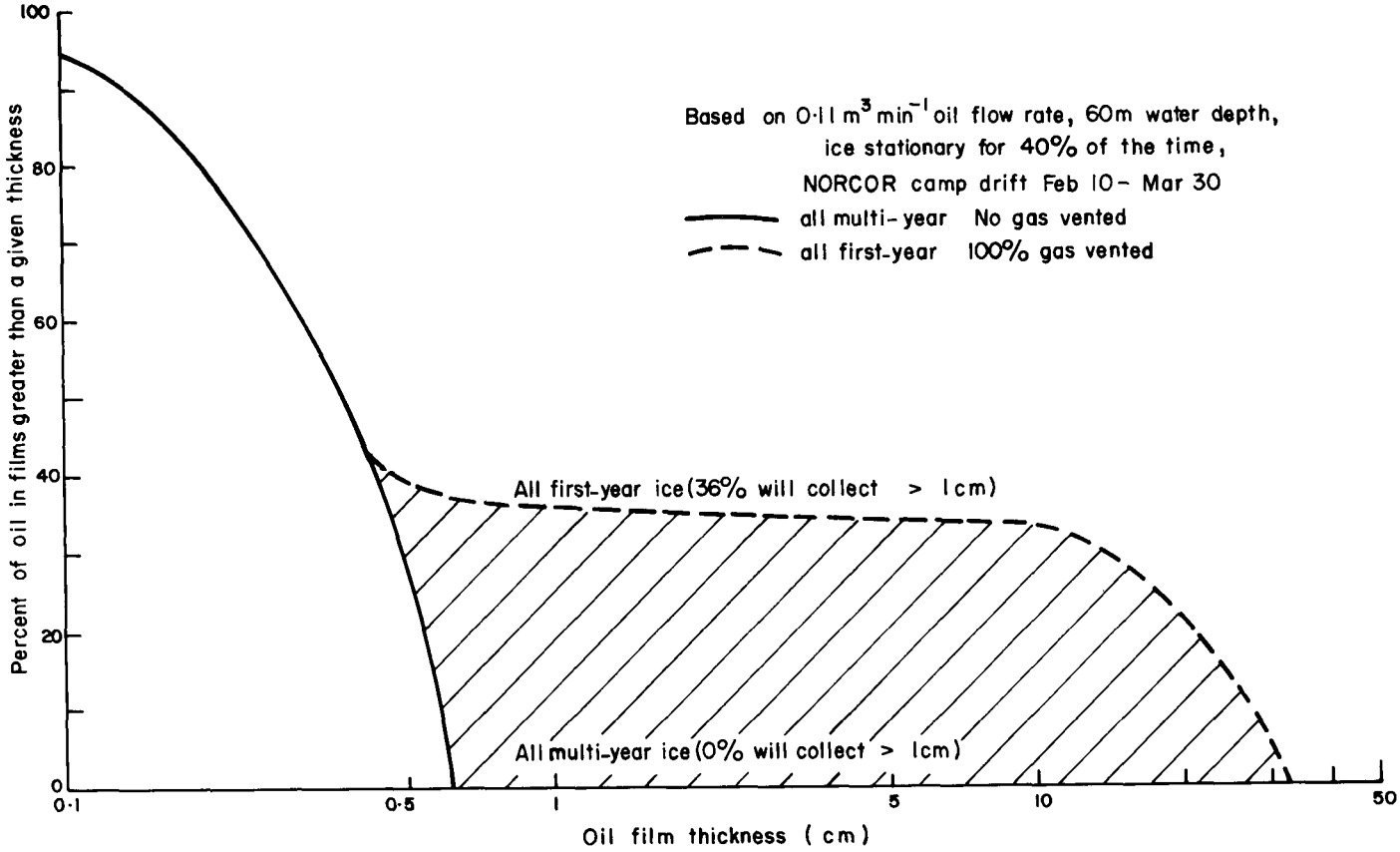

Figure 13 shows a drawing of 5/10 multi-year floes with refozen leads and ridges superimposed to make a graphic representation of mean ice conditions as observed in the March 6 overflight (Table 1). A typical 4-day drift track with corresponding contamination areas has been laid over this mean ice schematic. Two days of stationary ice movement have been included.

5 SPRING AND SUMMER OIL DISTRIBUTION

The final contaminated track prior to breakup in June can only be estimated by extrapolating winter ice movements measured in the transition zone into May, with suitable changes in ice velocity and increasing net westerly drift confirmed by the AIDJEX buoys. On this basis the oiled ice may easily extend several hundred kilometers west of the spill point. Depending on the variation in velocity vectors, the total distance contaminated may be several times greater.

As the ice velocity increases in April and May, the probability of having long stationary periods with thick oil films will become less. Figure 12 can be applied to the entire winter period by reducing the amount of stationary time. A typical ice type mix of 7/10 first-year and 3/10 multi-year will be used here. With these conditions only about 20% of the total oil volume spilled between October 1 and June 1 will be under the ice in films greater than 1 cm.

Detailed field studies conducted at Balaena Bay, Parry Peninsula (NORCOR 1975), found that oil discharged under first-year ice between October and April began to appear on the surface on May 9. By June 3 an estimated 50% of the oil had appeared in pools on the ice surface.

Fig. 13 SCHEMATIC OF OILED TRACK
IN A TYPICAL MIXTURE OF ICE CONDITIONS

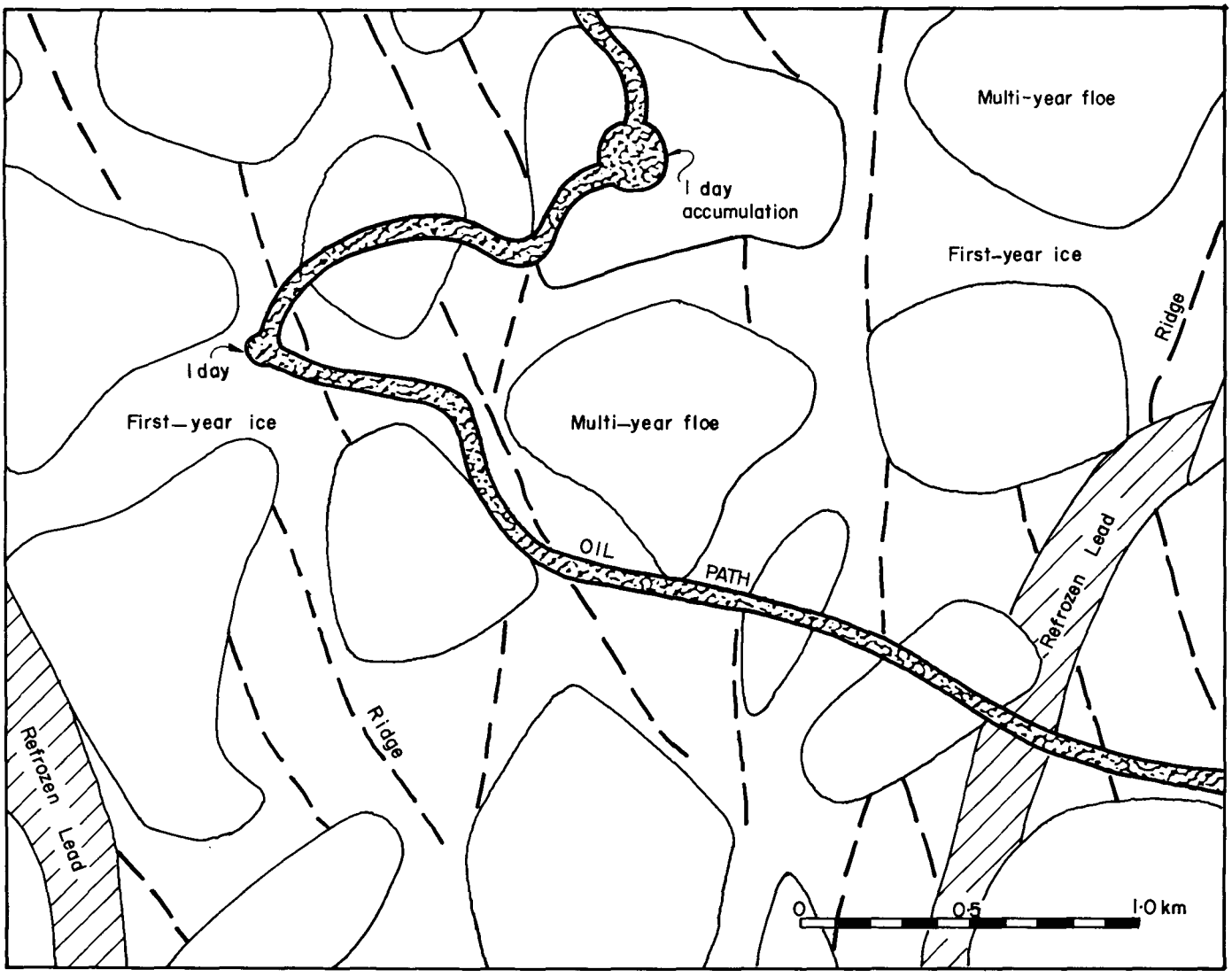

(Floe sizes, Ridges, and Refrozen Leads based on means from Mar 6 overflight (Table I))

NOTE : This diagram is simply a pictorial presentation of measured means and does not represent a specific area

Significant weathering occurs very rapidly when the oil surfaces. For instance, Norman Wells crude at 0°C undergoes 35% evaporation in 20 days (NORCOR 1975, Figure 14). Calculating the exact time taken for the oil to reach the surface is impossible, but field observations at Balaena Bay are generally applicable to any first-year ice in the Beaufort Sea. From that experience it is estimated that close to 100% of the oil will reach the ice surface in about 40 days (ie. June 20).

By applying progressive evaporation to discrete parcels of oil as they surface, it can be calculated that by the time the ice internal structure is free of oil only 70% of the oil will remain on the surface. Thereafter, the evaporation rate reduces the oil quantity logarithmically so that by September 15 only 35-38% of the oil originally spilled under the first-year ice remains on the surface. Figure 15 shows the percentage of oil on the ice surface or open water as a function of time. A band of possible conditions has been drawn by assuming a maximum 20-day annual variation in oil migration rate (May 1 to May 20). By September 15 this uncertainty would only mean a 3% difference in the amount remaining (Curves 1, 2 in Figure 15).

Essentially nothing is known about the migration of oil in multi-year ice. Coring in the spring of 1976 by D.F.E. in Byam Martin Channel and near Resolute Bay has indicated that an adequate brine channel network may exist to allow vertical transport (A. Milne, personal communication). Core holes have been observed to fill with liquid brine in a matter of hours. In terms of salinity, temperature and thickness, multi-year ice is significantly different from first-year ice. In the very best case, oil trapped within multi-year ice will rise to the surface along the curves shown in Figure 15 for first-year ice. In the worst case, the oil may not rise at all during the first summer following the blowout.

Figure 15 can be applied to a realistic average winter transition zone ice mix of 3/10 multi-year and 7/10 first-year. Using the two extremes of oil migration discussed above for this ice condition, a minimum of 38% and a maximum of 57% of the total winter oil discharge still present on September 15 is yielded. By this date the original contaminated track described for May will probably not exist. The oil will have moved with individual floes in a largely unpredicatble manner. Much of the oil originally discharged under first-year ice will have entered the water as the thinner floes break up and melt completely. Oil slicks will then continue to evaporate and recontaminate otherwise clean pieces of drifting ice.

With wind and wave action a substantial amount of emulsification may take place during the summer. However, large quantities of oil may not submerge. At Balaena Bay even the most severely burned residue still floated.

It appears that large amounts of oil would contact the shoreline only with strong NW winds moving the contaminated ice onshore after the breakup of the landfast ice. In an average year this landfast ice would act as a protective barrier to shore fouling by oil as late as July 5. By that date between 25 and 50% of the oil could have already evaporated (Figure 15). In the Beaufort Sea, for the period July through September, the wind is in the NW-NE quadrant for 45% of the time. However, any realistic model of possible oil-shore interception would be necessarily very complex. Such variables as percentage frequency of favourable wind directions for different speed classes, and mean duration of winds in those categories, would have to be applied to floes and slicks on water, taking into account the different

Fig. 14 EVAPORATION vs TIME
NORMAN WELLS CRUDE OIL

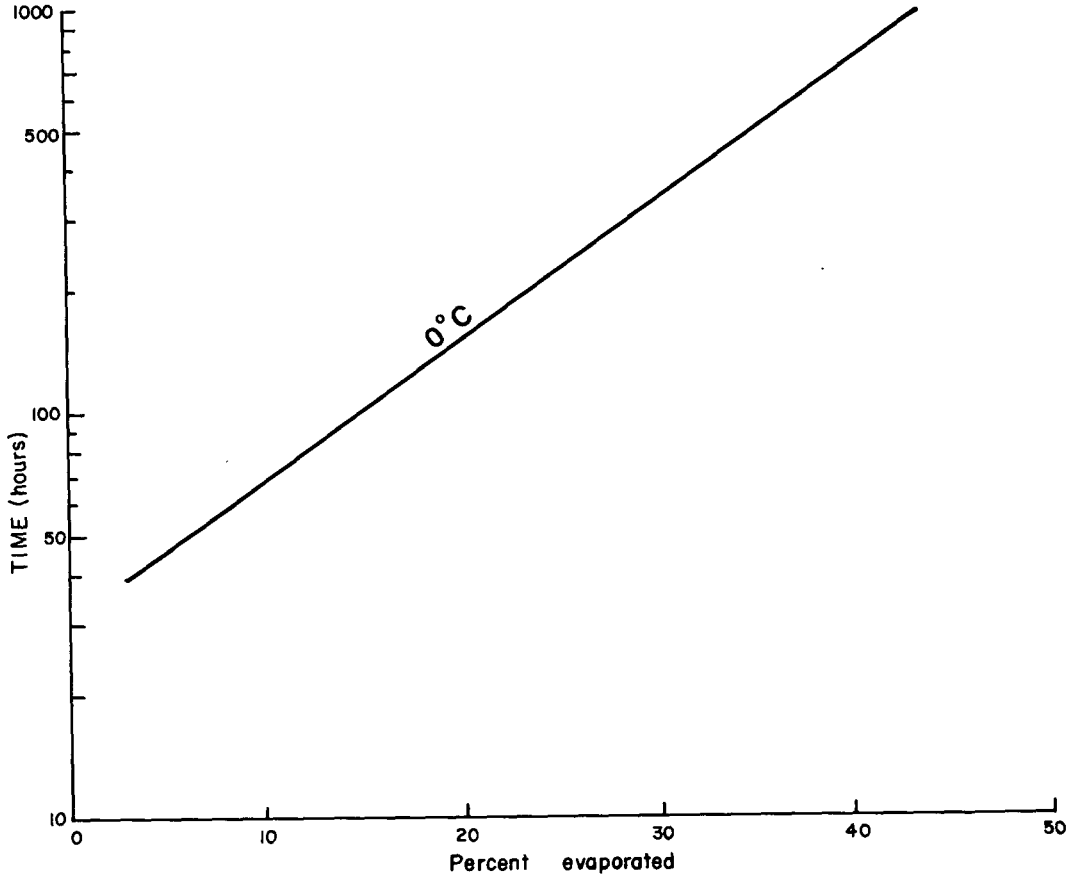

Fig. 15 PERCENTAGE OF OIL REMAINING
AS A FUNCTION OF TIME

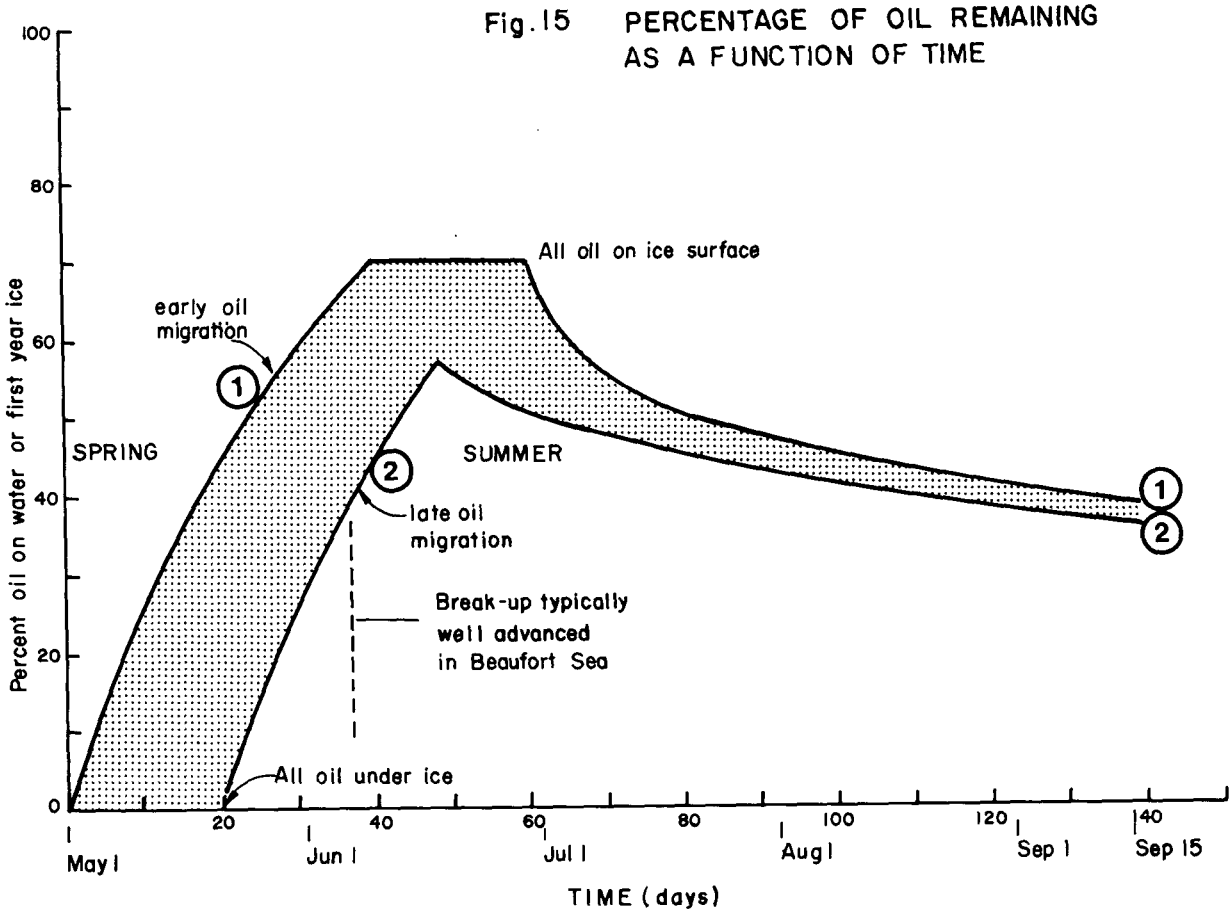

distances from various shore points along the contaminated track. Even if such an analysis is possible, it is beyond the scope of this report. Certainly some oil will reach shore. It is hard to imagine all the floes blown onto shore remaining to discharge oil. Even if half the oil on water and half of the floes contacted and adhered to shore, this would amount to no more than 15% of the total winter oil volume.

TABLE 6 ESTIMATES OF THE FATE OF OIL FROM A WINTER BLOWOUT

Location	Initial volume %	Disposed % (E) Evaporation (B) Burning	Final volume % September 15 (nearest 10%)
Trapped within or on surface of multi-year floes	30%	0 - 20% (E)	10 - 30
On surface of remaining first-year floes (1/2 assumed melted)	35%	7 1/2% (B) 16 1/2 (E)	11
In the water or on shore	35%	7 1/2 (B) 16 1/2 (E)	11
TOTALS	100%	15% (B) 33 - 53% (E) 48 - 68% (B,E)	30 - 50%

By the end of September any oil remaining on the ice from the previous winter will begin to be covered by snow. Oil still on the water will be incorporated into new ice as it forms.

A similar migration-evaporation process will occur during the next summer, but on a smaller scale. Much of the light ends will have already evaporated, and nothing is known about weathered oil migration through ice.

Although our simple model easily "disposes" of over 40% of the oil in the first summer, the remainder will be much more difficult to eliminate. Being weathered, it will resist burning and evaporate relatively slowly. Possibly over 30% of the oil will be present in visible forms for at least two years.

6 CONCLUSIONS

Beaufort Sea Reports 27 and 31 provided considerable insight into the possible physical behaviour of oil under ice and on the surface. Here that understanding has been combined with field observations, satellite analysis and overflights to provide a basis for predicting the interaction of oil and ice during the winter and spring. The data base is still very small, but this study represents an attempt to best utilize all available relevant information.

Velocity and distance probability distributions were developed from daily ice movement data spanning the period November 16, 1975 to March 30, 1976. These statistical values enabled quantitative calculations of a variety of contamination parameters. AIDJEX buoy movements in the polar pack were analyzed from January to August 1976. These results confirmed the general validity of measured movements in the transition zone and provided a basis for predicting the order of magnitude of spring movements in the area of interest. The concept of describing the natural ice thickness variation as a function of time was used, together with knowledge of ice movement, plume dynamics, and realistic blowout flow parameters, to evaluate typical blowout cases at 100 and 160 days after freeze-up (January and March respectively).

For a worst case flow rate of 5,000 barrels per day in 20 m of water, the mean oil film thickness was found to be 0.6 cm. With more representative long-term flow rates of 1,000 barrels per day and water depths of 60 m, the mean oil film thickness decreased to 0.1 cm. A figure of 0.5 cm is generally considered the minimum necessary for efficient in-situ burning at the current state of the art. When it is realized that between 70% and 80% of the total oil volume could be contained in films less than 0.5 cm, the enormity of the cleanup problem is readily apparent. In practice, the ice appears to remain stationary for as much as 30% of the time. With this magnitude of zero movement along a typical ice movement track, between zero and 30% of the total oil volume spilled could be present in thick films (greater than 0.5 cm; 100% to 0% multi-year ice). For example, the presence of 3/10 multi-year ice would result in about 20% oil by volume in thick films. When this oil surfaces in the spring, evaporation would further reduce the thick films significance to about 13% of the total oil discharged (October to May at "standard" flow rates).

It should be noted that as ice passes over the blowout plume some oil will likely rise through fractures and become mixed with snow on the ice surface. This relatively small fraction of the total will likely be weathered too much for burning by the time spring cleanup operations commence.

At the end of the winter the contaminated area could stretch several hundred kilometers from the blowout site in a meandering and broken path less than 100 m wide. Nothing is known about the behaviour of crude oil in multi-year ice. The extremes could be represented by:

1. Best Case - all oil surfaces in multi-year ice as rapidly as in first-year ice.

2. Worst Case - no oil surfaces in multi-year ice in the first summer (the maximum time might be the multi-year ice depletion rate: 4-11 years).

Using these criteria, field observations of oil migration in first-year ice, and measured curves of crude oil evaporation with time, an estimate can be made of the quantity of oil remaining from a winter oil spill by the end of the summer. According to the model used here, by September 15 between 30 and 50% of the oil will have evaporated between the time of the oil's initial appearance on the ice surface (about May 10) and freeze-up (about October 1). The remaining oil will still be on the ice surface in a weathered state in the water, still trapped within multi-year floes or on shore. About 15% of the oil might be burned.

With such a small information base it has been necessary throughout this report to use a number of crucial assumptions. In each case where these choices could have severely influenced the contamination calculations, a solution was worked out for two extremes (eg. per cent venting, per cent multi-year ice). The resulting range of possible winter oil volumes remaining at the end of a summer represents a combination of several extreme cases.

Several major conclusions can be made regarding the probable behaviour and fate of a winter oil spill in the Beaufort Sea. Evaporation in the first summer will likely be extremely effective in quickly reducing the volume of contaminant (by up to 50%) and the level of toxicity. Unless ice in the spill area is stationary for more than a third of the time, less than 20% of the oil will form films greater than 0.5 cm on the ice surface in the spring. With evaporation and varying amounts of multi-year ice the final volume in thick films will likely be even less. Therefore, possibilities for any significant cleanup using conventional burning techniques appear extremely limited.

During the following summer opportunities for effective cleanup would be even less with weathered, thin films spread over a large area.

In spite of these rather grim conclusions, the end result even without human intervention would be a very small oil loading/km^2 expressed in terms of the Beaufort Sea area. If burning techniques could be developed to cope with thin films, then the impact could be reduced further. Further studies will hopefully allow a safe estimate which could be made of oil spillage to be tolerated in the Beaufort Sea.

REFERENCES

AYERS, R.C., JOHNS, H.D., and GLAESER, J.L. November 1974: Oil Spills in the Arctic Ocean - Extent of Spreading and Possibility of Large-Scale Thermal Effects. Letter in Science Vol. 186, pp 843-4, with a reply by CAMPBELL, W.J. and MARTIN, S. on following pages.

BROWN, W.P.: Personal Communication. Polar Research Laboratory, Santa Barbara, California.

BURNS, B.M. 1974: The Climate of the Mackenzie Valley - Beaufort Sea, Vols. I & II. Environment Canada, Climatological Studies No. 24. Toronto, Ontario.

CAMPBELL, W.J. and MARTIN, S. July 1973: Oil and Ice in the Arctic Ocean: Possible Large-Scale Interactions. Vol. 181, pp 56-58 Science.

CHEN, E.C., OVERALL, J.C.K., and PHILLIPS, C.R. February 1974: Spreading of Crude Oil on an Ice Surface. The Canadian Journal of Chemical Engineering, Vol. 52, pp 71-74, Ottawa, Ontario.

EIDE, L.I. and MARTIN, S. 1974: The Formation of Brine Drainage Features in Young Sea Ice. Department of Oceanography WB-10, University of Washington, Seattle.

GLAESER, LtJg John L. and VANCE, Lcdr George P. February 1971: A Study of the Behaviour of Oil Spills in the Arctic. Project No. 714108/A/001,002, Office of Research & Development, U.S. Coast Guard, Washington, D.C.

GOLDEN, LtJg Paul C. January 1974: Oil Removal Techniques in an Arctic Environment. Vol. 8, No. 8, pp 38-43 MTS Journal.

HIBLER, W.D. III, WEEKS, W.F. and MOCK, S.J. 1972: Statistical Aspects of Sea Ice Ridge Distributions. J. Geophys. Res., 77(30), pp 5954-5970.

HIBLER, W.D. III, ACKLEY, S.F., CROWDER, W.K., MCKIM, H.L., ANDERSON, D.M. 1974a: Analysis of Shear Zone Ice Deformation in the Beaufort Sea Using Satellite Imagery. In the Coast and Shelf of the Beaufort Sea, Arctic Inst. of N. Amer., Arlington, Va. pp 285-296.

HIBLER, W.D. III, MOCK, S.J. and TUCKER, W.B. III 1974b: Classification and Variation of Sea Ice Ridging in the Western Arctic Basin. J. Geophys. Res., 79(18), pp 2735-2743.

HOULT, D.P., O'DEA, S., PATUREAU, J.P., and WOLFE, S. 1975: Oil in the Arctic Report No. CG-D-96-75, prepared for Department of Transportation, United States Coast Guard, Office of Research & Development, Washington, D.C.

KEEVIL, B.E. and RAMSEIER, R.O. 1975: Behaviour of Oil Spilled Under Floating Ice. Proc. Conf. on Prevention and Control of Oil Pollution, March 25-27, 1975, pp 497-501. San Francisco.

KETCHUM, R.D. Jr. 1971: Airborne Laser Profiling of the Arctic Pack Ice. Remote Sensing of Environment, 2, pp 41-52.

KOVACS, A. and MELLOR, M. 1974: Sea Ice Morphology and Ice as a Geologic Agent in the Southern Beaufort Sea. In the Coast and Shelf of the Beaufort Sea, Arctic Inst. of N. Amer., Arlington, Va., pp 113-161.

LEINONEN, P.J. and MACKAY, D. February 1975: A Mathematical Model of the Evaporation and Dissolution of Oil on Land, on Ice, and Under Ice, paper presented at the 11th Annual Symposium on Water Research to be published in the proceedings.

LYON, W. 1967: Under Surface Profiles of Sea Ice Observed by Submarine. In Physics of Snow and Ice, Intl. Conf. on Low Temp. Science, Institute of Low-Temperature Science, Hokkaido Univ., Sapporo, Japan, 1(1), pp 707-711.

MACKAY, A., MEDIR, M. and THORNTON, D.E. 1975: Interfacial Behaviour of Oil Under Ice. In Press. Can. J. Chem. Eng.

MACKAY, D., LEINONEN, P.J., OVERALL, J.C.K., and WOOD, B.R. March 1975: The Behaviour of Crude Oil Spilled on Snow. Journal of the Arctic Institute of North America, Vol. 28, No. 1, Montreal.

MARKO, J. 1975: Satellite Observations of the Beaufort Sea Ice Cover. Beaufort Sea Project Technical Report No. 34, Department of the Environment, Victoria, B.C.

MARTIN, P. and STATEMAN, M.: Personal Communication. Aidjex, Seattle, Washington.

MARTIN, S. 1976: A Laboratory Study of the Dispersion of Crude Oil Within Sea Ice Grown in a Wave Field. Department of Oceanography, University of Washington, Special Report 69, Seattle, Washington.

MILNE, A.R.: Personal Communication. Department of the Environment, Victoria, B.C.

MOCK, S.J., HARTWELL, A.D. and HIBLER, W.D. III 1972: Spatial Aspects of Pressure Ridge Statistics. J. Geophys. Res. 77(30), pp 5945-5953.

MOIR, J.R. and LAU, Y.L. 1975: Some Observations of Oil Slick Containment by Simulated Ice Ridge Keels. Unpubl. Report, Canada Centre for Inland Waters, Burlington, Ontario.

NORCOR Engineering and Research Limited 1975: The Interaction of Crude Oil with Arctic Sea Ice. Beaufort Sea Project Technical Report No. 27. Department of the Environment, Victoria, B.C.

NORCOR Engineering and Research Limited 1975: Contribution to Beaufort Sea H Studies Overview Report. Department of the Environment, Environmental Protection Service, Burlington, Ontario.

NORCOR Engineering and Research Limited 1975: Investigation of Techniques for the Recovery of Crude Oil from Under Solid Ice Cover, internal document for Panarctic Oils Limited.

PARAMERTER, R.R. and COON, M.D. 1973: Mechanical Models of Ridging in the Arctic Sea Ice Cover. AIDJEX Bull., 19, pp 59-112.

RAMSEIER, R.O., GANTCHEFF, G.S., and COLBY, L. 1973: Oil Spill at Deception Bay, Hudson Strait. Scientific Series No. 29, Inland Waters Directorate, Water Resources Branch, Ottawa.

ROSENEGGER, L.W. 1975: Oil-In-Ice Studies. Lab. Report L-12075, Imperial Oil Co. Ltd., Resource Production and Technical Services Laboratory, Calgary, Alberta.

SCOTT, B.F. and CHATTERJEE, R.M. 1975: Behaviour of Oil Under Canadian Climatic Conditions. Scientific Series No. 50, Inland Waters Directorate, Water Quality Branch, Ottawa.

SWITHINBANK, C.W.M. 1972: Arctic Pack Ice from Below. In Sea Ice, Proc. Intl. Sea Ice Conf., Reykjavik, Natl. Res. Council of Iceland, Reykjavik, pp 246-254.

TOPHAM, D.R. 1975: Hydrodynamics of an Oil Well Blowout. Beaufort Sea Project Technical Report No. 33. Department of the Environment, Victoria, B.C.

TOPHAM, D.R. 1976: The Deflection of an Ice Sheet by a Submerged Gas Source. Frozen Sea Research Group, Internal Report No. 36, Department of the Environment, Victoria, B.C.

WADHAMS, P. 1975: Sea Ice Morphology in the Beaufort Sea. Beaufort Sea Project Technical Report No. 36, Department of the Environment, Victoria, B.C.

WALKER, E.R. 1976: Oil, Ice and Climate in the Beaufort Sea. Beaufort Sea Project Technical Report No. 35. Department of the Environment, Victoria, B.C.

WILLIAMS, E., SWITHINBANK, C.W.M. and de Q. ROBIN, G. 1975: A Submarine Sonar Study of the Arctic Pack Ice. J. Glaciol, 15(73), pp 349-362.

APPENDIX A - ANALYTICAL & FIELD TECHNIQUES

APPENDIX A - ANALYTICAL & FIELD TECHNIQUES

Detailed Field Studies

On November 16, 1975, a 4-man camp was established on a large multi-year floe in the shear zone, approximately 50 km north of the Tuktoyaktuk Peninsula. The floe, which measured about 2 km in diameter, was surrounded by large refrozen leads which permitted the use of fixed wing aircraft. The camp was placed at the intersection of two medium-sized multi-year ridges. In early February a very large first-year ridge intersected the floe, but was deflected by the multi-year ridge and missed the camp by less than 100 m.

The sail of the ridge measured 10 m and contained blocks up to 2.5 m thick. The self-sufficient camp was manned until December 9 and again from February 10 to March 30, 1976.

In general, conditions around the camp were representative of the entire band of ice north of the Tuktoyaktuk Peninsula. During the initial phase of the field work large and erratic movements were common. New leads were continually opening and refreezing. As the ice shifted, the intensity of ridges progressively increased. At all times open water could be located within 10 km of the camp. During February and March conditions tended to stabilize. With the exception of small cracks, which quickly refroze, open water was essentially limited to the lead along the outer edge of the landfast ice. Due to the increased ice thickness, ridging occurred less frequently, but was more severe.

Surface weather was measured on a daily basis.

At prescribed depths at the base camp and stations in the landfast ice and polar pack, the following oceanographic parameters were measured:

- ice thickness;
- water temperature;
- conductivity;
- salinity;
- transmissivity;
- water depth.

Water samples were also taken for biological and water quality studies.

Initially, a GNS 500 navigational system was installed in the helicopter to determine the position of the camp and high-frequency beacons placed on the ice. However, the system had difficulty stabilizing due to the cold air temperatures. With the camp continuously drifting, the system had to be set up daily at a known benchmark on the shore. This was not always possible due to white-out conditions and fog. Consequently, the GNS 500 was removed and the position determined by means of a range and bearing from the DEW Line Station BAR 4 at Nicholson Peninsula. With repeated points, a position could be determined to within 1.0 km. A high-powered radar transponder was installed at the camp, but it was impossible to obtain sufficient altitude for radar positioning.

Overflights

Two types of overflights were undertaken. In the immediate vicinity of the camp, transects were flown at regular intervals from the edge of the landfast ice to the permanent polar pack. To determine the relative movement across the transition zone, two strings of high-frequency beacons were installed in parallel lines running roughly perpendicular to the shoreline. On each overflight continuous video coverage was maintained between the beacons and their position determined by means of a range and bearing to the DEW Line Station BAR 4 at Nicholson Peninsula. A Bell 206 helicopter was used for these overflights to permit detailed oceanographic studies at selected stations.

A Cessna 402 was used for six aerial reconnaissance flights along the length of the transition zone between January 20 and July 14, 1976. The flights were designed to provide an extrapolation to the detailed studies, while also filling gaps in the 1976 LANDSAT coverage. Video and still photographic coverage was maintained along the entire track. The tapes were subsequently analyzed to obtain statistical data on ice concentration and types, the frequency and orientation of leads and cracks, and the size and frequency of ridges. Following breakup, the landfast ice edge and polar pack southern perimeter were mapped, and the data evaluated in terms of ridges, per cent open water, and mean floe size.

Satellite Imagery

Two types of imagery were employed in the analysis: LANDSAT (formerly known as ERTS) and NOAA. The characteristics of these images are summarized in the following:

	LANDSAT	NOAA
Scale	1:1,000,000	≃ 1:12,235,000 (horiz.)
Resolution	86 m x 86 m	800 m x 800 m
Scaling Error (corrected)	10 km	N/A
Frequency	Visible	Infrared (winter) Visible (summer)
Cycle (days)	9	.5
Overlap (at 70°N)	x3	
Period of Operation	Mar. – Oct.	All year

The NOAA imagery is particularly useful to delineate general ice and lead patterns throughout the Beaufort and Chukchee Seas. Because the imagery is available in infrared, coverage can be maintained year round. However, the large-scale and realtively poor resolution limits its effectiveness for detailed studies.

The LANDSAT-1 imagery is available from July 26, 1972 and LANDSAT-2 imagery from April 9, 1975. Each satellite has a period of 18 days, but they are positioned in such a manner as to provide coverage every ninth day.

There is sufficient overlap of the tracks over the Beaufort Sea that a given point is covered on three successive days. The principal limitation with LANDSAT is that coverage is terminated from late October to early March due to the low-light levels. As well, because the imagery is in the visible range, it is severely limited by cloud cover. The problem is particularly pronounced during freeze-up and breakup when the temperature differential between water and the ice results in almost continuous ground fog.

Frames 9, 10, and 11 on tracks 65 through 73 were used. This selection provided coverage from the shoreline to latitude 72°N and from longitudes 126°W to 139°W. In analysing the LANDSAT imagery each frame was divided into 21 subsections, such that the areas covered by adjacent frames were repeatable and unique. As a result, it was possible to trace the change in conditions for a specific area over three successive days. The centre of each subsection is shown in Figure B1 of Appendix B. Only frames with less than 60% cloud cover were used.

Due to heavy cloud cover much of the 1976 LANDSAT imagery of the Beaufort Sea is of limited value. However, on June 12 and 13 conditions allowed a direct comparison to be made between three different data sources, overflights (scale 1 mm = 15 m), LANDSAT (scale 1 mm = 1 km) and NOAA (1 mm = 12 km) over a 20-hour period. A number of other significant NOAA images are available for the period March 8 to June 18.

APPENDIX B - ICE CONDITIONS 1974 - 1976

APPENDIX B - ICE CONDITIONS 1974, 1975

On March 10, 1975, narrow shore leads were evident along the west side of Banks Island and across Mackenzie Bay from Herschel Island to north of Atkinson Point. Due to cloud cover, it was impossible to determine if the two leads were connected. The ice concentration north and west of the leads in the permanent polar pack was 9/10 to 10/10. The band of landfast ice was intact. By late April (Figure B3) a single lead ran from the west side of Banks Island across the Amundsen Gulf and along the Tuktoyaktuk Peninsula. The lead edge ranged between 20 and 40 km from shore, except near Bathurst Peninsula where it came within several kilometers of Baillie Island. The lead was approximately 12 km wide in the Amundsen Gulf and the concentration of ice on the west side had fallen to between 6/10 and 8/10. By early May the lead had widened and moved closer to the shore along the Tuktoyaktuk Peninsula. Across the mouth of Amundsen Gulf the lead was close to 100 km wide. By late May (Figure B6) there was open water from Baillie Island to Cape Kellet. Through Amundsen Gulf the lead was 150 km wide, but decreased to between 20 and 30 km along the west side of Banks Island and the Tuktoyaktuk Peninsula. The clearing of ice from the mouth of Amundsen Gulf is due to the westward drift of the pack. By late June the pack had receded and the entire offshore area was free of ice, with the exception of a number of large floes that had broken free in the mouth of the Gulf. The landfast ice was intact with only a small passage on the west side of the Mackenzie Delta, and clearings at the mouth of the Horton River and near Sachs Harbour. By July 12 the permanent polar pack was north of latitude 72°N and the entire southern Beaufort Sea was free of ice.

During the first half of August the pack had advanced to about 71°N (Figure B9). Along the southern edge of the pack there was a band of ice (1/10 to 3/10) varying in width from 20 to 50 km. By late September the pack was tight against Banks Island. A tongue of 6/10 ice extended into the Amundsen Gulf. By October 12 a band of fast ice had developed along the shore and the pack was less than 100 km off the Tuktoyaktuk Peninsula. In Mackenzie Bay the shore lead was about 30 km wide, but terminated near Shingle Point.

Due to the limited data, it is difficult to produce meaningful statistics for either the average or extreme conditions. However, the general pattern of breakup and freeze-up in 1975 was reasonably typical for the southern Beaufort Sea. In comparison, the conditons during the summer of 1974 were very severe and likely close to an extreme year.

The ice concentrations from June to late September, 1974 are shown in Figures B12 through B17, Appendix B. By mid-June, 1974, both the polar pack and landfast zones were still solid. A very narrow lead extended from Richards Island to Cape Brown, but otherwise there was no open water. Conditions were similar to what would normally be expected in early March. One month later Liverpool Bay and a small area off Cape Kellet were free of ice (Figure B13). The pack was tight onshore and the landfast ice reasonably intact. By August 5 the landfast ice had cleared in Mackenzie Bay and along the Tuktoyaktuk Peninsula, but the pack was less than 10 km offshore. Conditions improved slightly during the latter half of August and early part of September. By September 9 the pack was 80 km off the Tuktoyaktuk Peninsula and there was a wide band of 2/10 to 4/10 ice along the inner edge. The mouth

of the Amundsen Gulf was still heavily congested. By the end of September the pack was tight against the outer islands of the Mackenzie Delta and the Tuktoyaktuk Peninsula (Figure B17). New ice was beginning to form in Liverpool Bay and other sheltered areas along the coast.

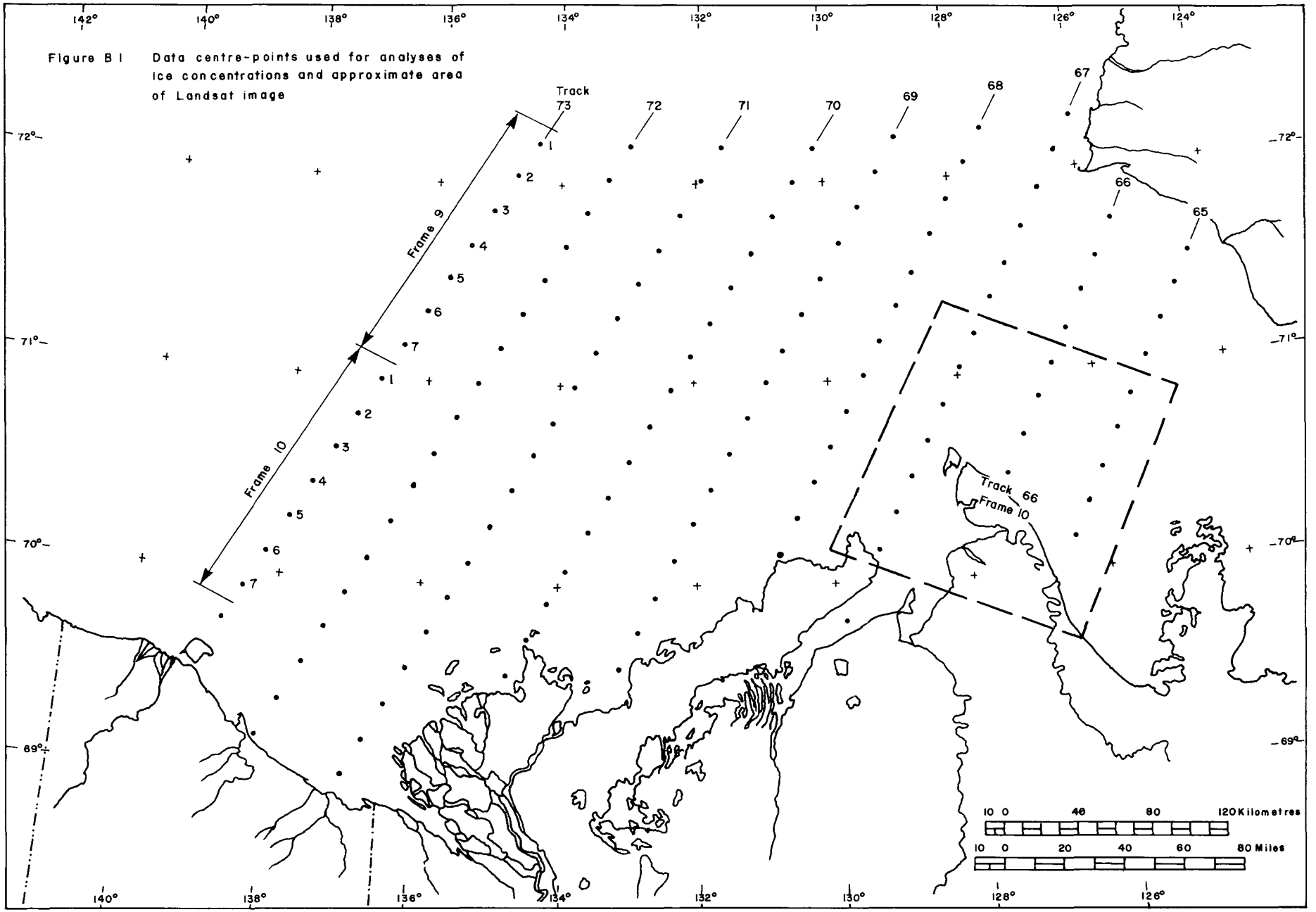

Figure B 1 Data centre-points used for analyses of ice concentrations and approximate area of Landsat image

Figure B2 ICE CONCENTRATION MAR 10 - 14 1975
(compiled from Landsat 1&2 imagery)

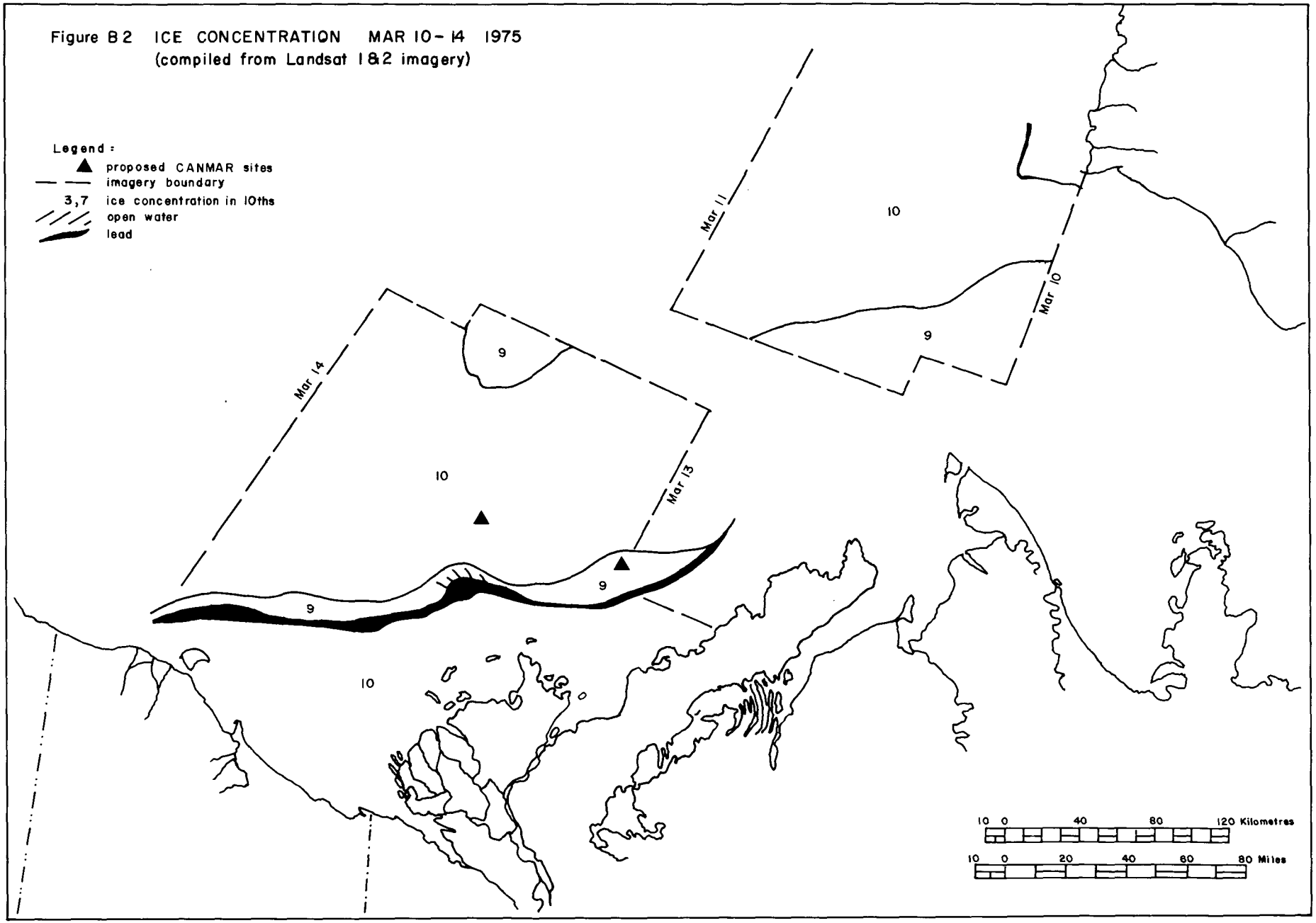

Figure B3 ICE CONCENTRATION APR 22-26 1975
(compiled from Landsat 1&2 imagery)

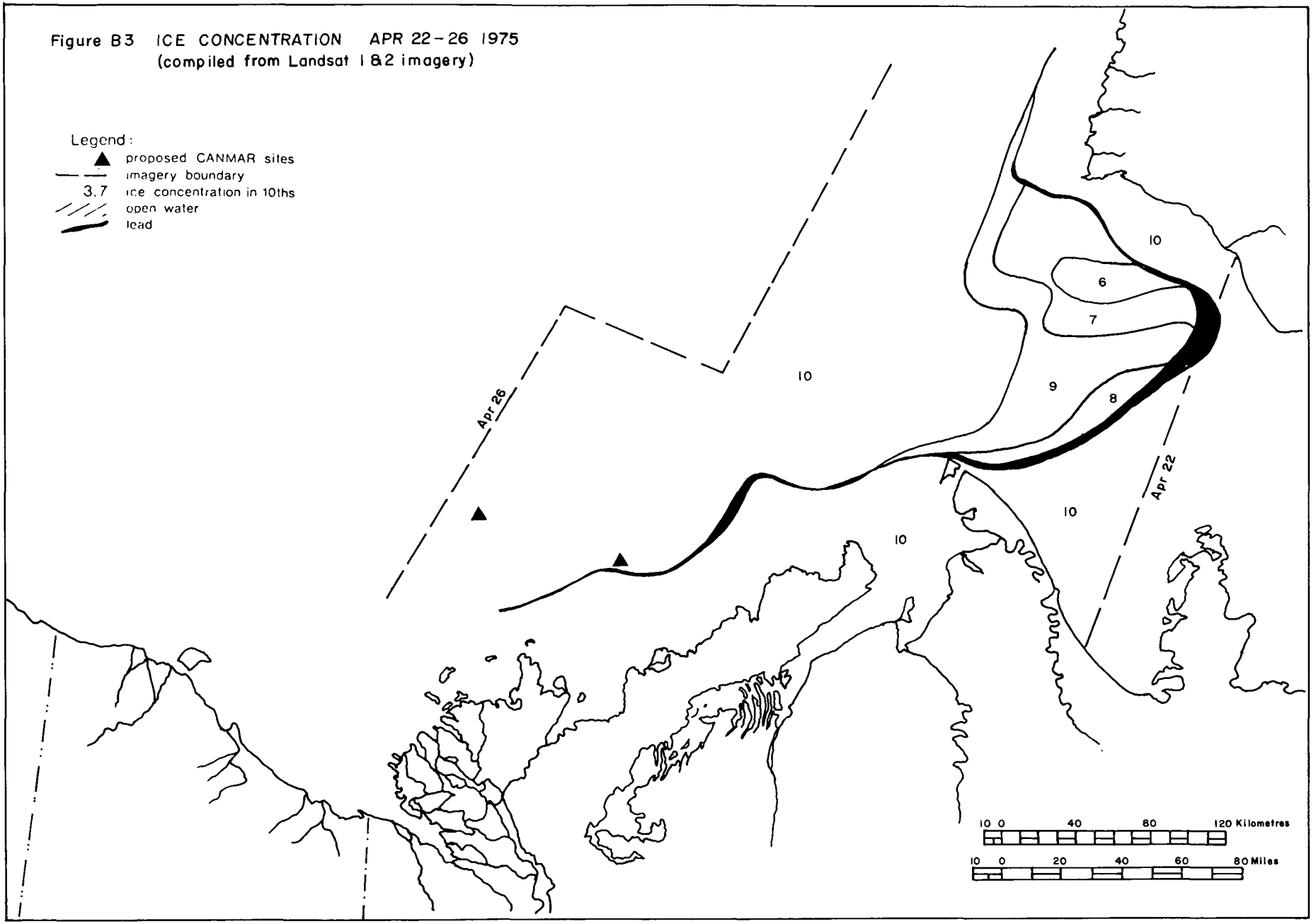

Figure B4 ICE CONCENTRATION MAY 2-5 1975
(compiled from Landsat 1 &2 imagery)

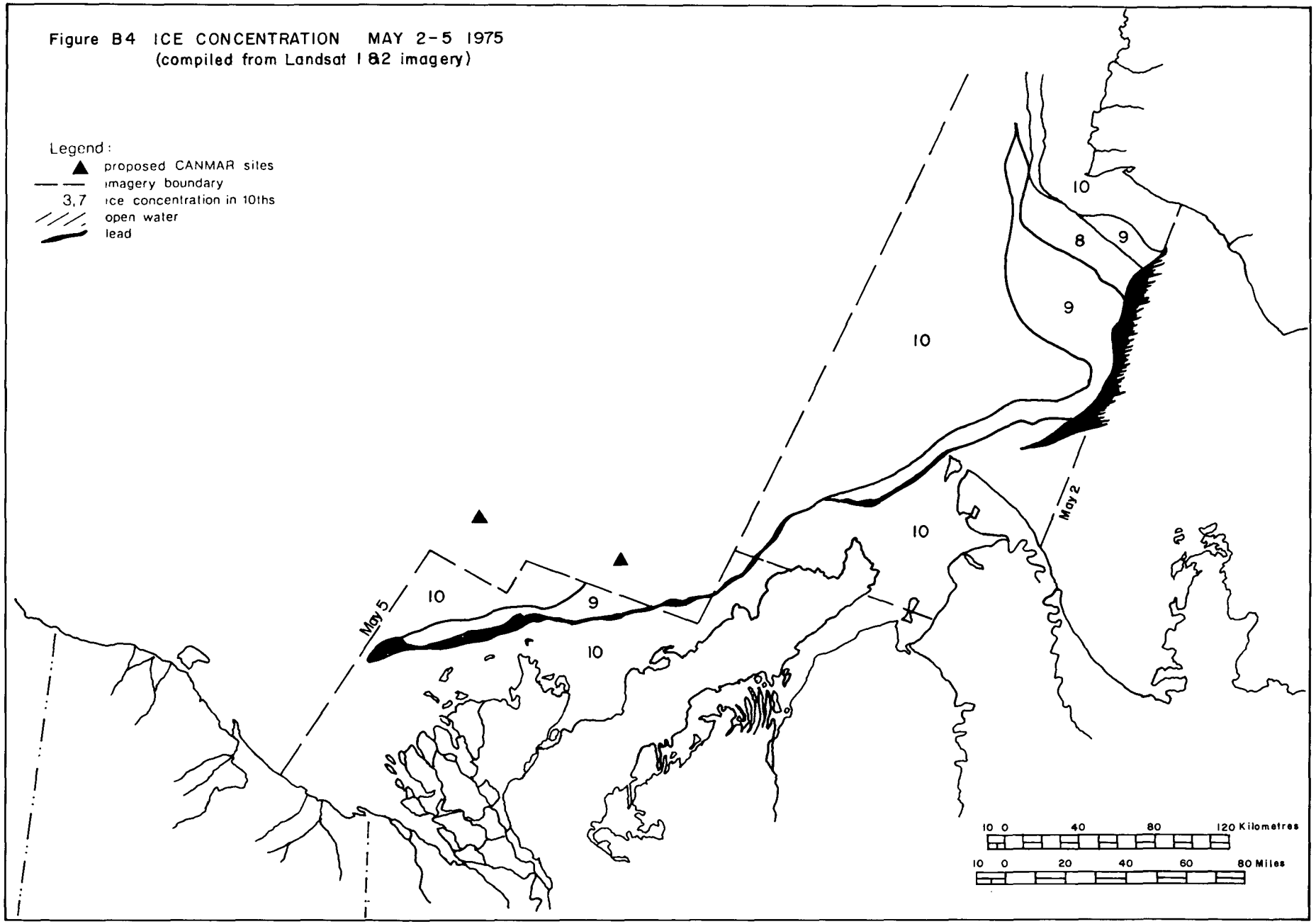

Figure B5 ICE CONCENTRATION MAY 10 1975
(compiled from Landsat 1&2 imagery)

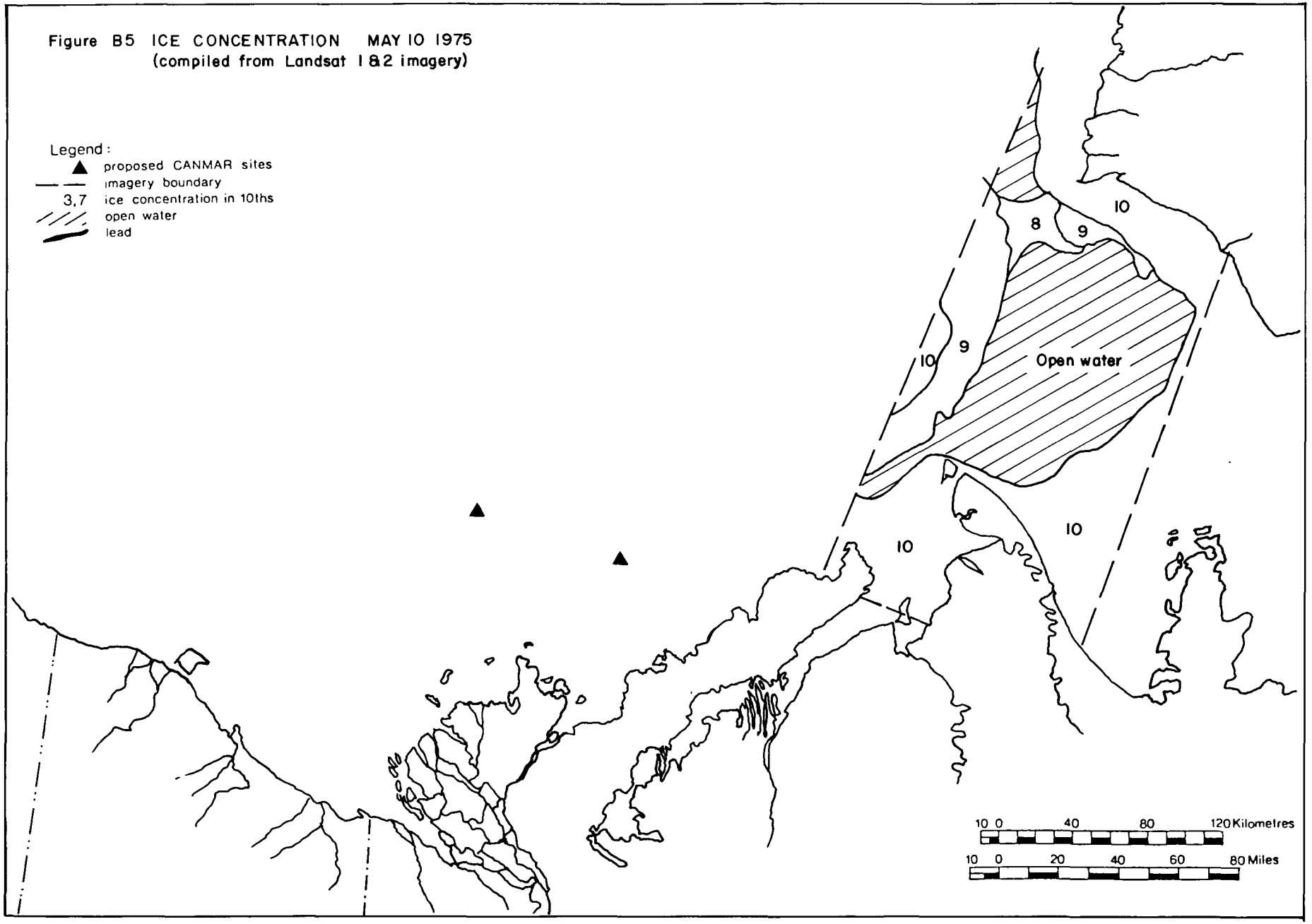

Figure B6 ICE CONCENTRATION MAY 22, 28, & 29 1975
(compiled from Landsat 1 & 2 imagery)

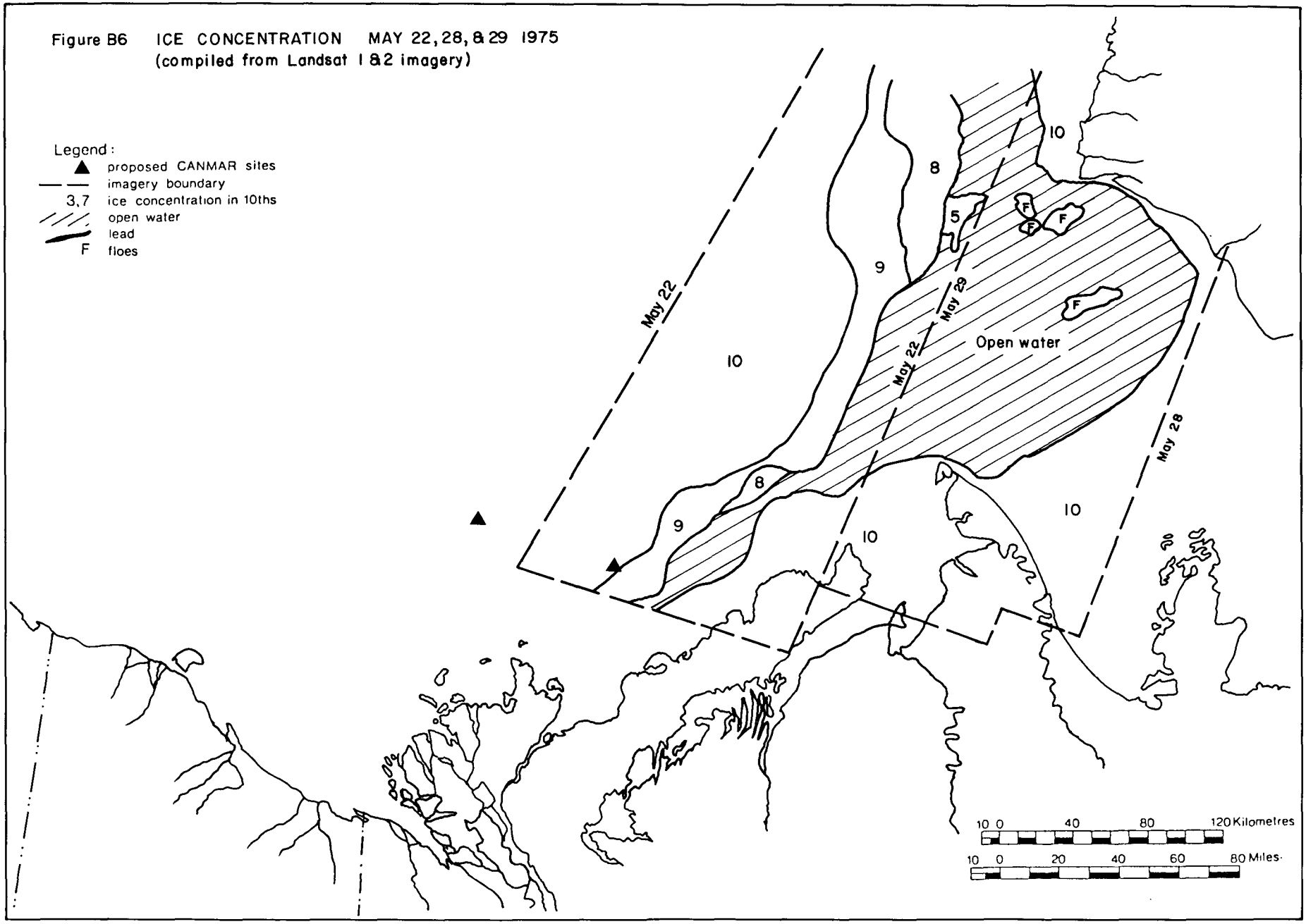

Figure B7 ICE CONCENTRATION JUNE 24 – 30 1975
(compiled from Landsat 1 & 2 imagery)

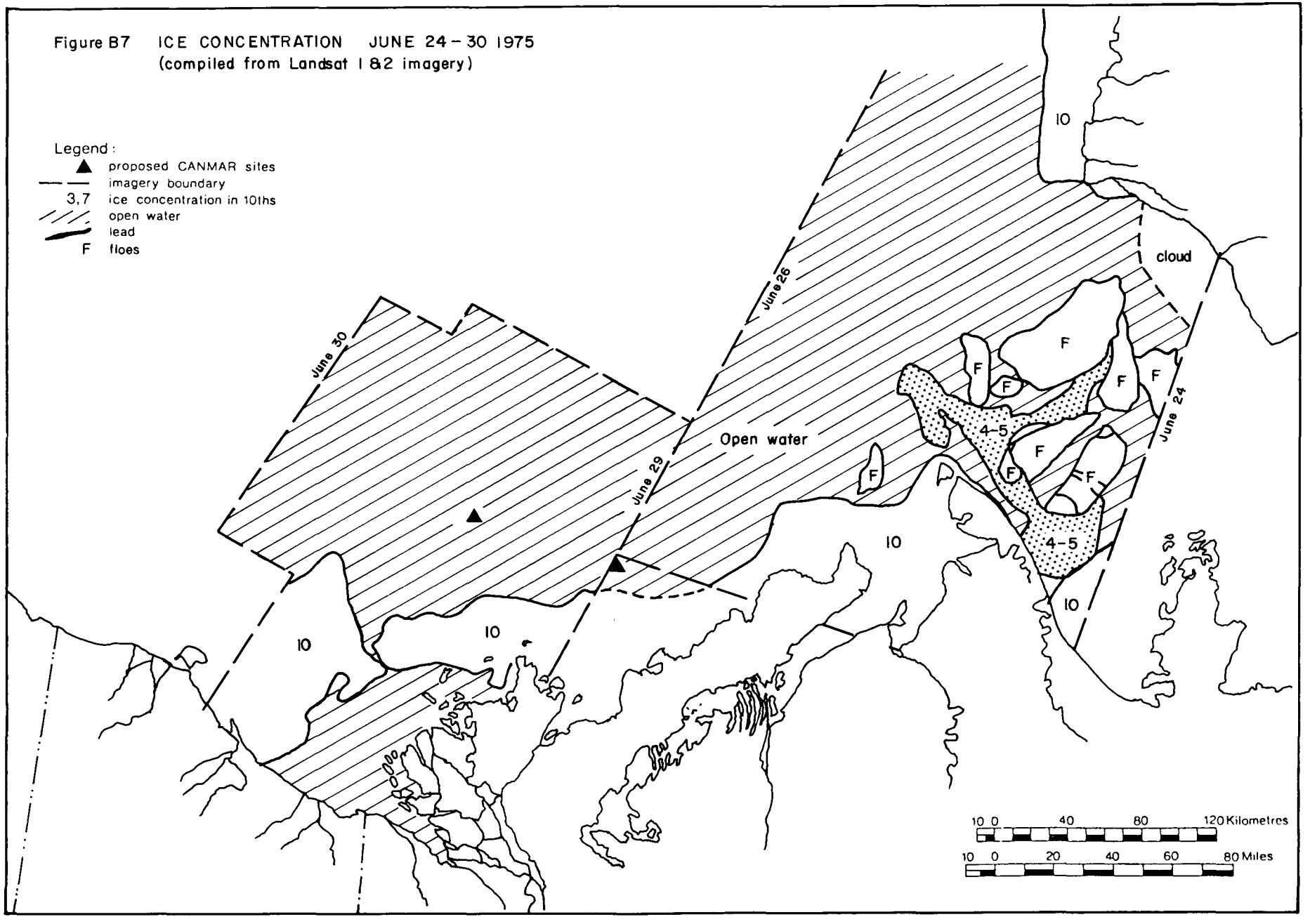

Figure B8 ICE CONCENTRATION JULY 12–18 1975
(compiled from Landsat 1&2 imagery)

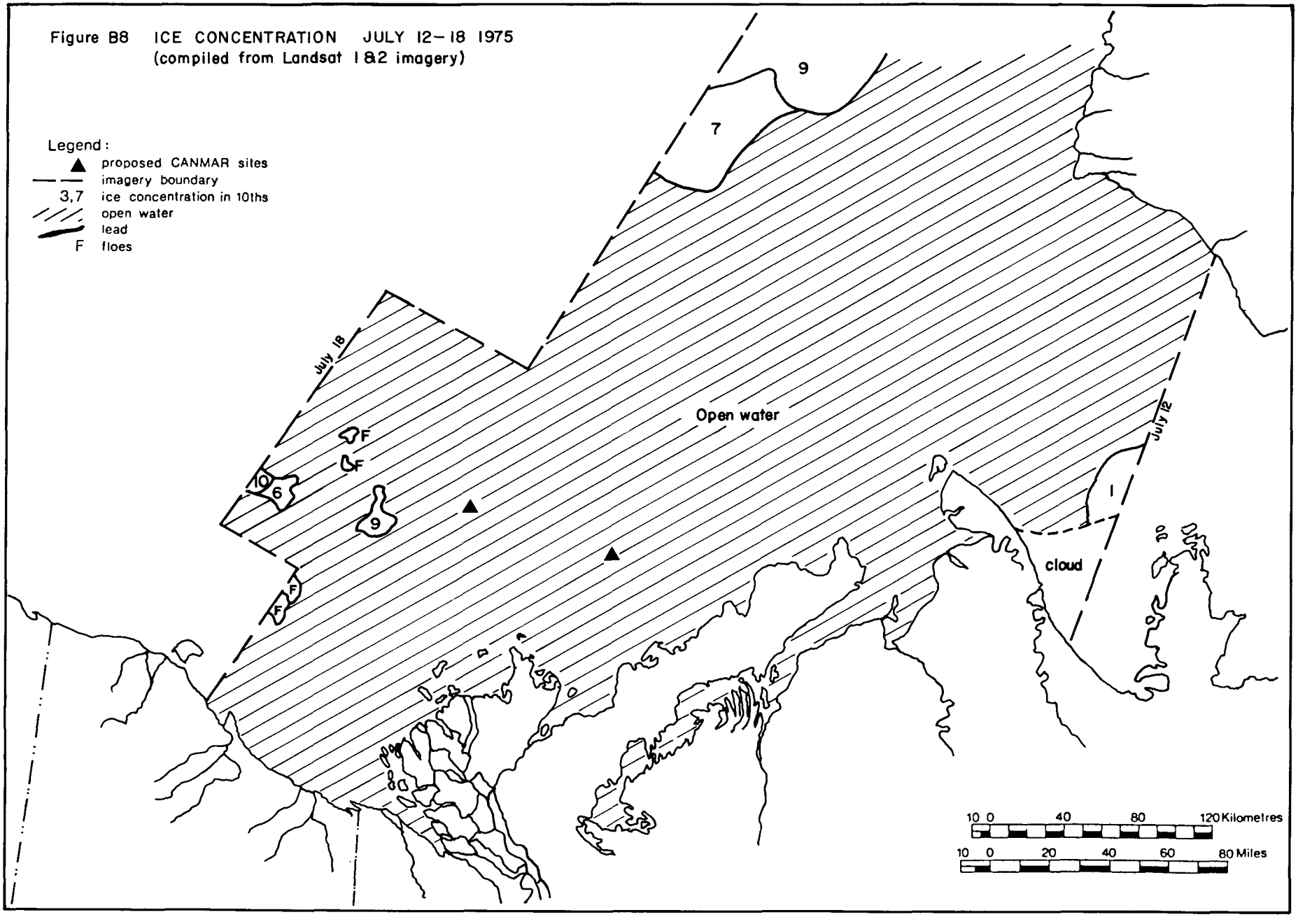

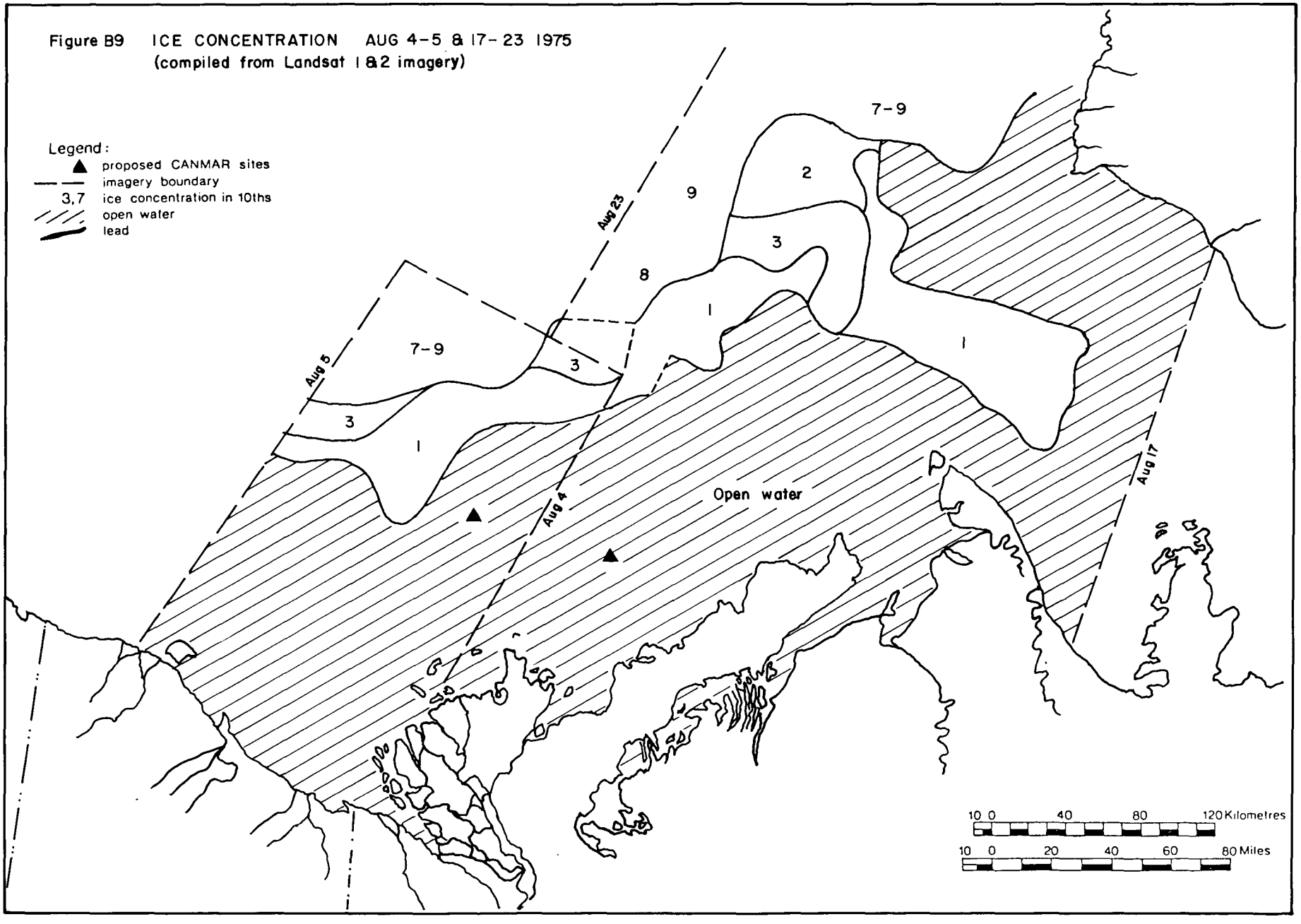
Figure B9 ICE CONCENTRATION AUG 4-5 & 17-23 1975
(compiled from Landsat 1 & 2 imagery)
Legend:
proposed CANMAR sites
imagery boundary
3,7 ice concentration in 10ths
open water
lead
7-9
2
9
3
8
1
1
7-9
3
3
1
Aug 23
Aug 5
Aug 4
Aug 17
Open water
10 0 40 80 120 Kilometres
10 0 20 40 60 80 Miles

Figure B 10 ICE CONCENTRATION SEPT 23–26 1975
(compiled from Landsat 1 &2 imagery)

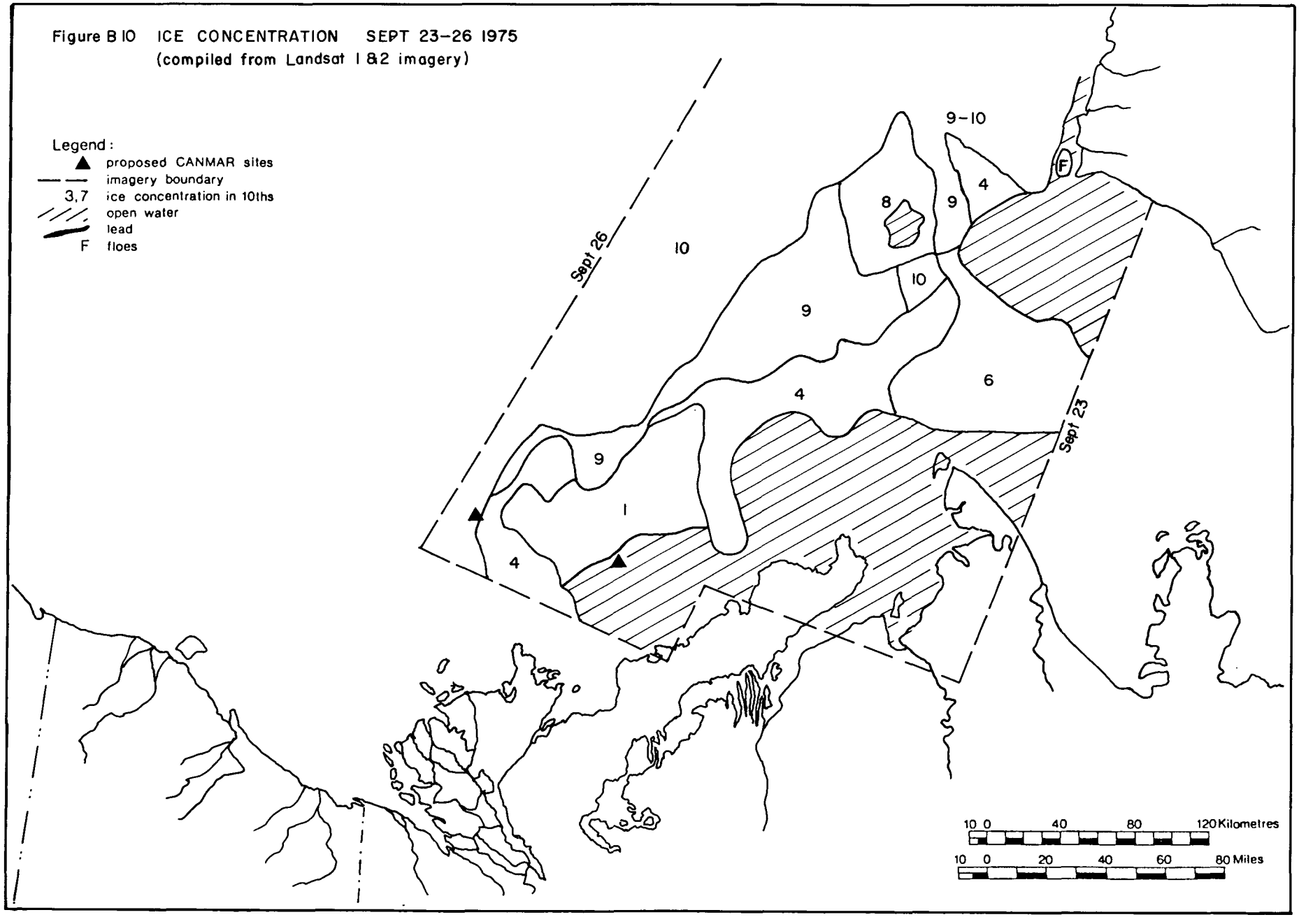

Figure B11 ICE CONCENTRATION OCT 2, 7, & 12 1975
(compiled from Landsat 1 & 2 imagery)

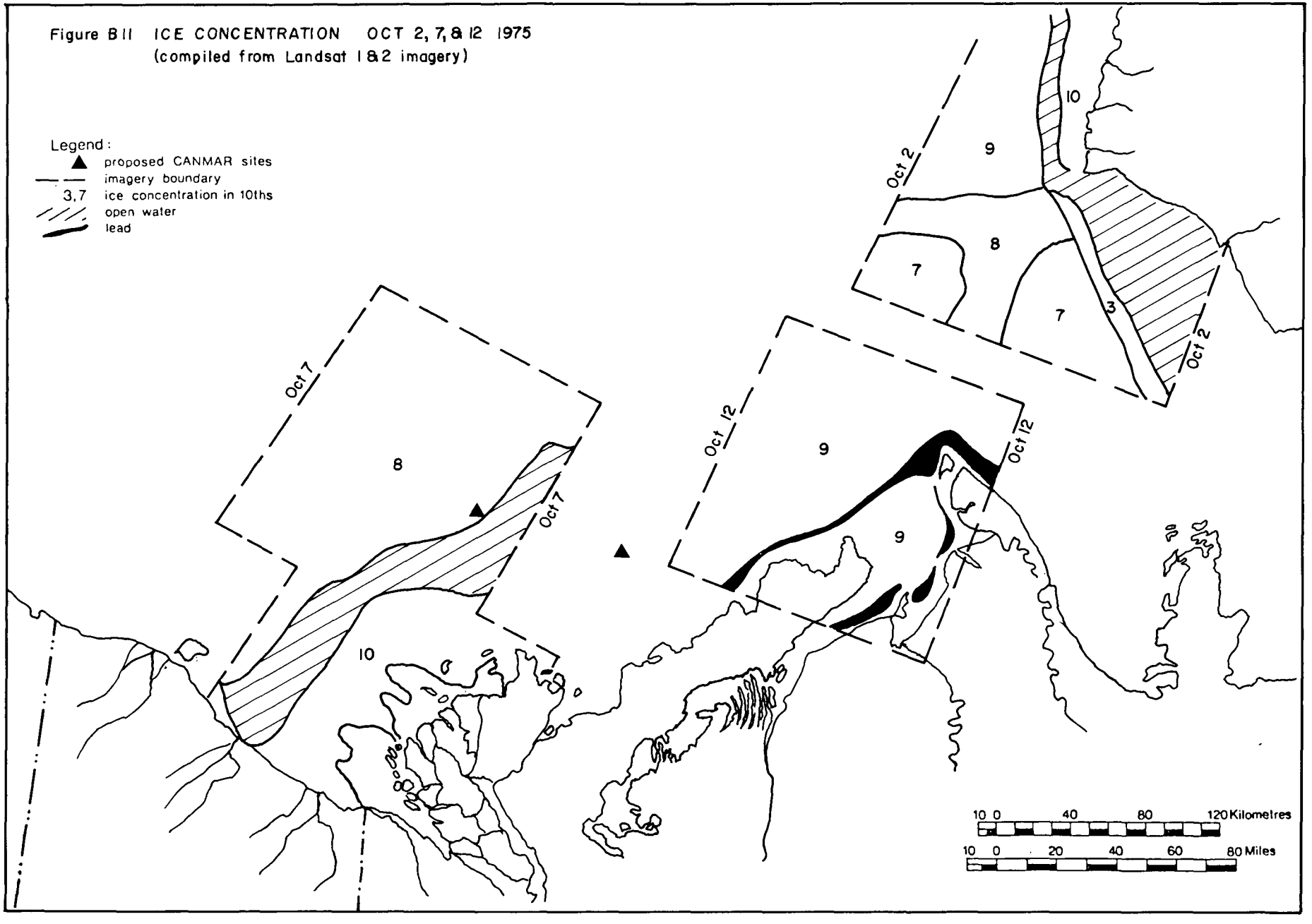

Figure B12 ICE CONCENTRATION JUNE 13-15 1974
(compiled from Landsat 1&2 imagery)

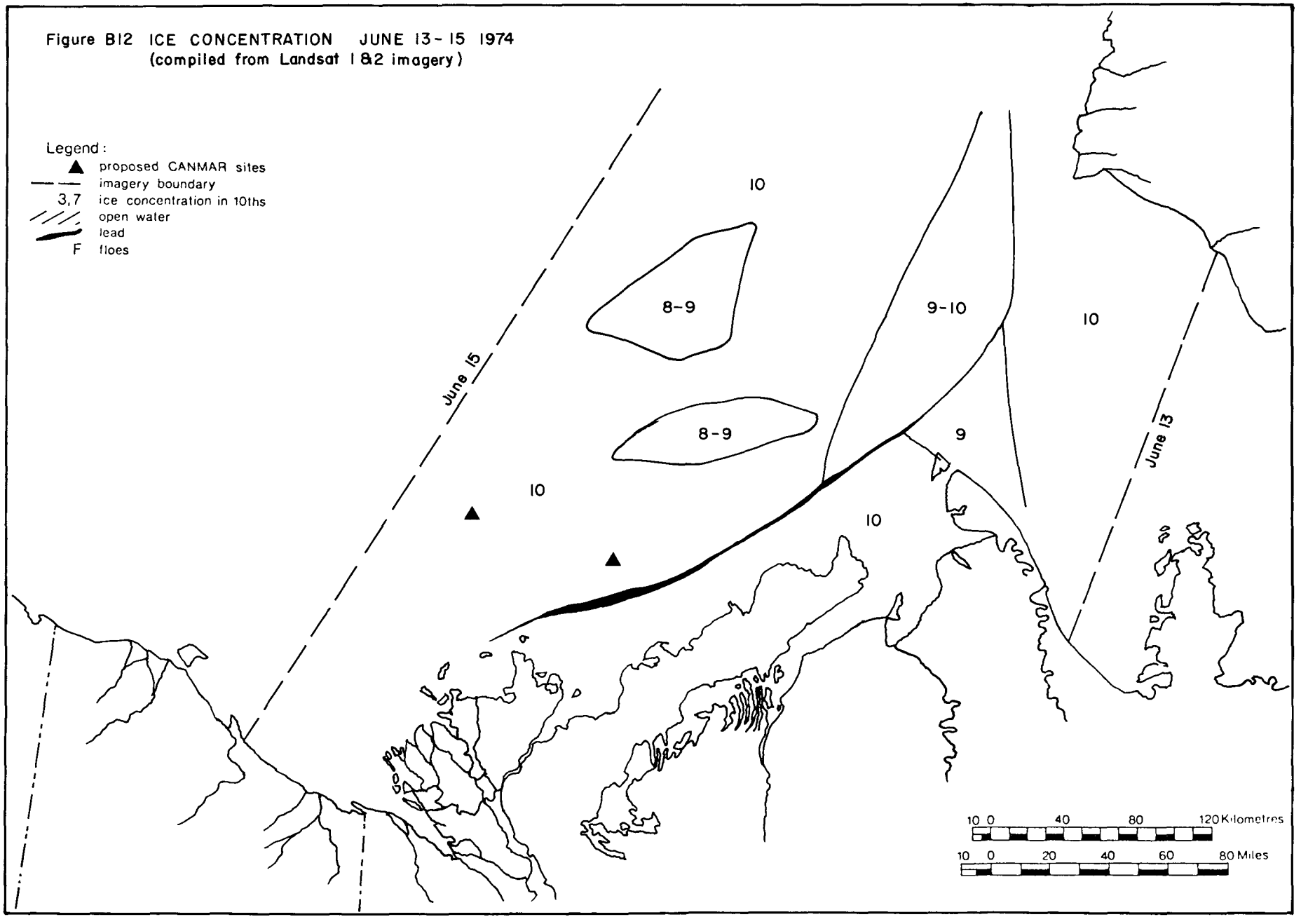

Figure B 13 ICE CONCENTRATION JULY 17-21 1974
(compiled from Landsat 1&2 imagery)

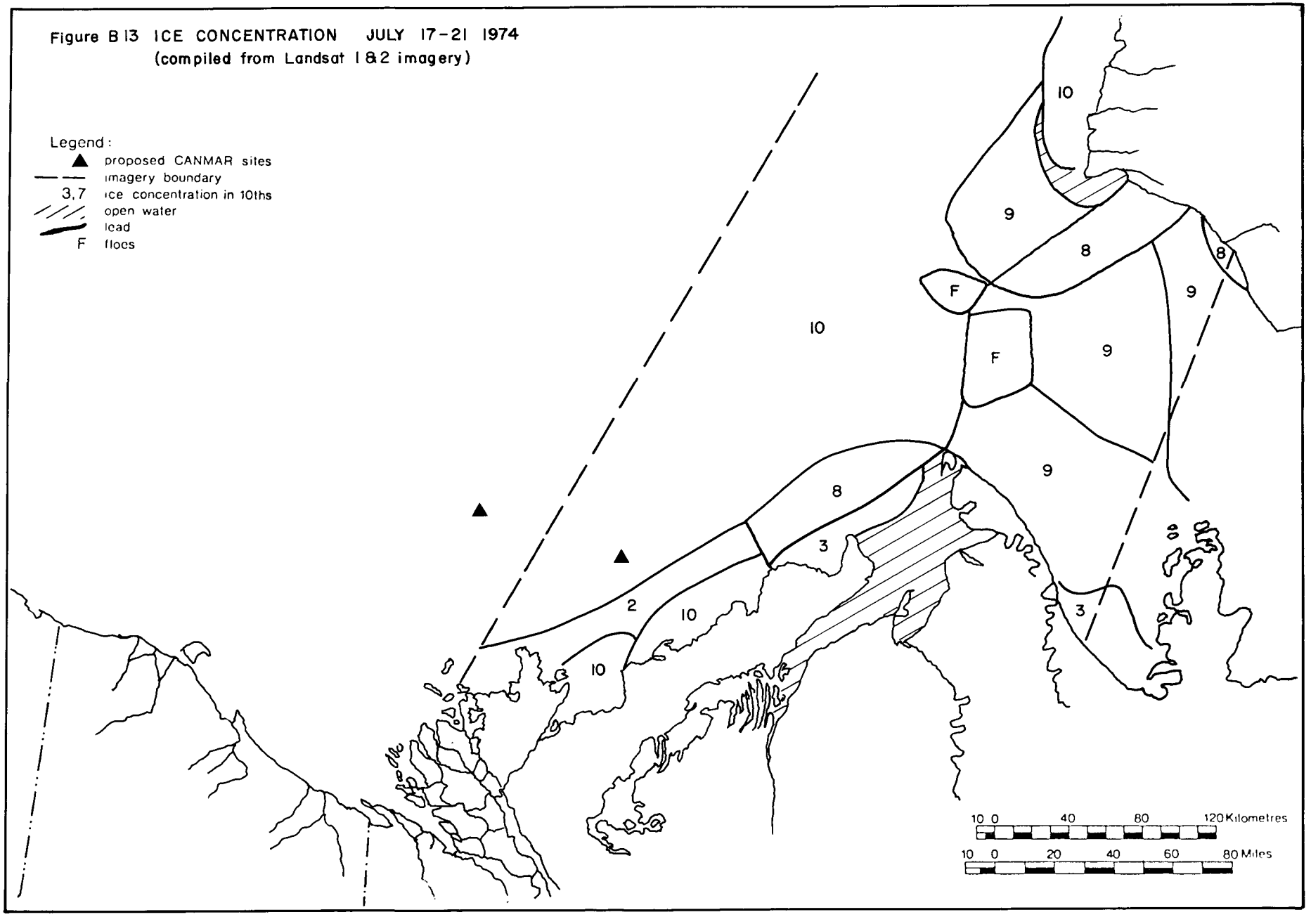

Figure B14 ICE CONCENTRATION AUG 5-10 1974
(compiled from Landsat 1&2 imagery)

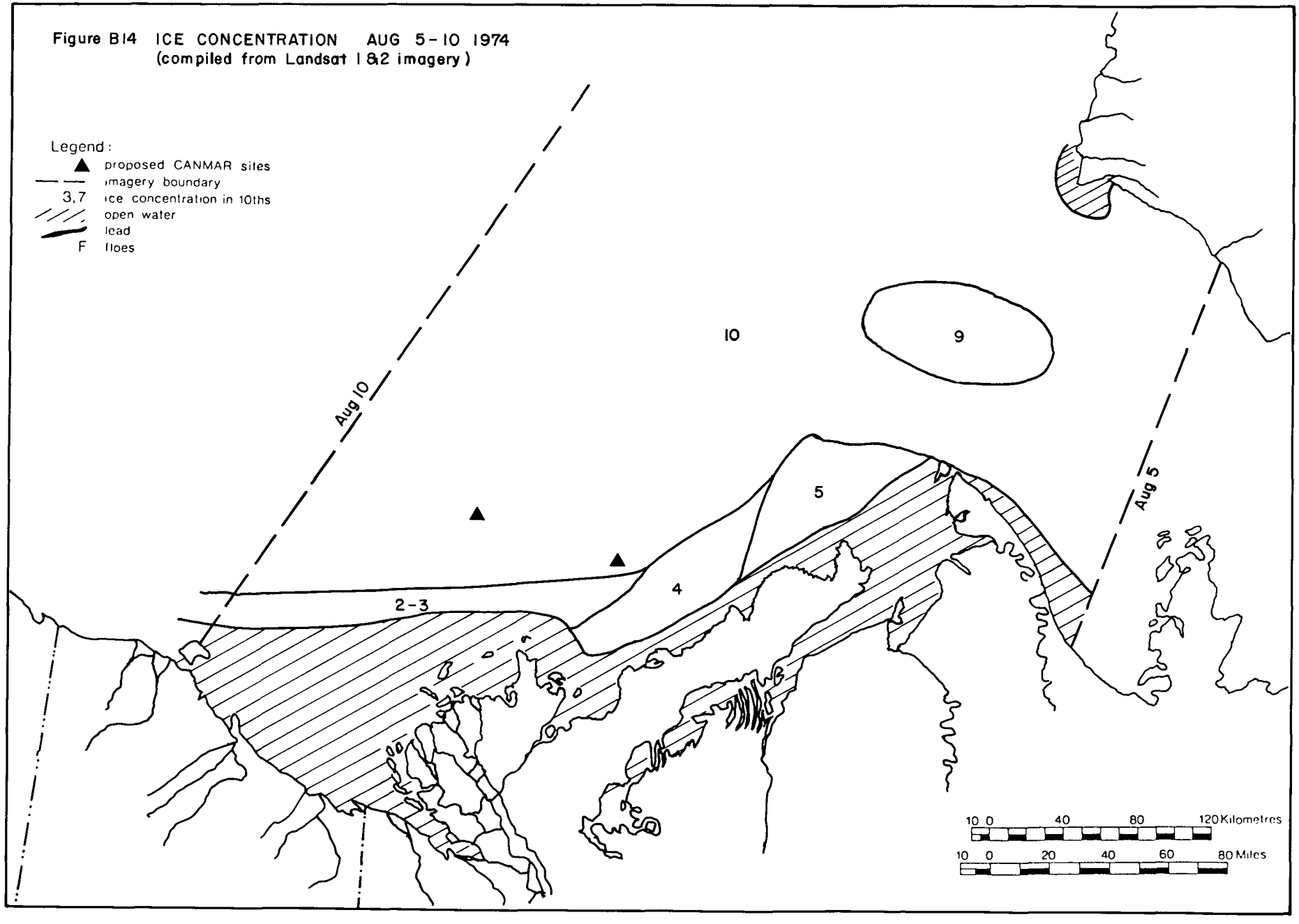

Figure B 15 ICE CONCENTRATION AUG 22 – 26 1974
(compiled from Landsat 1 & 2 imagery)

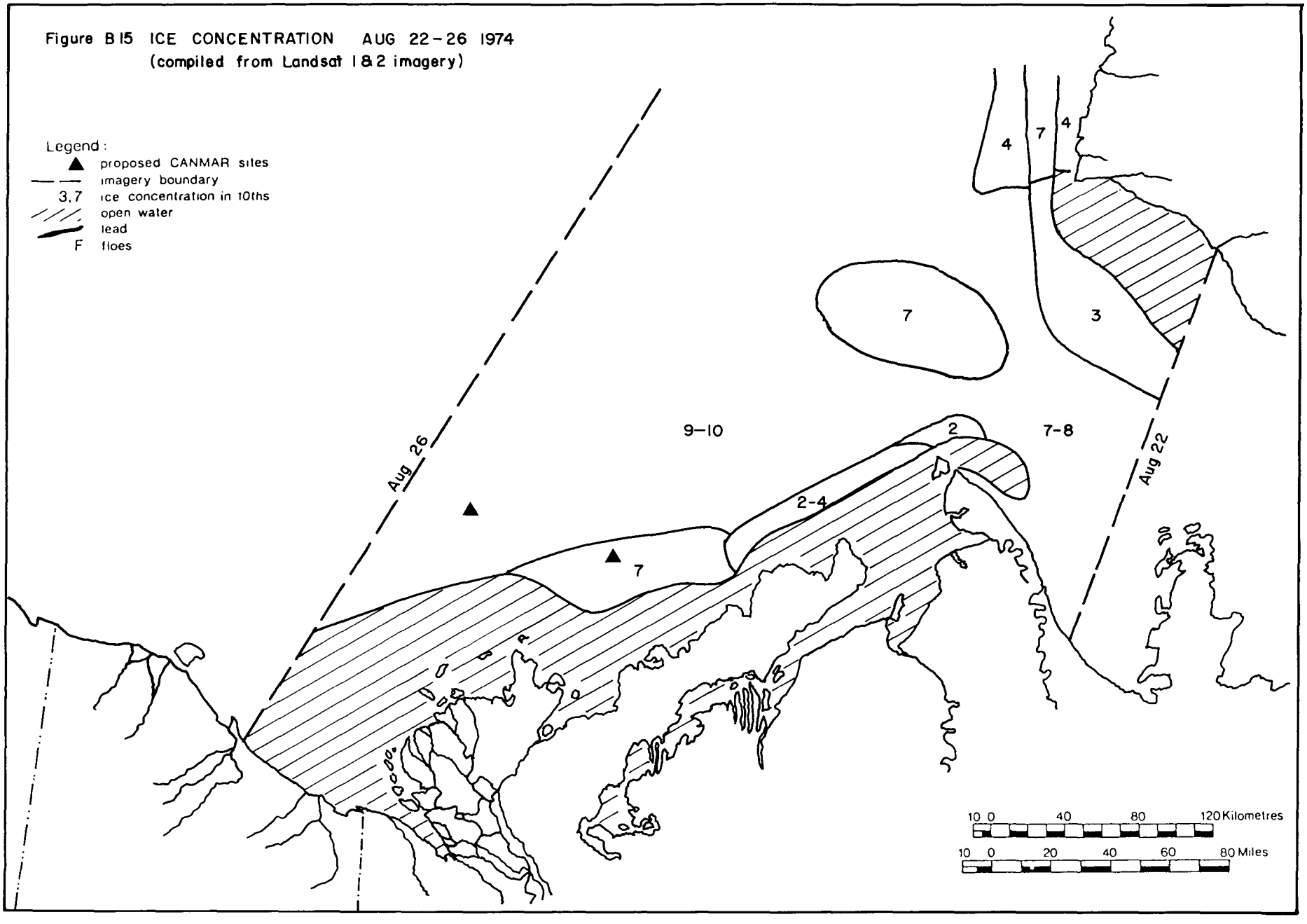

Figure B16 ICE CONCENTRATION SEPT 9-11 1974
(compiled from Landsat 1&2 imagery)

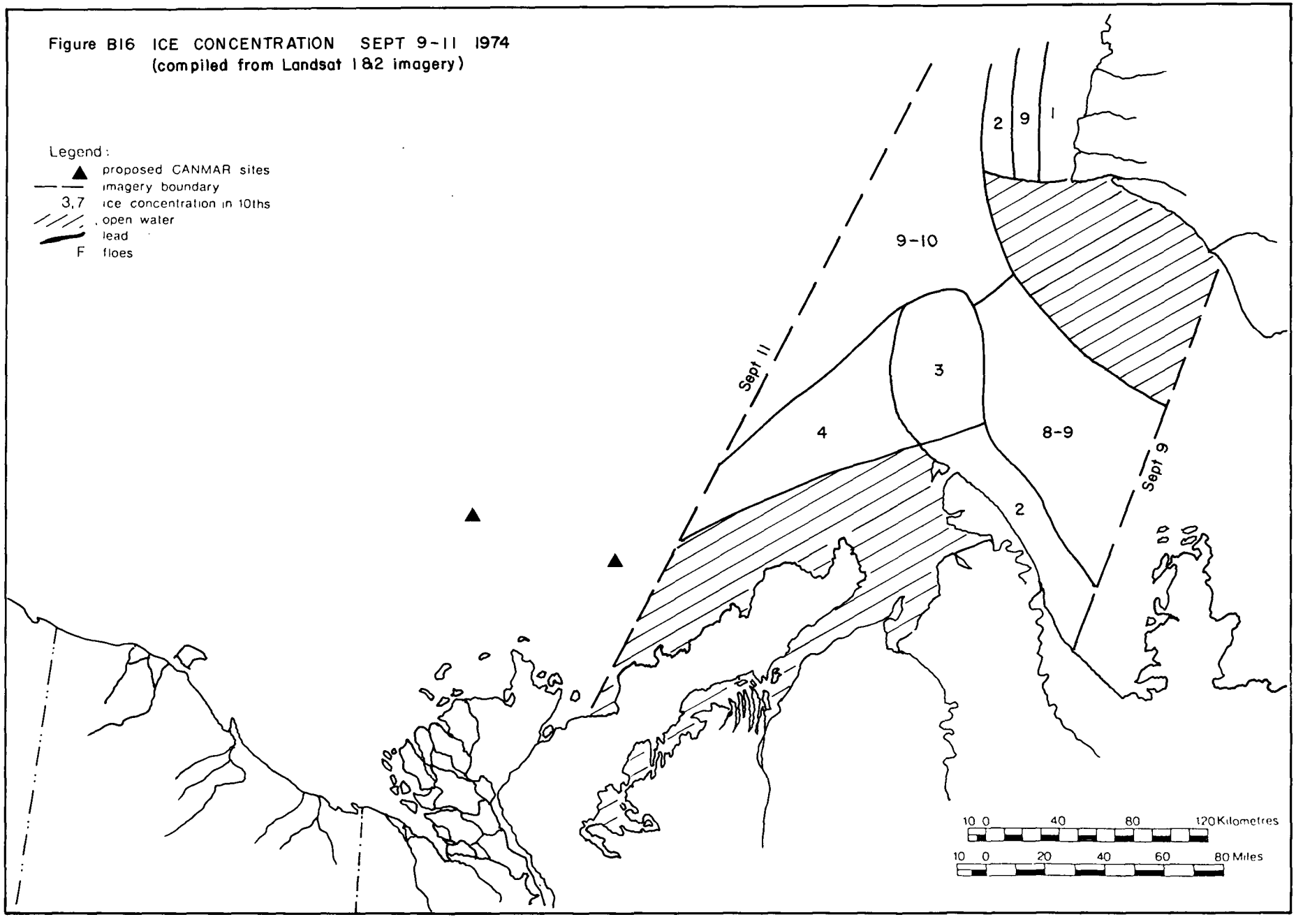

Figure B17 ICE CONCENTRATION SEPT 28 & OCT 1 1974
(compiled from Landsat 1 & 2 imagery)

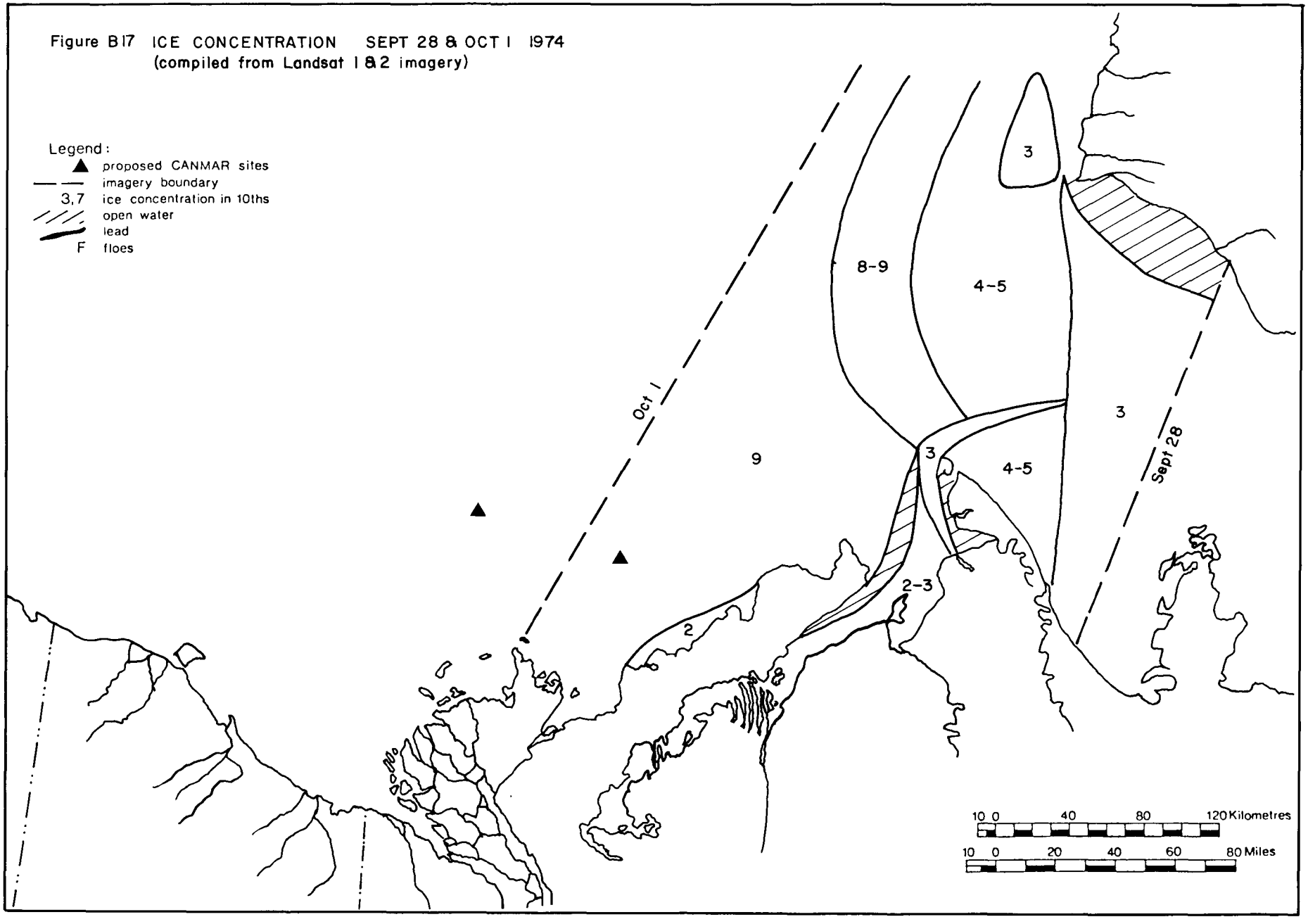

Figure B 18 ICE RECONNAISSANCE FLIGHT JAN 20 1976
MULTI-YEAR FLOE FREQUENCY AND SIZE

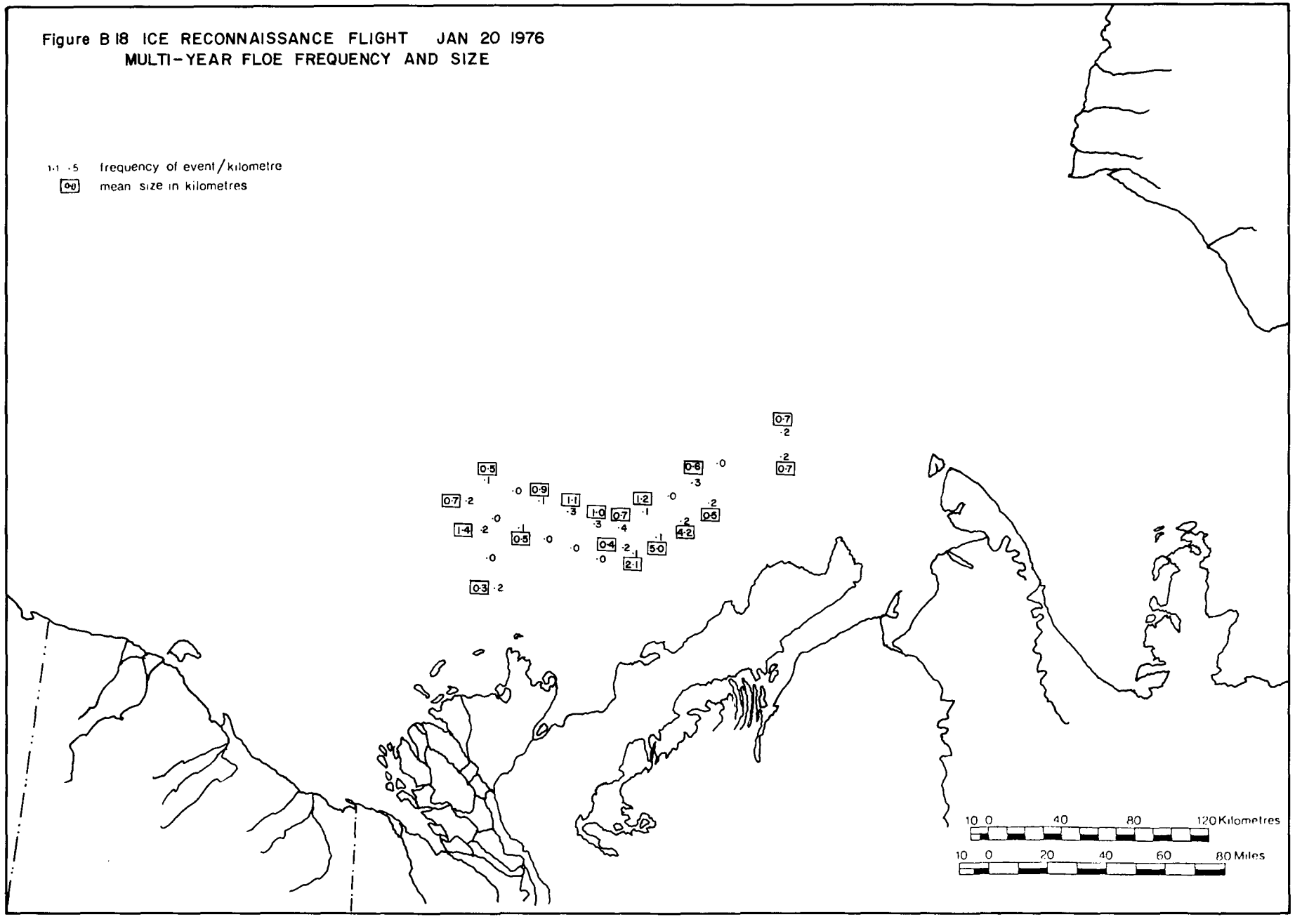

Figure B19 ICE RECONNAISSANCE FLIGHT JAN 20 1976
RIDGE FREQUENCY AND ORIENTATION

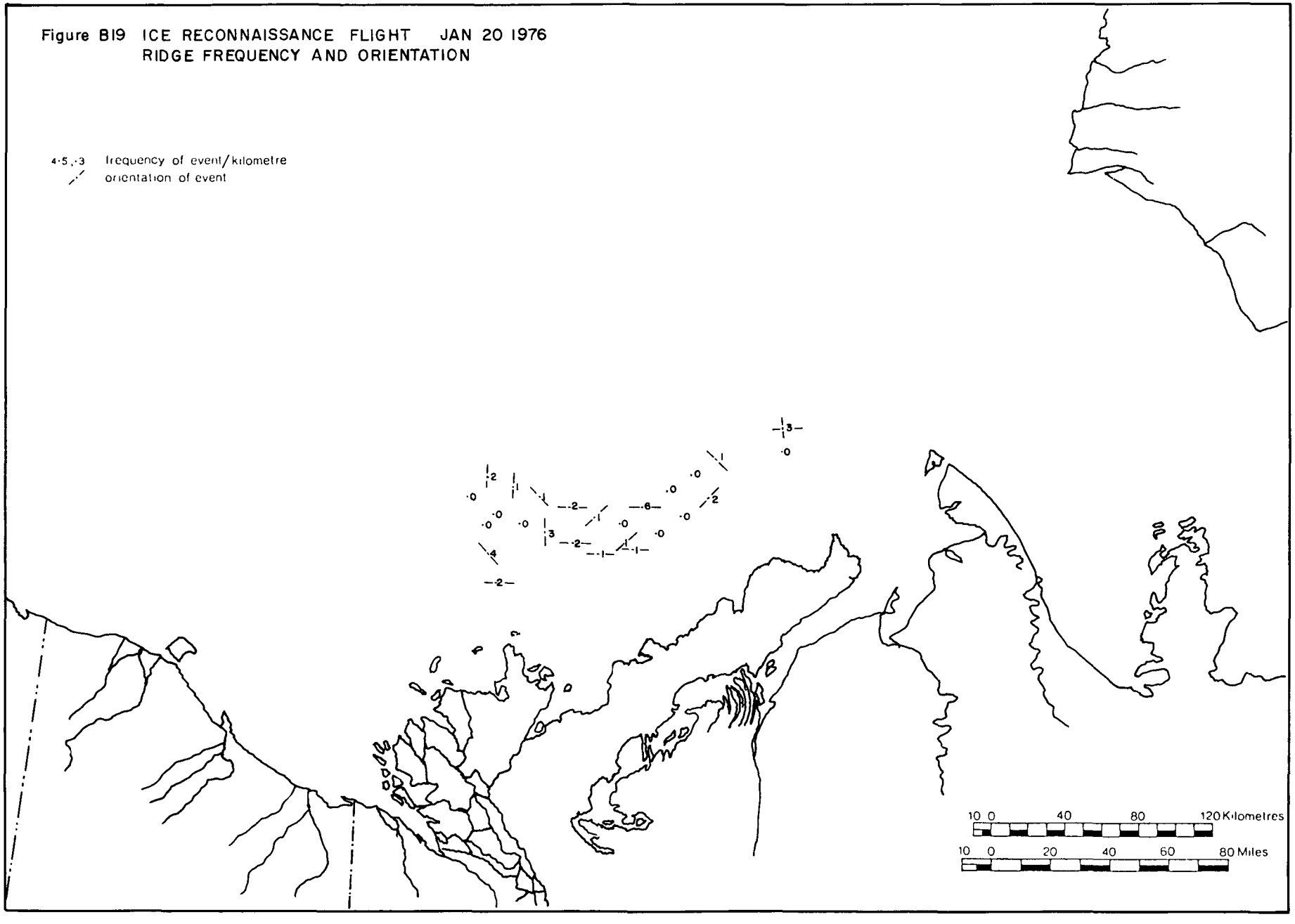

Figure B20 ICE RECONNAISSANCE FLIGHT JAN 20 1976
CRACK/LEAD FREQUENCY AND ORIENTATION

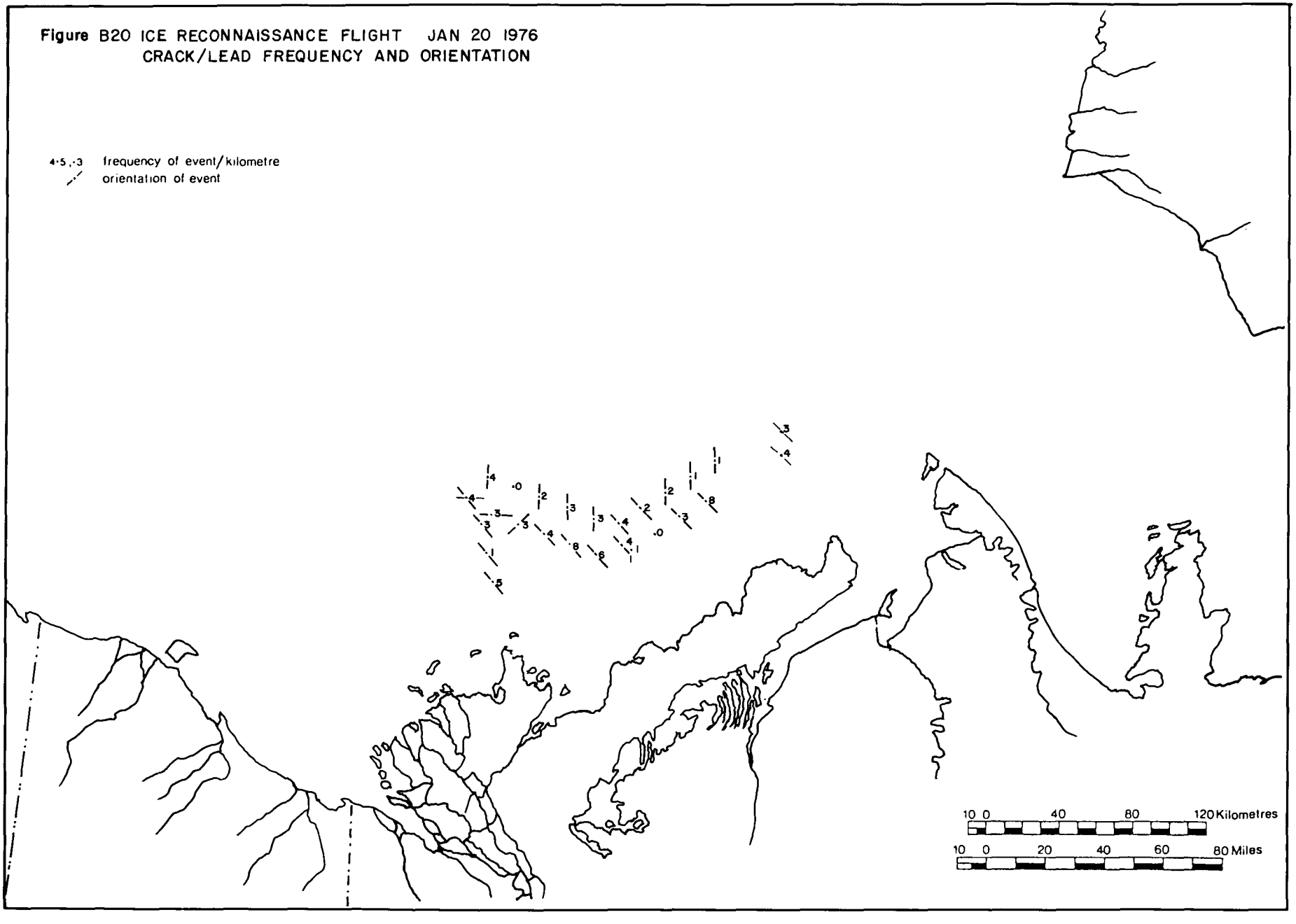

Figure B21 ICE RECONNAISSANCE FLIGHT MAR 6 1976
MULTI-YEAR FLOE FREQUENCY AND SIZE

1·1, ·5 frequency of event/kilometre
[0·8] mean size in kilometres

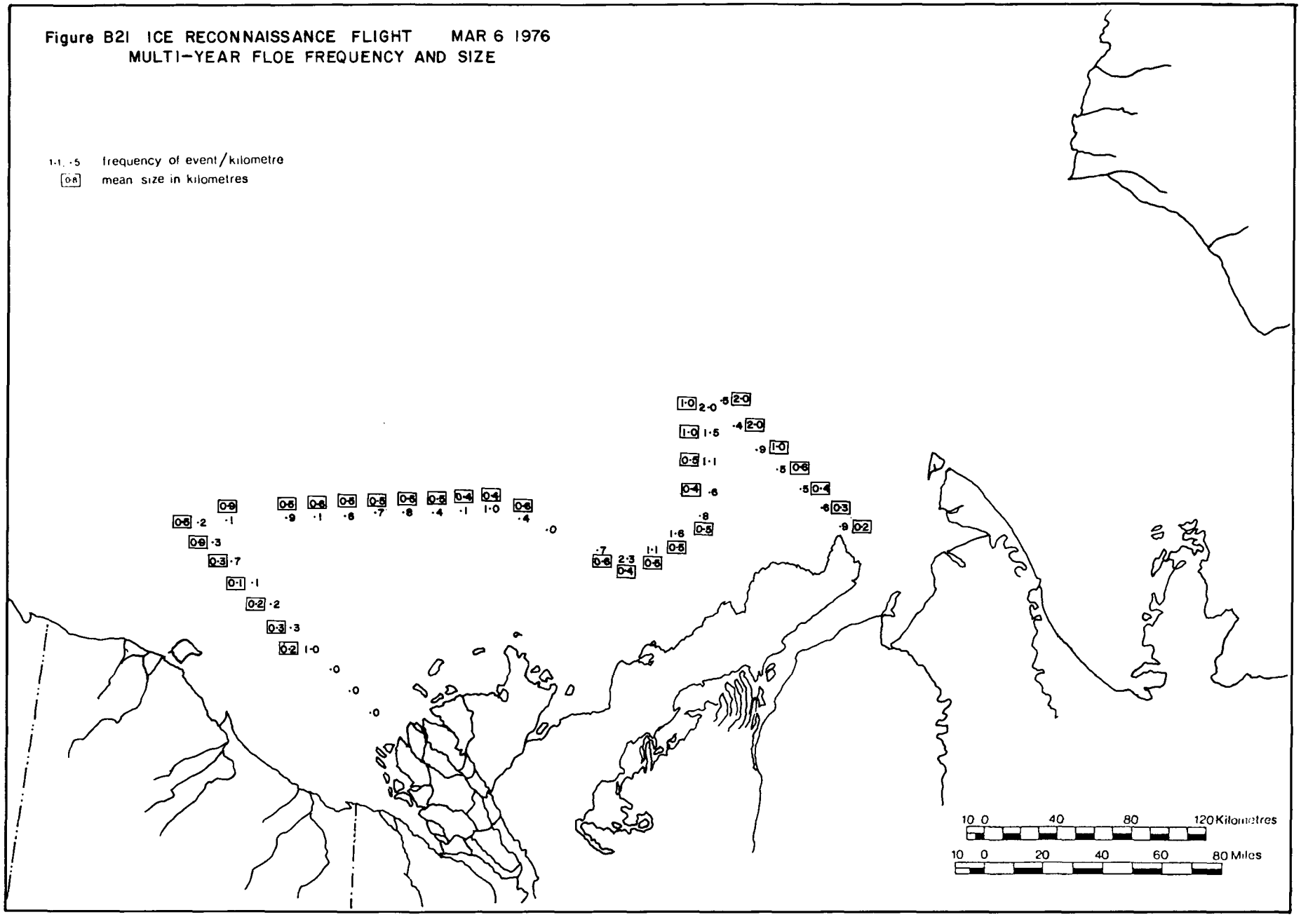

Figure B22 ICE RECONNAISSANCE FLIGHT MAR 6 1976
RIDGE FREQUENCY AND ORIENTATION

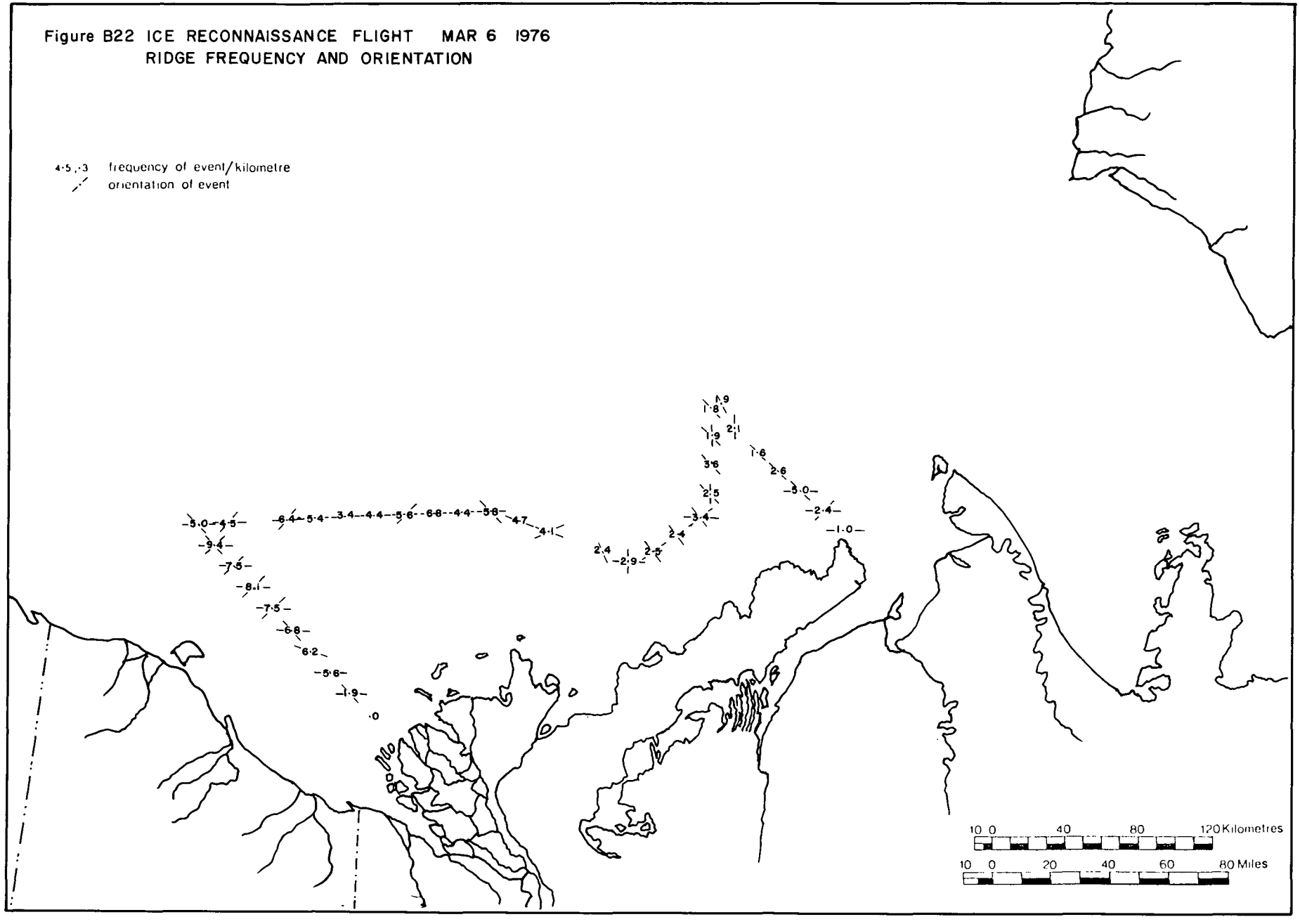

Figure B 23 ICE RECONNAISSANCE FLIGHT MAR 6 1976
CRACK/LEAD FREQUENCY AND ORIENTATION

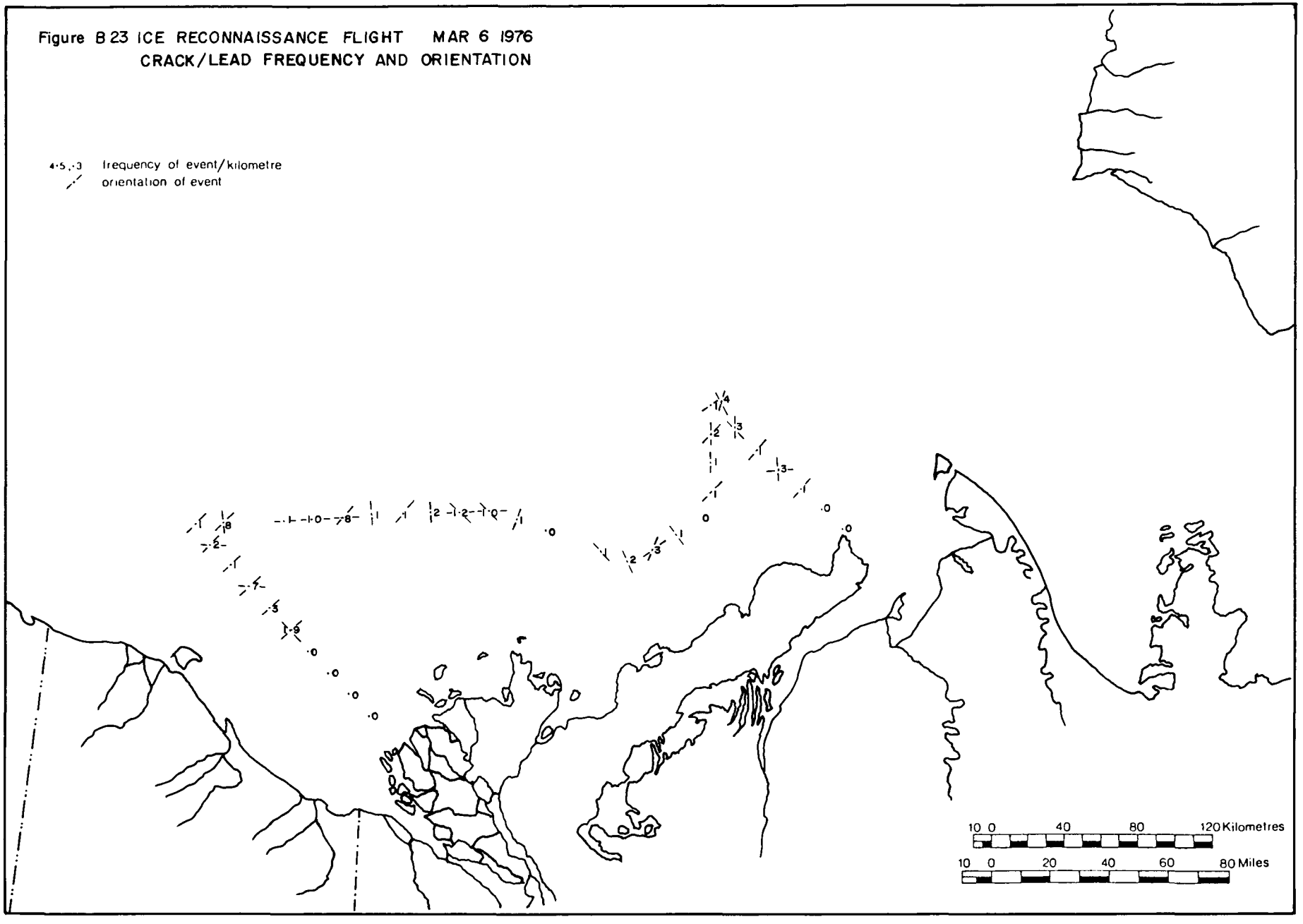

Figure B24 ICE RECONNAISSANCE FLIGHT APR 29 1976
MULTI-YEAR FLOE FREQUENCY AND SIZE

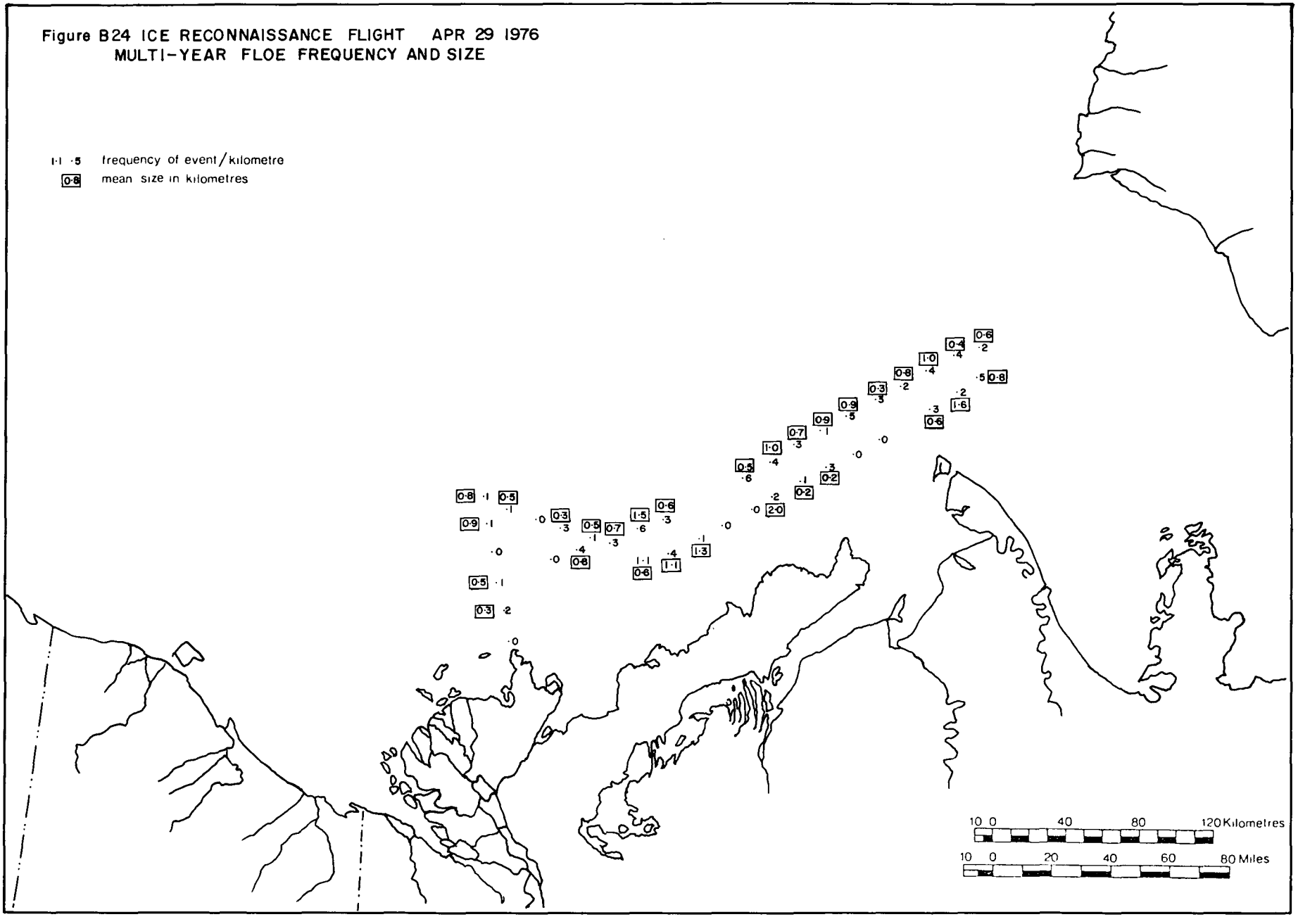

Figure B25 ICE RECONNAISSANCE FLIGHT APR 29 1976
RIDGE FREQUENCY AND ORIENTATION

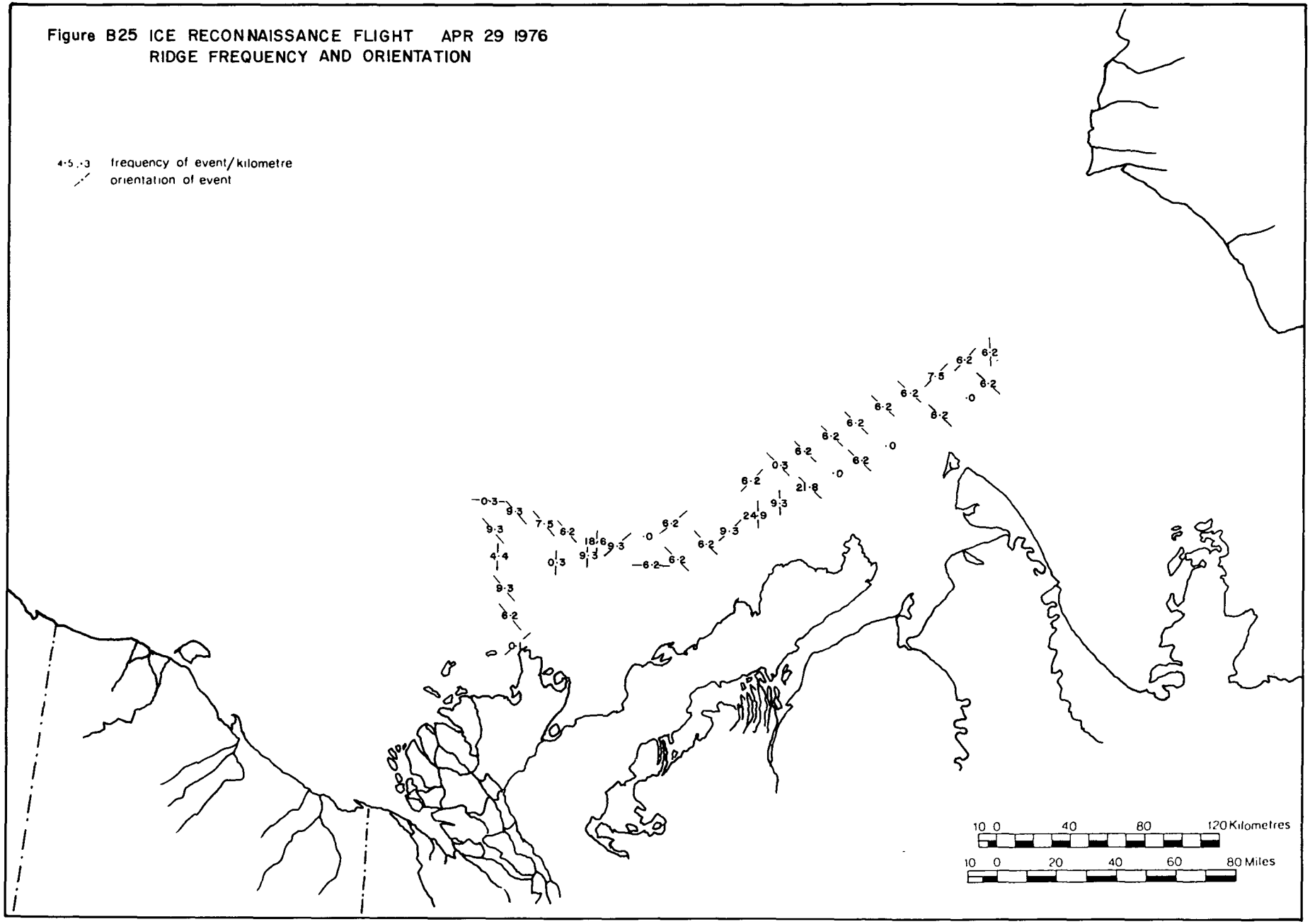

Figure B26 ICE RECONNAISSANCE FLIGHT APR 29 1976
CRACK/LEAD FREQUENCY AND ORIENTATION

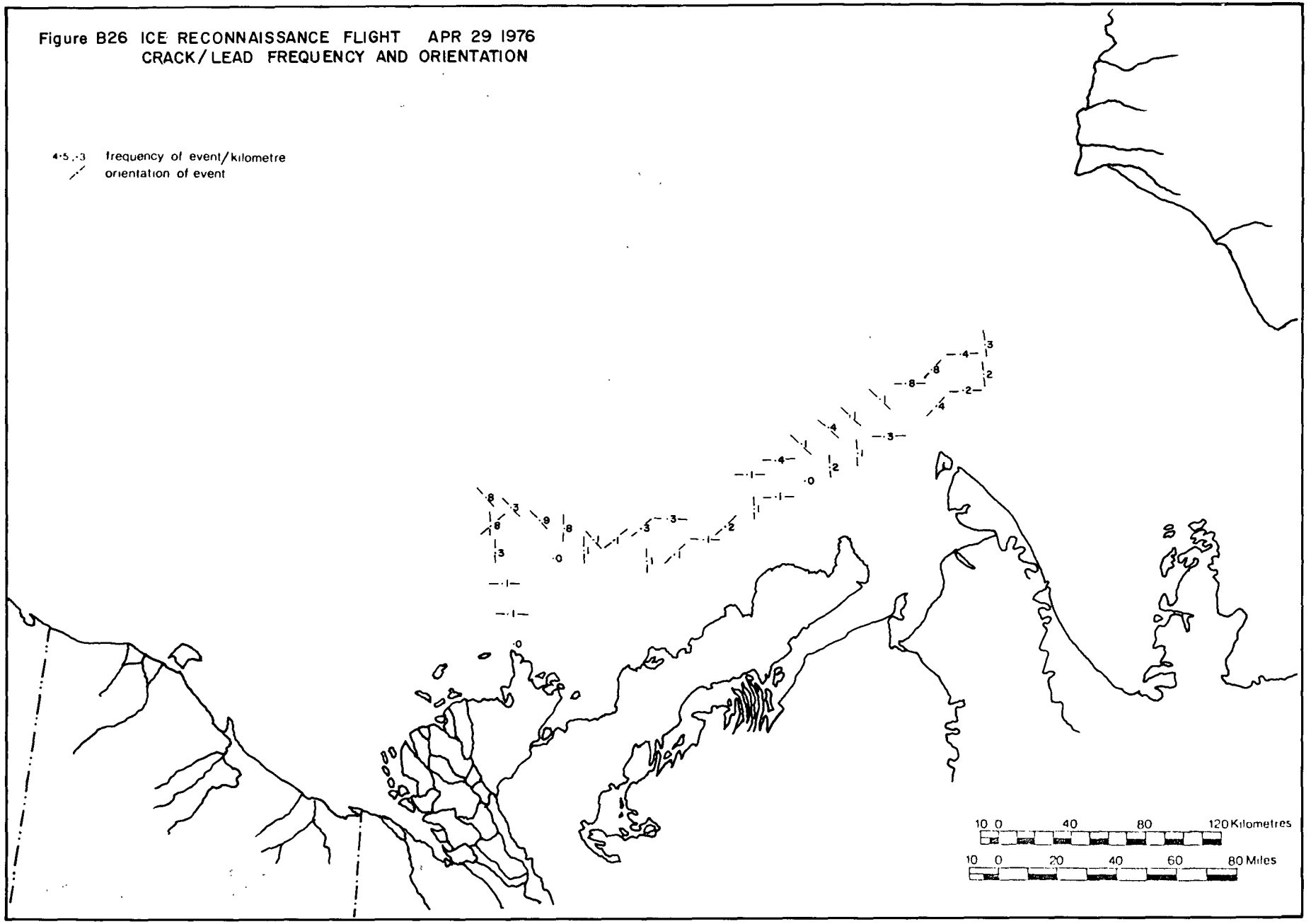

Figure B27 ICE RECONNAISSANCE FLIGHT JUNE 2-3 1976
PERCENT AREA OF OPEN WATER & SMALL FLOES

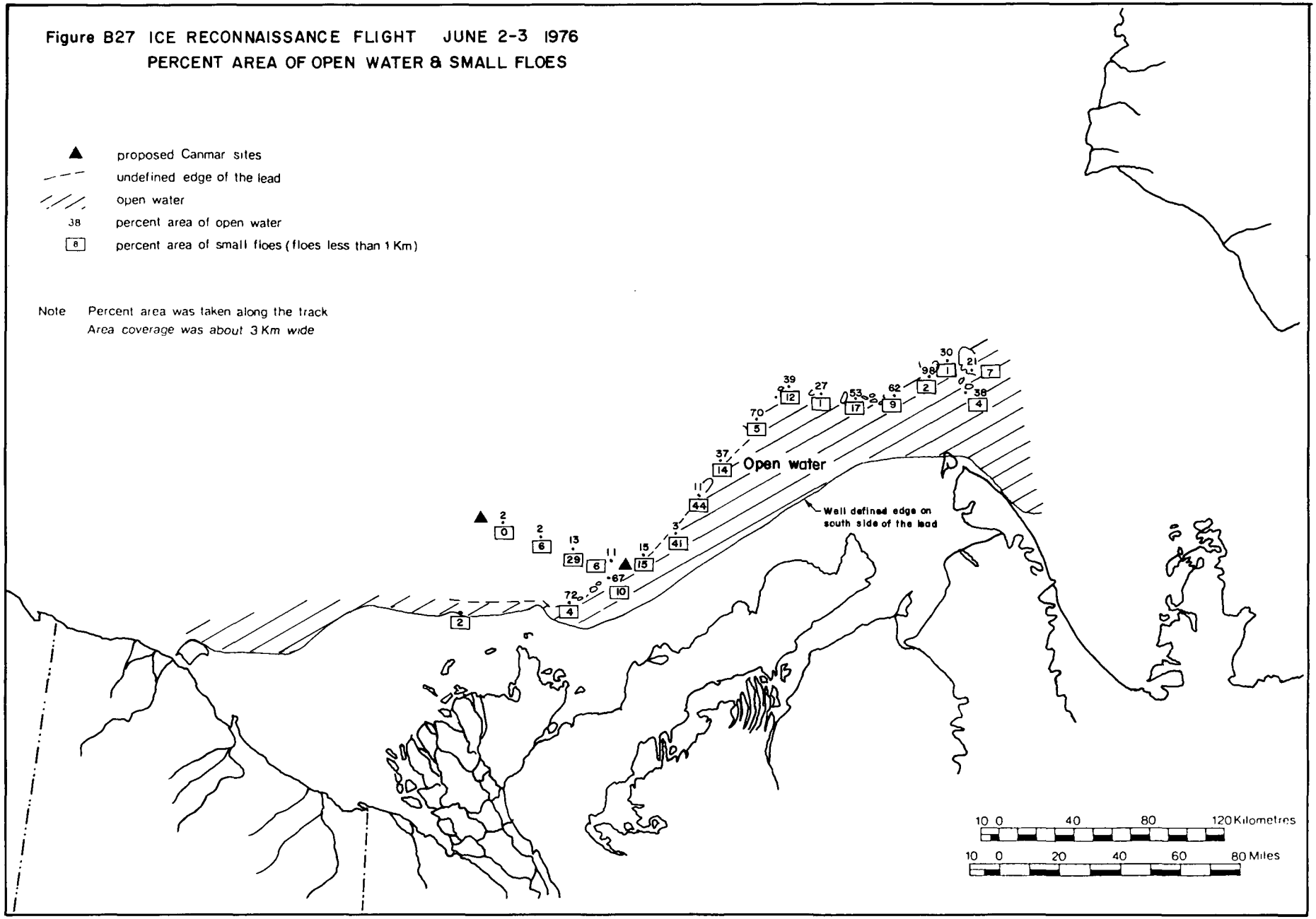

Figure B28 ICE RECONNAISSANCE FLIGHT JUNE 2-3 1976
RIDGE FREQUENCY AND ORIENTATION

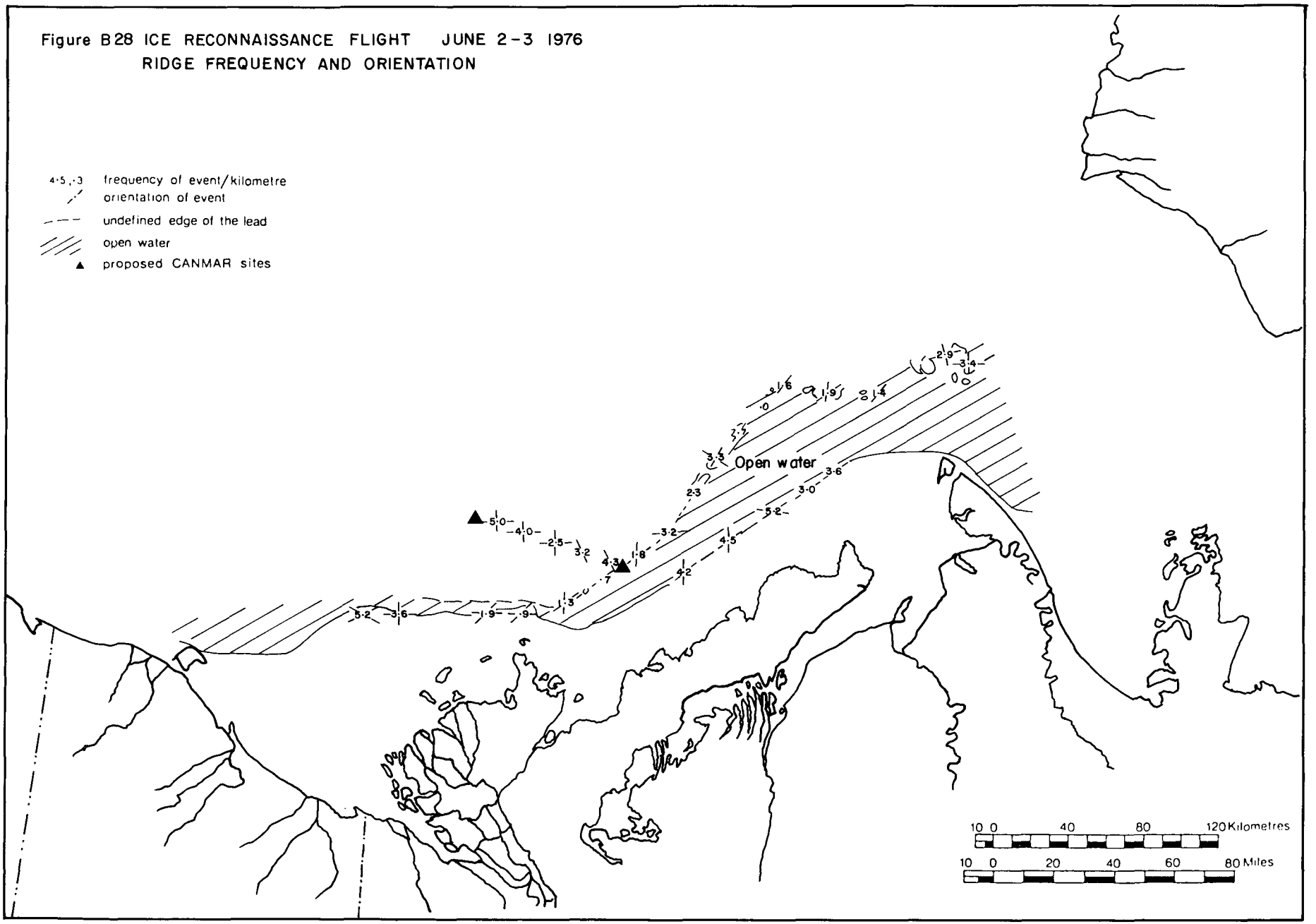

Figure B29 ICE RECONNAISSANCE FLIGHT JUNE 2-3 1976
MEAN SIZE OF FLOES

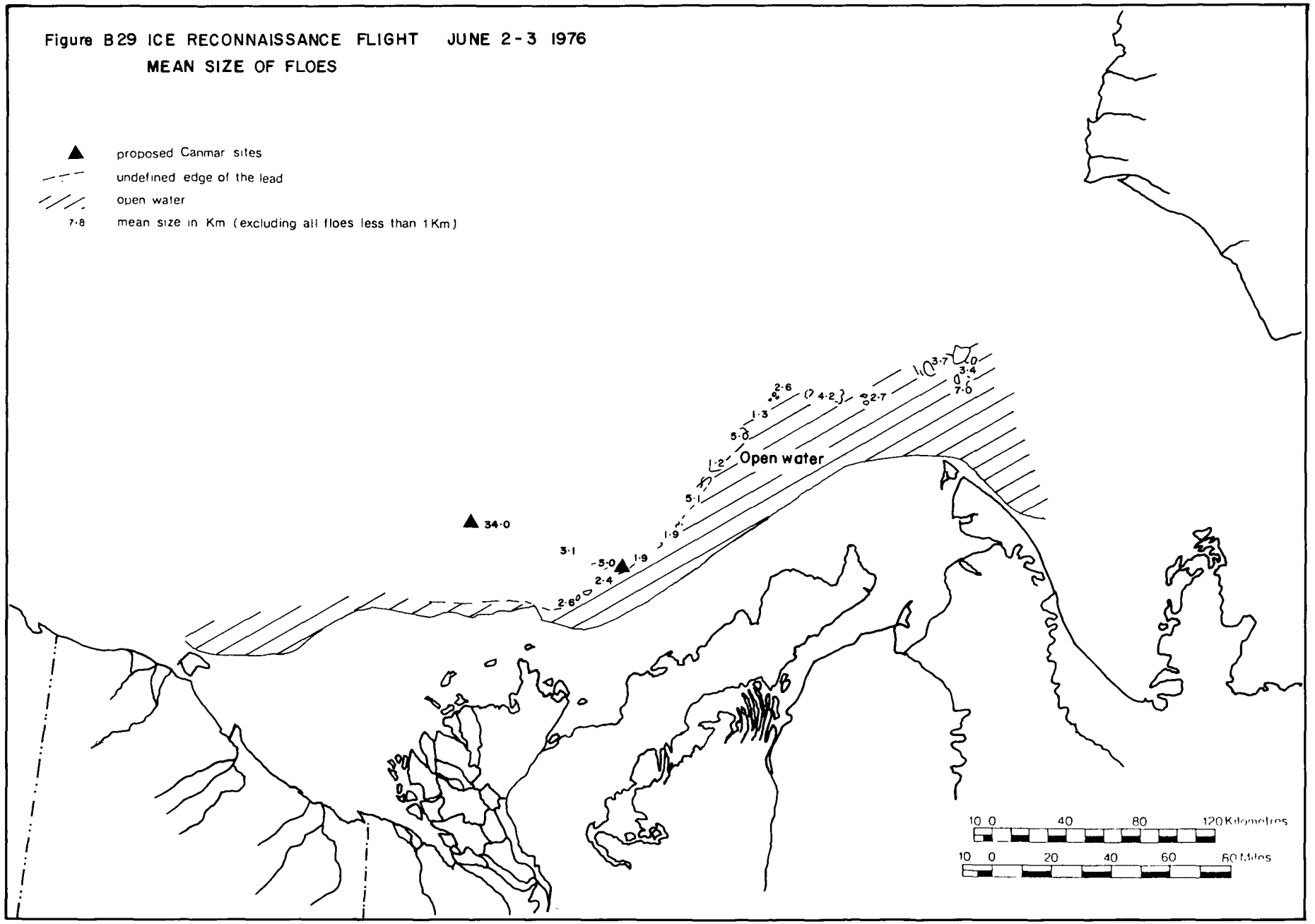

Figure B30 ICE RECONNAISSANCE FLIGHT JUNE 12 - 13 1976
PERCENT AREA OF OPEN WATER & SMALL FLOES

▲ proposed Canmar sites

undefined edge of the lead

open water

38 percent area of open water

[8] percent area of small floes (floes less than 1 Km)

Note: Percent area was taken along the track
Area coverage was about 3 Km wide

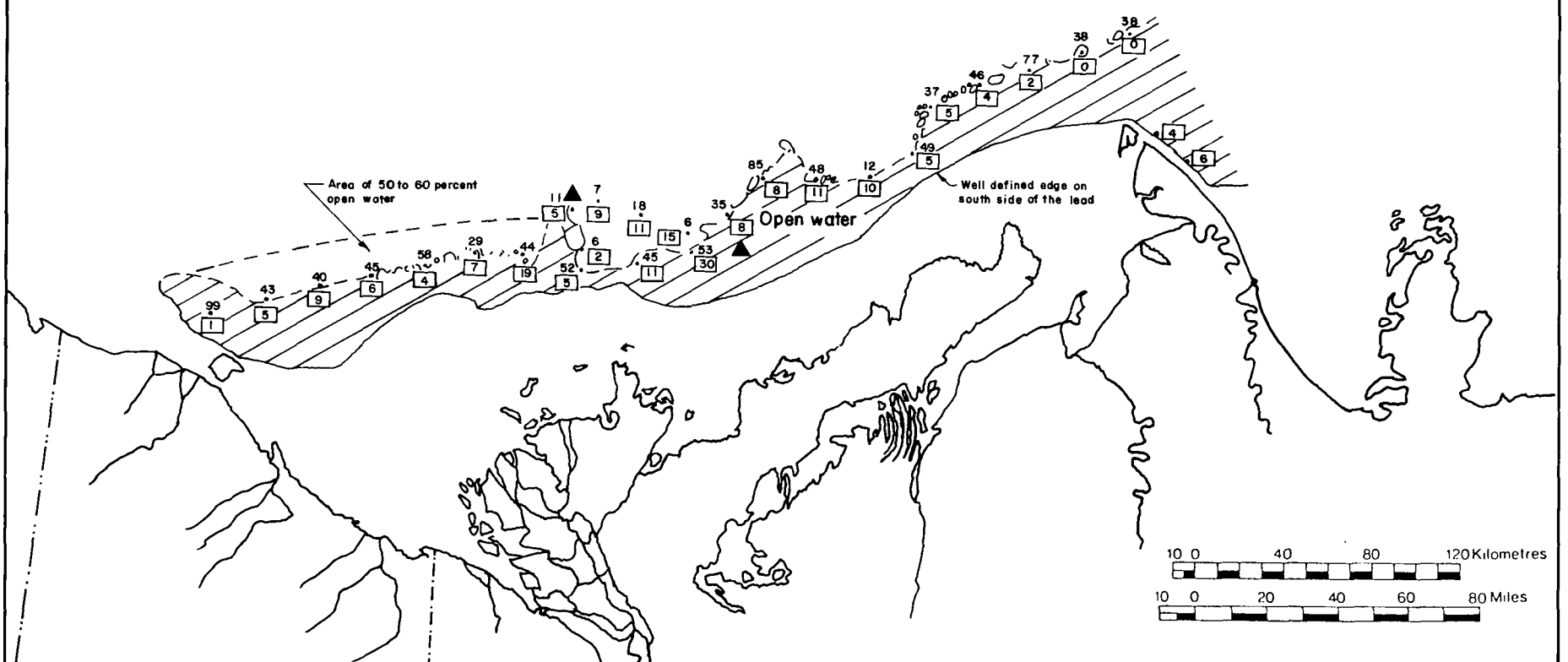

Figure B31 ICE RECONNAISSANCE FLIGHT JUNE 12 - 13 1976
RIDGE FREQUENCY AND ORIENTATION

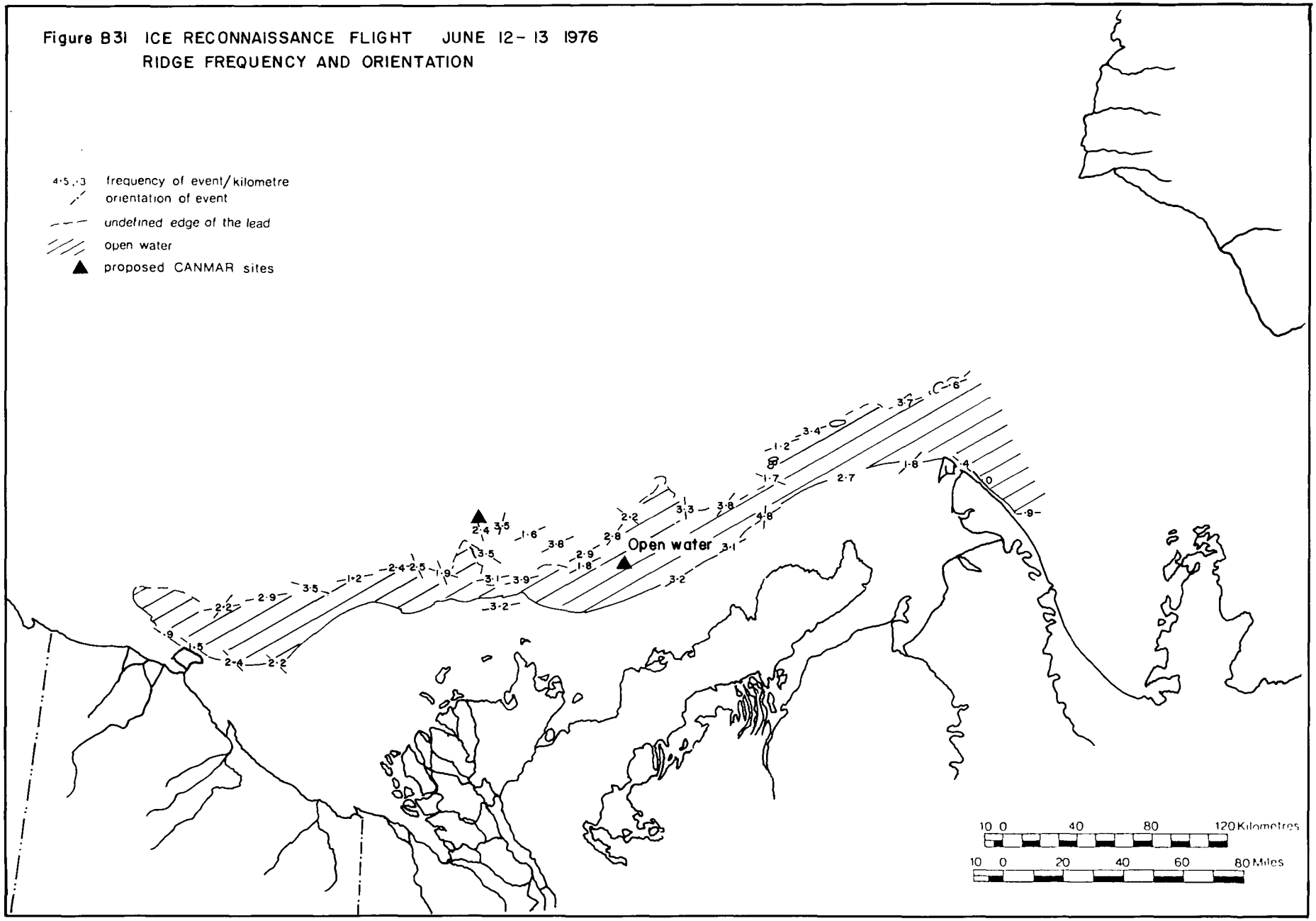

Figure B32 ICE RECONNAISSANCE FLIGHT JUNE 12-13 1976
MEAN SIZE OF FLOES

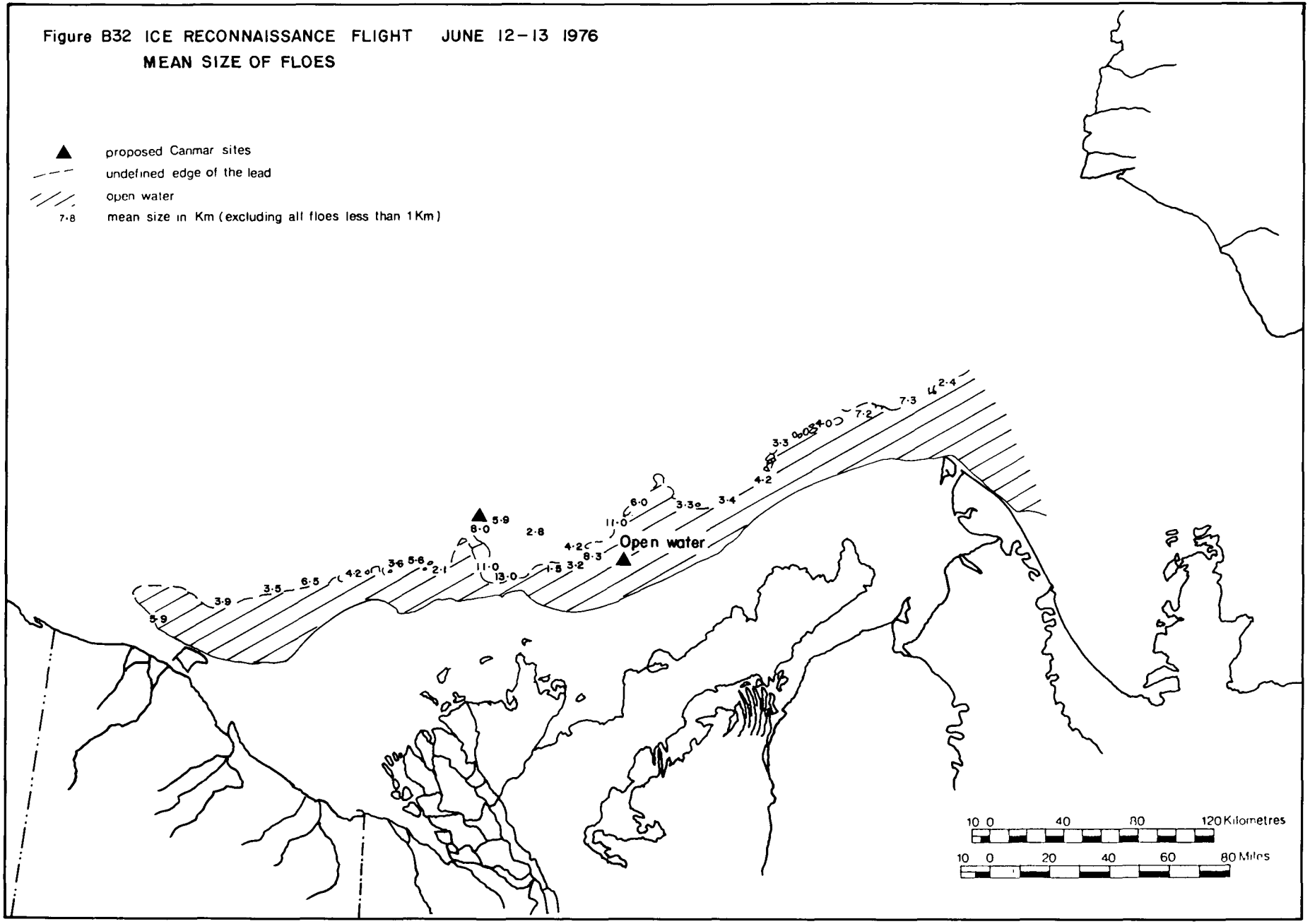

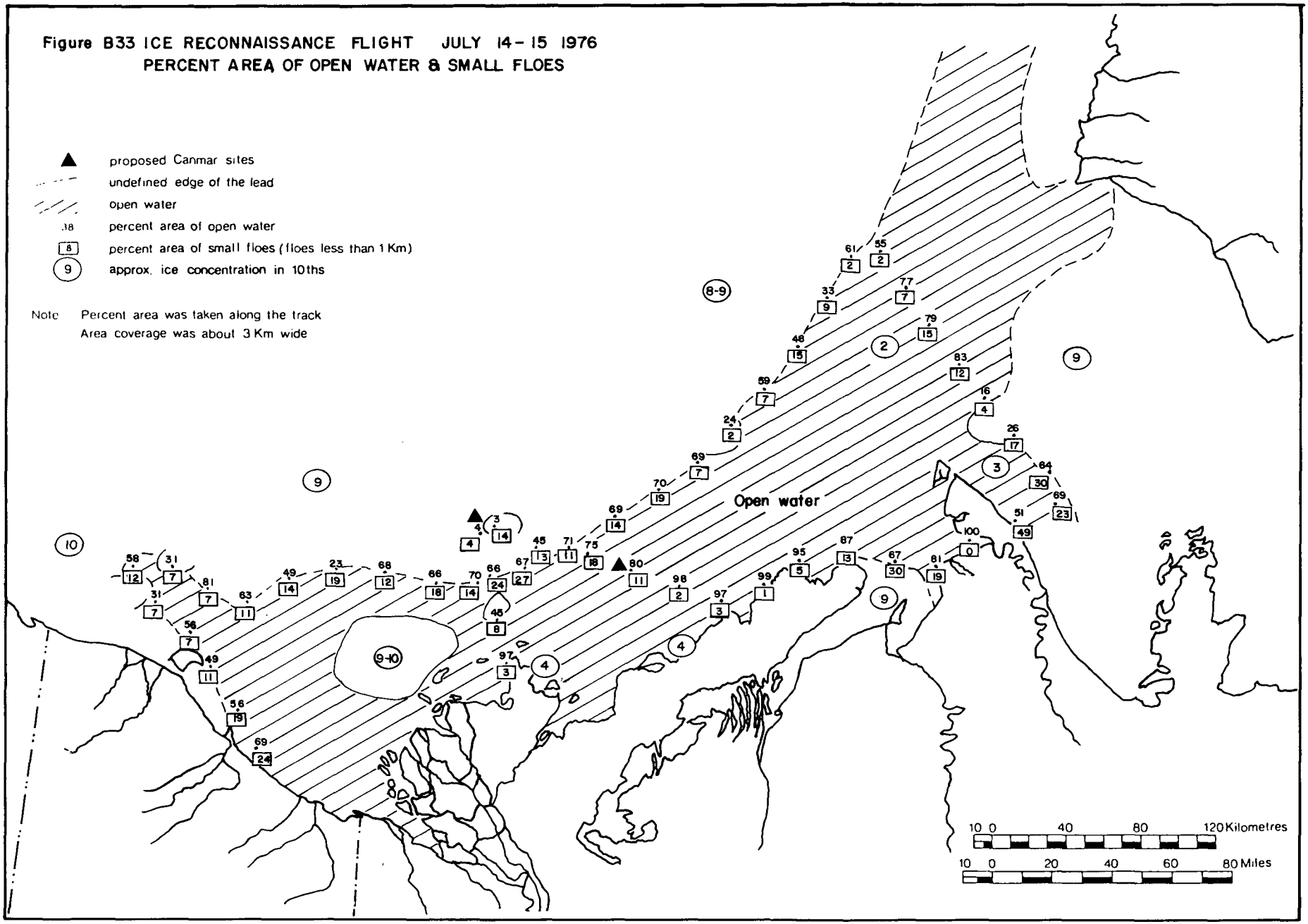
Figure B33 ICE RECONNAISSANCE FLIGHT JULY 14 - 15 1976
PERCENT AREA OF OPEN WATER & SMALL FLOES
proposed Canmar sites
undefined edge of the lead
open water
18 percent area of open water
8 percent area of small floes (floes less than 1 Km)
9 approx. ice concentration in 10ths
Note Percent area was taken along the track
Area coverage was about 3 Km wide
Open water
10 0 40 80 120 Kilometres
10 0 20 40 60 80 Miles

Figure B34 ICE RECONNAISSANCE FLIGHT JULY 14-15 1976
RIDGE FREQUENCY AND ORIENTATION

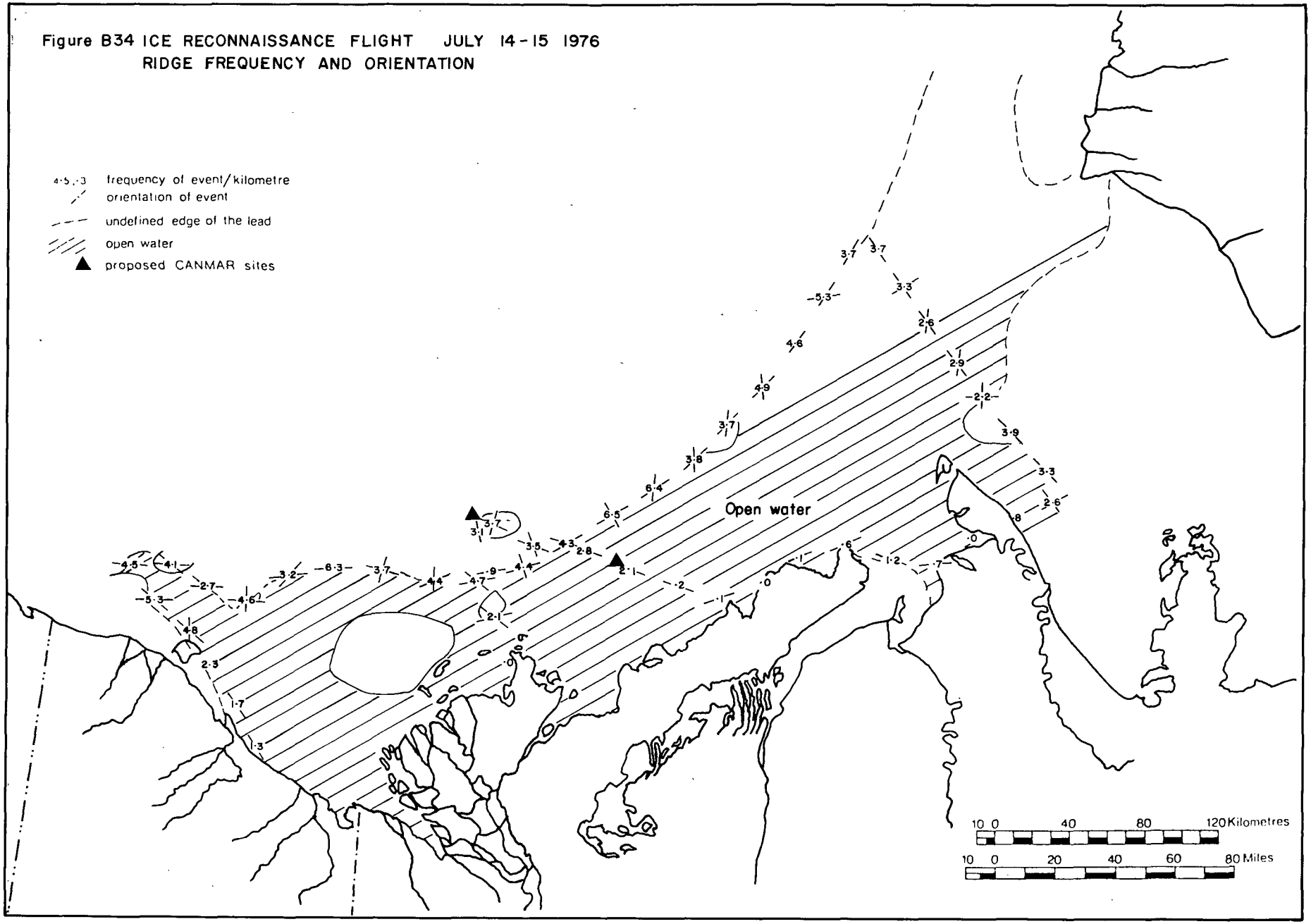

Figure B35 ICE RECONNAISSANCE FLIGHT JULY 14 – 15 1976
MEAN SIZE OF FLOES

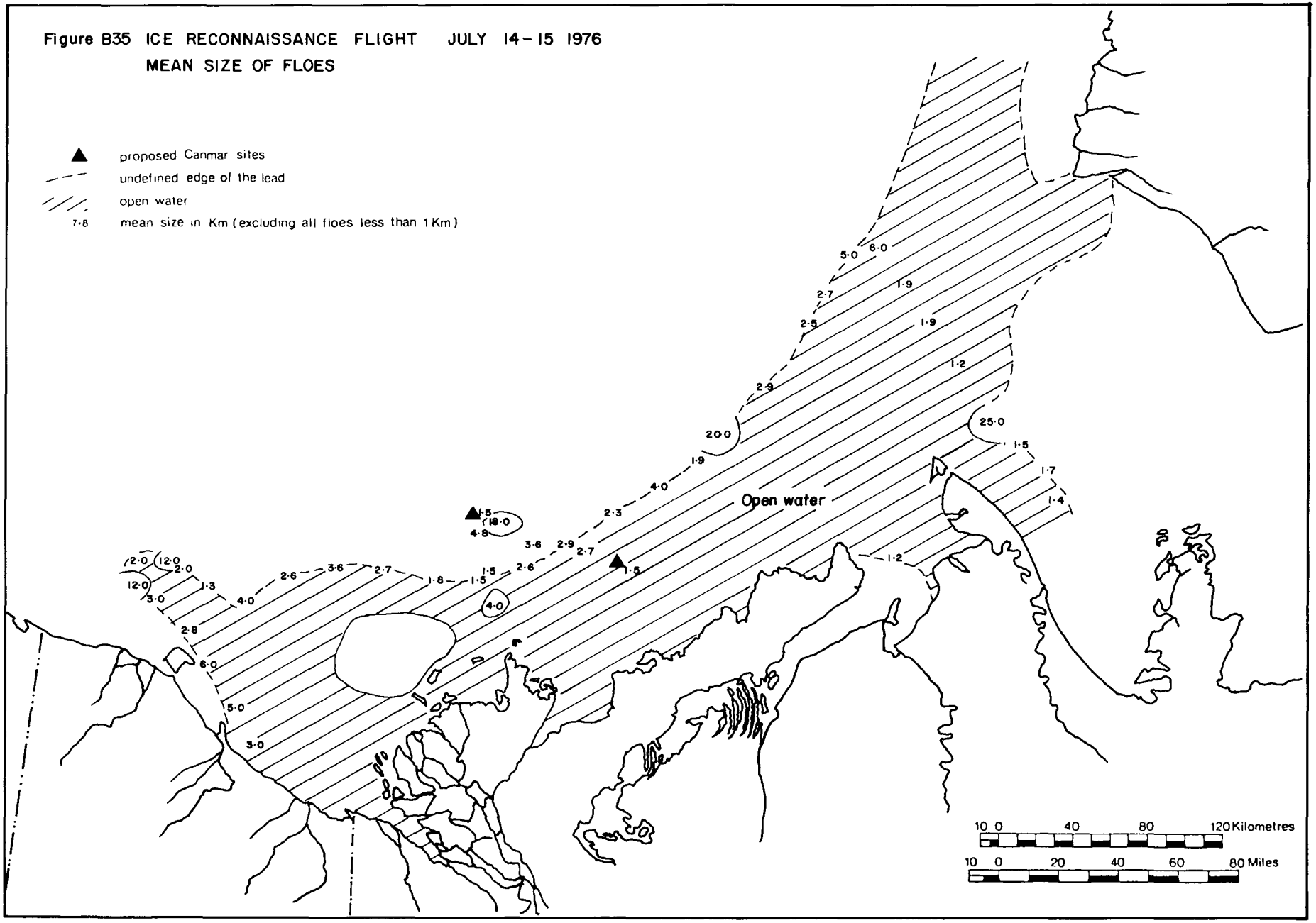

APPENDIX C - ICE MOVEMENT

Fig C1
NORCOR CAMP DRIFT
Feb 10, 76 to Mar 30, 76

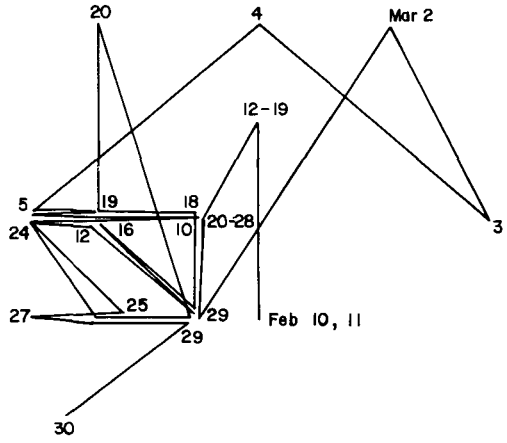

Fig C2
AIDJEX BUOY No 10
Daily Drift Plot, Feb 10, 76 to Mar 30, 76

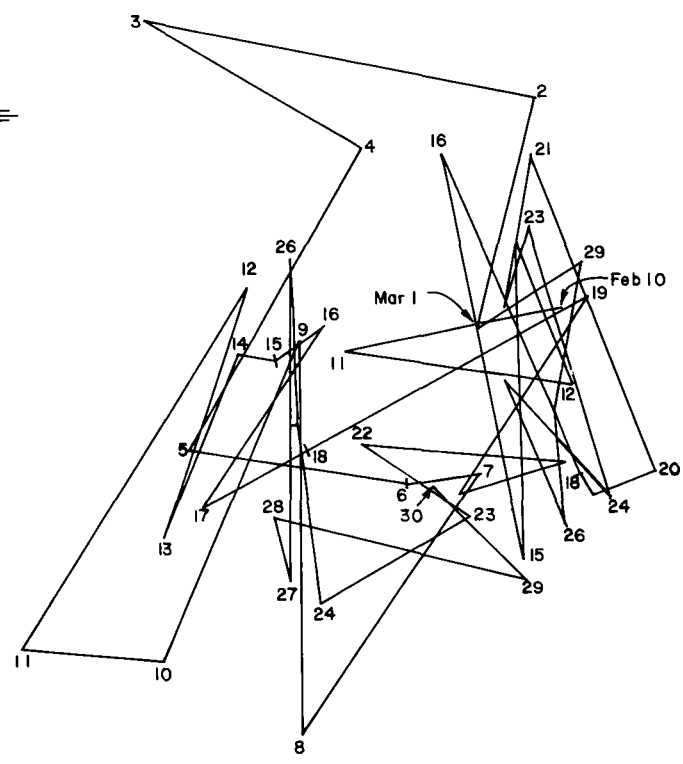

Fig. C3 AIDJEX BUOY No 1273
Daily Drift Plot, Feb 10, 76 to Mar 30, 76

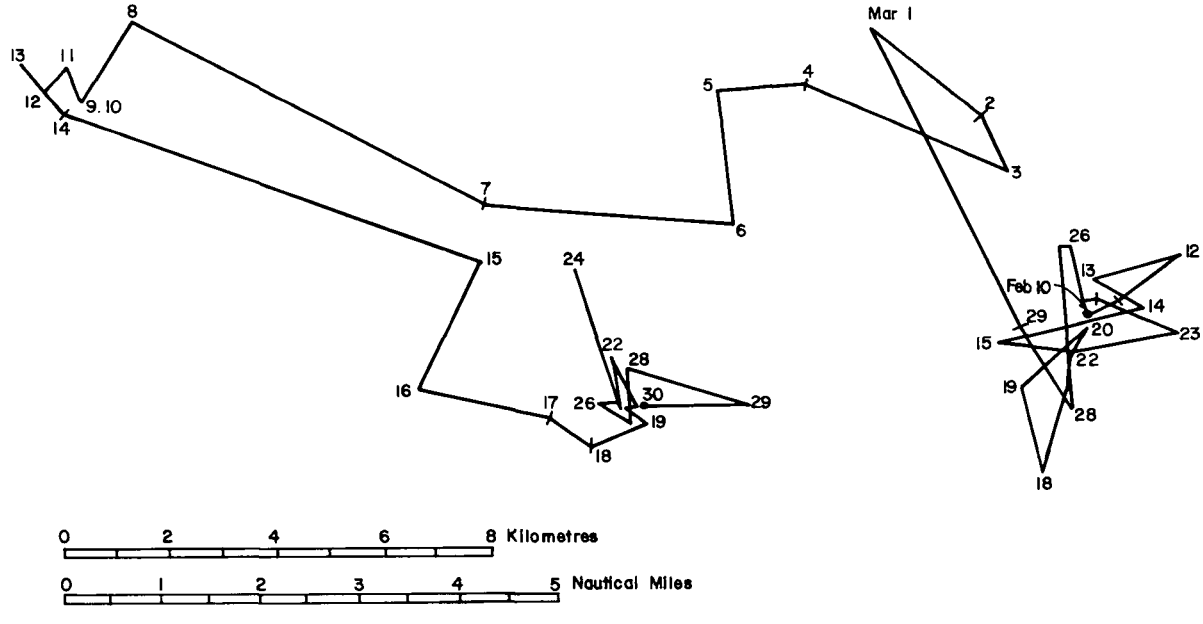

Fig. C 4 AIDJEX BUOY No 320
Daily Drift Plot, Feb 10, 76 to Mar 30, 76

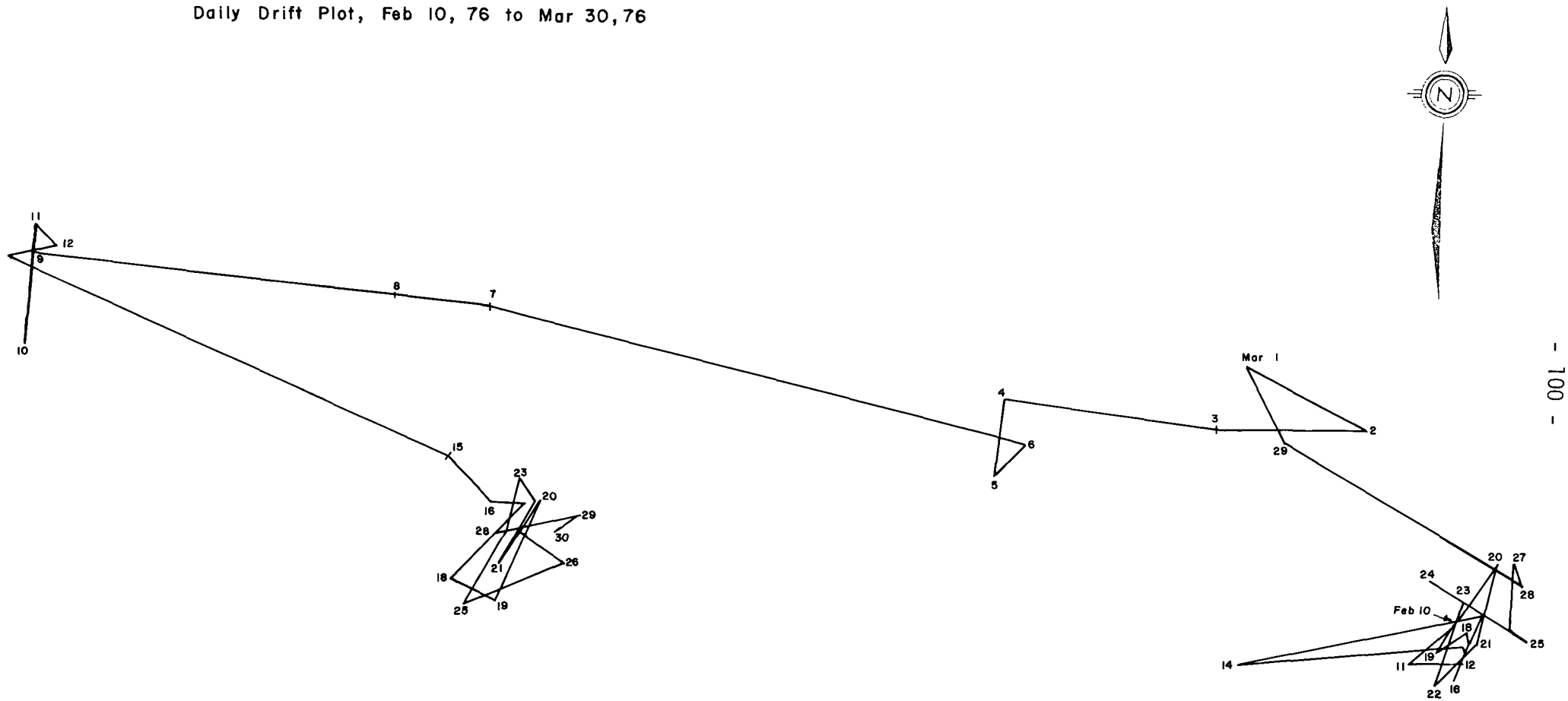

Fig. C 5 AIDJEX BUOY No 502
Daily Drift Plot, Feb 10, 76 to Mar 30, 76

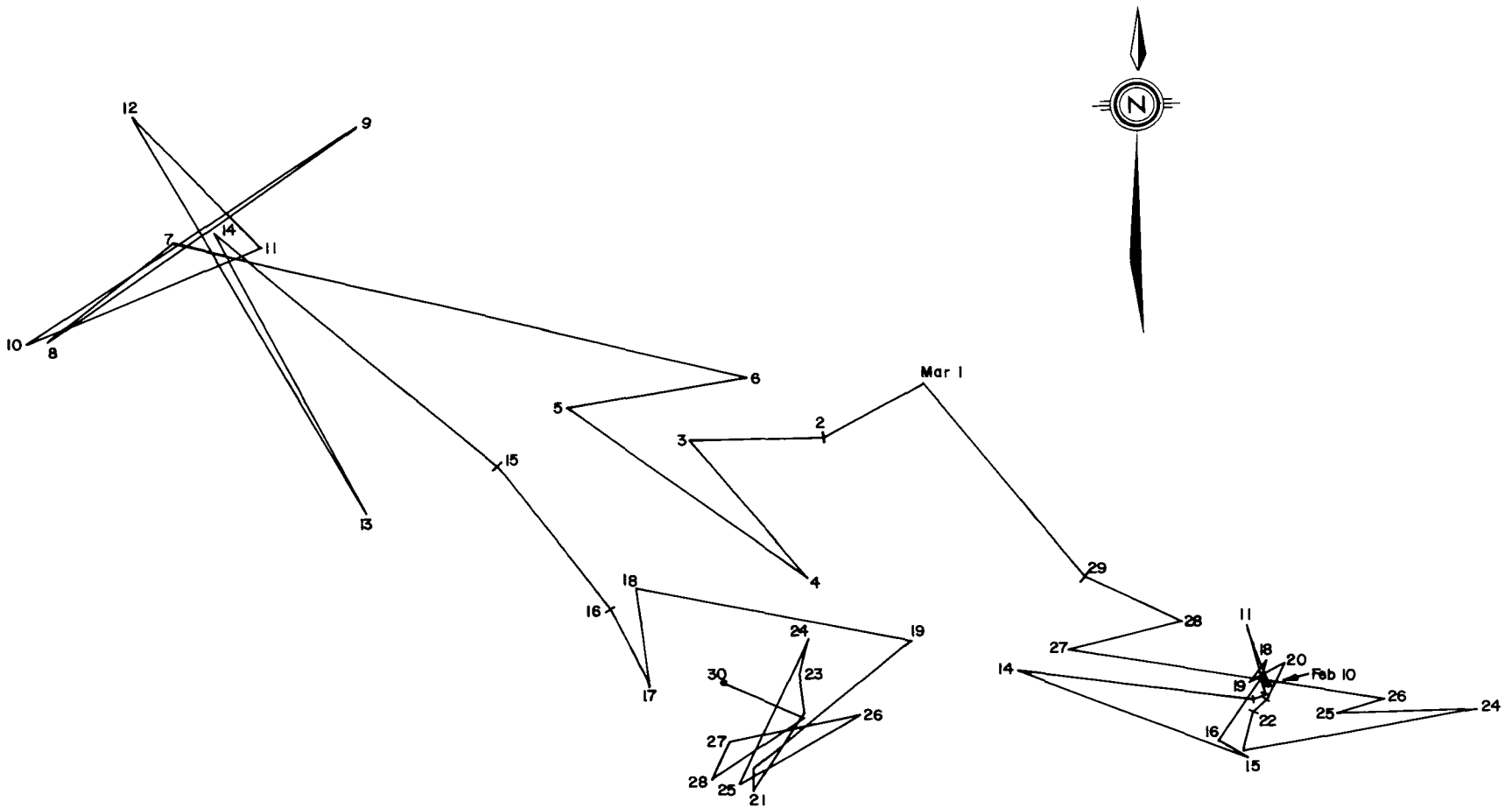

Fig. C6 AIDJEX BUOY No 1003
Daily Drift Plot, Feb 10, 76 to Mar 30, 76

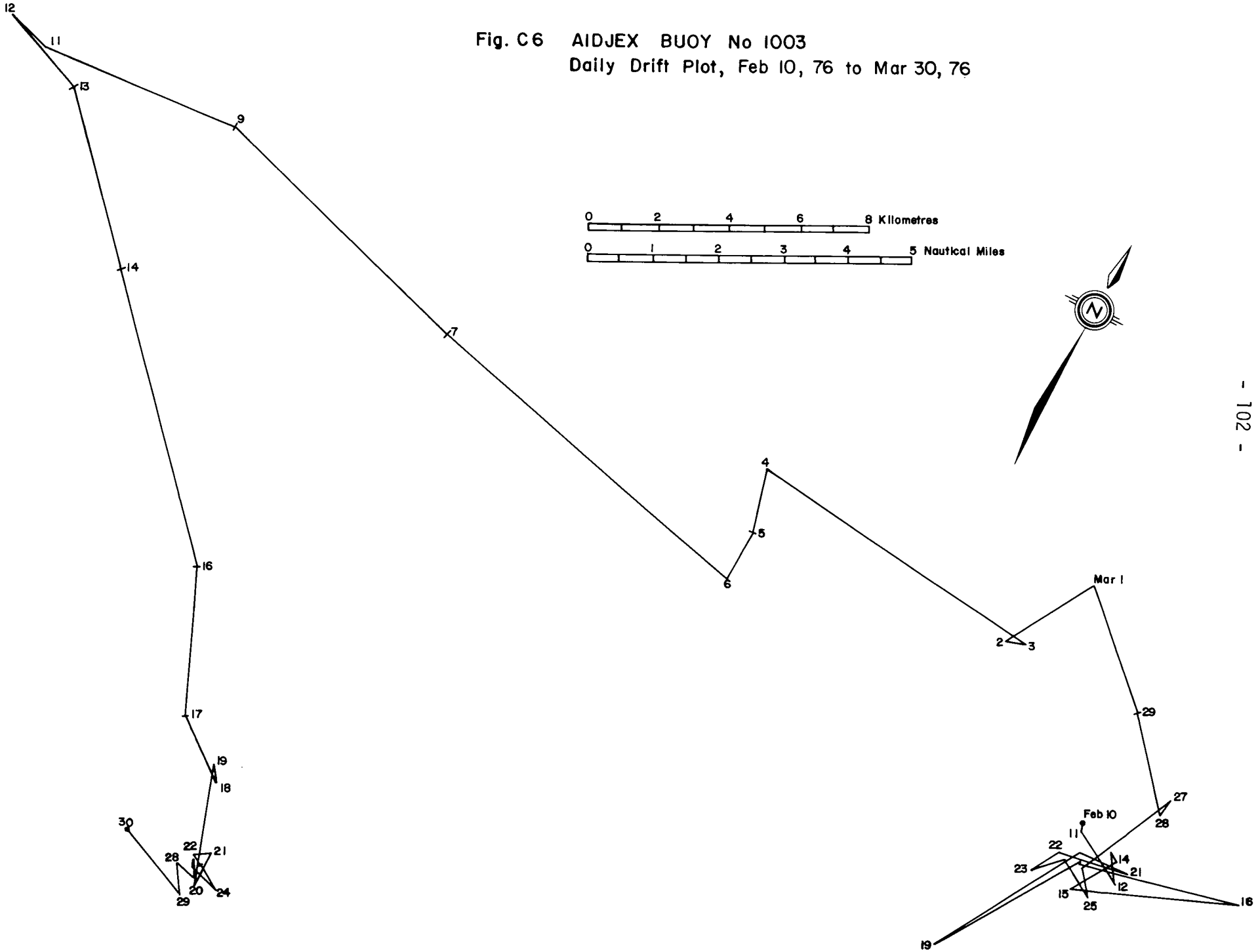

TABLE C1 CAMP DRIFT

Date	Latitude	Longitude	Displacement[1]	
			Distance (km)	Bearing (°T)
Nov.				
16	70°36'N	130°01'W		
17	70°36'N	130°07'W	3.7	270°03'
18	70°36'N	130°07'W	0	–
19	70°36'N	130°09'W	1.2	270°01'
20	70°36'N	130°11'W	1.2	270°01'
21	70°36'N	130°18'W	4.3	270°03'
22	70°40'N	130°29'W	10.0	317°43'
23	70°44'N	130°34'W	8.0	337°36'
24	70°44'N	130°34'W	0	–
25	70°43'N	130°34'W	1.9	360°00'
26	70°39'N	130°49'W	11.8	231°15'
27	–	–	–	–
28	70°42'N	130°52'W	5.9	341°41'
29	70°41'N	130°59'W	4.7	246°41'
30	70°41'N	130°59'W	0	–
DEC.				
1	–	–	–	–
2	70°38'N	130°36'W	15.2	111°19'
3	70°38'N	130°38'W	0	–
4	70°38'N	130°38'W	0	–
5	70°38'N	130°36'W	0	–
6	70°38'N	130°38'W	0	–
7	70°38'N	130°36'W	0	–
JAN.				
20	70°42'N	130°43'W	8.6	329°59'
FEB.				
10	70°35'N	130°59'W	16.2	217°17'
11	70°35'N	130°59'W	0	–
12	70°37'N	130°59'W	3.7	360°00'
13	70°37'N	130°59'W	0	–
14	–	–	–	–
15	–	–	–	–
16	–	–	–	–
17	70°37'N	130°59'W	0	–
18	–	–	–	–
19	70°37'N	130°59'W	0	–
20	70°36'N	131°01'W	2.2	213°42'

21	70°36'N	131°01'W	0	–
22	70°36'N	131°01'W	0	–
23	70°36'N	131°01'W	0	–
24	70°36'N	131°01'W	0	–
25	70°36'N	131°01'W	0	–
26	70°36'N	131°01'W	0	–
27	70°36'N	131°01'W	0	–
28	70°36'N	131°01'W	0	–
29	70°35'N	131°01'W	1.9	180°00'
MAR.				
1	–	–	–	–
2	70°38'N	130°55'W	6.7	33°32'
3	70°36'N	130°52'W	4.1	153°33'
4	70°38'N	130°59'W	5.7	310°47'
5	70°36'N	131°06'W	5.7	229°20'
6	70°36'N	131°04'W	1.2	89°59'
7	70°36'N	131°04'W	0	–
8	70°36'N	131°06'W	1.2	270°01'
9	70°36'N	131°04'W	1.2	89°59'
10	70°36'N	131°01'W	1.8	89°59'
11	70°36'N	131°06'W	3.1	270°01'
12	70°36'N	131°04'W	1.2	89°59'
13	70°36'N	131°04'W	0	–
14	–	–	–	–
15	70°35'N	131°01'W	2.6	135°05'
16	70°36'N	131°04'W	2.6	315°08'
17	70°35'N	131°01'W	2.6	135°05'
18	70°36'N	131°01'W	1.9	360°00'
19	70°36'N	131°04'W	1.8	270°01'
20	70°38'N	131°04'W	3.7	360°00'
21	70°35'N	131°01'W	5.9	161°36'
22	70°35'N	131°01'W	0	–
23	70°35'N	131°04'W	1.9	270°01'
24	70°36'N	131°06'W	2.2	326°24'
25	70°35'N	131°03'W	2.6	135°08'
26	70°35'N	131°04'W	0.6	270°01'
27	70°35'N	131°06'W	1.2	270°02'
28	70°35'N	131°04'W	1.2	89°59'
29	70°35'N	131°01'W	1.9	89°59'
30	70°34'N	131°05'W	3.1	233°06'

[1] The displacements listed in this table are those between consecutive camp positions.

TABLE C2 BEACON MOVEMENT

Date	Latitude	Longitude	Displacement (km)	Bearing (°T)
Beacon No. 1				
Feb. 24/76	70°44'N	131°21'W	Initial Set Up	
Mar. 4/76	70°49'N	131°15'W	9.97	21
Mar. 9/76	70°46'N	131°21'W	6.65	213
Mar. 18/76	70°49'N	131°15'W	6.65	33
Mar. 25/76	70°45'N	131°19'W	7.80	198
		NET	2.22	33°
Beacon No. 2				
Feb. 24/76	70°51'N	131°43'W	Initial Set Up	
Mar. 4/76	70°54'N	131°47'W	6.0	336
Mar. 11/76	70°54'N	131°47'W	0	-
Mar. 18/76	70°54'N	131°47'W	0	-
Mar. 22/76	70°50'W	131°56'W	15	131
Mar. 25/76	70°52'W	131°50'W	5.3	44
		NET	4.6	293
Beacon No. 3				
Feb. 24/76	71°02'N	132°44'W	Initial Set Up	
Mar. 9/76	71°03'N	132°33'W	6.9	74
Mar. 16/76	71°05'N	132°42'W	New Beacon	
Mar. 22/76	71°02'N	132°38'W	5.7	168
Mar. 26/76	71°03'N	132°41'W	2.6	316
Mar. 19/76	71°03'N	132°33'W	4.8	90
		NET	5.6	131
Beacon No. 4				
Feb. 25/76	70°46'N	132°02'W	Initial Set Up	
Mar. 4/76	70°48'N	132°04'W	3.9	342
Mar. 11/76	70°47'N	132°06'W	3.1	307
Mar. 25/76	70°46'N	132°07'W	1.9	198
		NET	3.1	270
Beacon No. 5				
Feb. 25/76	70°29'N	131°18'W	Initial Set Up	
Mar. 4/76	70°29'N	131°14'W	2.5	90
Mar. 11/76	70°30'N	131°17'W	2.6	315
Mar. 16/76	70°30'N	131°25'W	4.9	270
Mar. 25/76	70°27'N	131°19'W	6.7	146
		NET	3.8	190

Beacon No. 6				
Feb. 21/76	70°25'N	130°27'W	Initial Set Up	
Mar. 3/76	70°26'N	130°32'W	3.6	301
Mar. 9/76	70°24'N	130°26'W	5.3	135
Mar. 12/76	70°24'N	130°26'W	0	-
Mar. 18/76	70°25'N	130°25'W	2.0	19
Mar. 25/76	70°23'N	130°22'W	4.2	153
		NET	4.8	140

TABLE C3 NET CAMP DISPLACEMENTS (km) AND BEARING (DEGREES TRUE)

NOVEMBER 16								
21.8	280°02′	DECEMBER 7						
28.0	293°39′	8.6	329°59′	JANUARY 20				
35.7	367°30′	15.2	248°44′	16.2	217°17′	FEBRUARY 10		
39.5	265°08′	19.3	247°41′	20.0	222°33′	2.2	243°26′	MARCH 30

TABLE C4 AVERAGE ICE DRIFT VELOCITIES (km/day^{-1})
Calculated from *Net* Displacements

NOVEMBER 16				
1.0	DECEMBER 7			
0.4	0.2	JANUARY 20		
0.4	0.2	0.8	FEBRUARY 10	
0.3	0.2	0.8	0.04	MARCH 30

TABLE C5 GROUPING OF ICE MOVEMENT DATA ACCORDING TO DAILY VELOCITY - NORCOR ICE STATION (November 16 - March 30)

Velocity Range (km/day^{-1})	Frequency (ie. # days)	Probability of Velocity within a range	Probability of Velocity > V	
			V	P(V)
0 - 1	25	0.373	0	1.0
1 - 2	17	0.254	1	0.63
2 - 3	5	0.075	2	0.37
3 - 4	9	0.134	3	0.30
4 - 5	3	0.045	4	0.16
5 - 6	3	0.045	5	0.12
6 - 7	0	-	6	0.07
7 - 8	2	0.030	7	0.07
8 - 9	1	0.015	8	0.04
9 - 10	0	-	9	0.03
10 - 11	1	0.015	10	0.03
11 - 12	1	0.015	11	0.01
		1.000		

Note: Mean Velocity $\bar{V} = 2.16$ km/day^{-1}

TABLE C6 GROUPING OF ICE MOVEMENT DATA ACCORDING TO DISTANCE - NORCOR ICE STATION (November 16 - March 30)

Velocity range (km/day^{-1})	Mean velocity (km/day^{-1})	Frequency	Distance (km)	% Total distance	Cumulative % Total distance
0 - 1	0.5	25	12.5	8	8
1 - 2	1.5	17	25.5	16	24
2 - 3	2.5	5	12.5	8	32
3 - 4	3.5	9	31.5	20	52
4 - 5	4.5	3	13.5	9	61
5 - 6	5.5	3	16.5	10	71
6 - 7	6.5	0	0	-	-
7 - 8	7.5	2	15	10	81
8 - 9	8.5	1	8.5	5	86
9 - 10	9.5	0	0	-	-
10 - 11	10.5	1	10.5	7	93
11 - 12	11.5	1	11.5	7	100
			142.5	100%	

TABLE C7 AIDJEX BUOYS 10, 320, 502, 1003, 1273 MEAN DAILY VELOCITIES BRACKETS - (NET MONTHLY DISPLACEMENT/TIME) (km/day^{-1})

Month	Buoy 10	Buoy 320	Buoy 502	Buoy 1003	Buoy 1273
Jan	4.10 (.4)	4.7 (.2)	5.8 (.3)	6.4 (.6)	5.3 (.7)
Feb	3.6 (.7)	2.6 (.7)	3.8 (.7)	3.2 (1.0)	3.0 (.9)
March	4.2 (.2)	2.9 (.6)	4.1 (.2)	2.8 (.7)	2.1 (.2)
April	5.7 (1.3)	3.0 (1.1)	4.8 (.8)	3.5 (1.3)	2.3 (.8)
May	7.8 (2.0)	4.9 (2.7)	5.5 (2.1)	6.6 (4.2)	4.9 (2.4)
June	-	5.6 (2.0)	-	7.1 (1.2)	5.8 (1.5)
July	-	5.7 (4.0)	-	5.3 (3.4)	5.8 (3.8)
Mean daily velocity (km/day^{-1})	5.1	4.2	4.8	5.0	4.2
Mean standard deviation in daily velocity (km/day^{-1})	±2.9	±4.4	±4.2	±3.7	±3.3

TABLE C8 AIDJEX BUOYS 10, 320, 502, 1003, 1273 MONTHLY DISPLACEMENT (km) AND DIRECTION (°TRUE)

Month	Buoy 10	Buoy 320	Buoy 502	Buoy 1003	Buoy 1273
Jan	12.5 - 241°	4.8 - 266°	9.3 - 245°	18.0 - 231°	21.0 - 287°
Feb	19.6 - 121°	19.3 - 105°	21.0 - 114°	28.4 - 116°	27.2 - 127°
March	6.8 - 171°	17.4 - 258°	7.4 - 261°	23.2 - 228°	7.4 - 264°
April	38.6 - 281°	32.8 - 296°	23.9 - 306°	39.9 - 300°	25.6 - 300°
May	56.2 - 225°	83.8 - 290°	66.1 - 288°	130.0 - 275°	76.2 - 275°
June		60.5 - 293°		37.4 - 293°	45.3 - 279°
July		128.7 - 294°		106.4 - 299°	116.6 - 287°

TABLE C9 RATIO – TOTAL MONTHLY DRIFT (SUM DAILY)/NET MONTHLY DISPLACEMENT

Month	Camp	#10	#320	#502	#1003	#1273
Jan		10.2	29.7	19.3	10.0	7.9
Feb	6.5	5.3	3.9	5.3	3.3	3.2
March	6.3	19.0	5.1	17.1	3.7	8.5
April		4.4	2.7	6.1	2.6	2.8
May		3.9	1.8	2.6	1.6	2.0
June			2.8		5.7	3.9
July			1.4		1.6	1.5

TABLE C10 DAILY VELOCITY PROBABILITIES FEBRUARY 10 TO MARCH 30, 1976 CAMP AND AIDJEX BUOYS

Velocity range (km/day^{-1})	Velocity probabilities						Mean for AIDJEX Buoys
	Camp	#10	#320	#502	#1003	#1273	#320 – 1273
0 – 1	0.37	0.14	0.35	0.24	0.41	0.47	.37
1 – 2	0.28	0.20	0.35	0.18	0.20	0.24	.24
2 – 3	0.14	0.18	0.16	0.24	0.18	0.14	.18
3 – 4	0.09	0.20	0.02	0.08	0.06	0.08	.06
4 – 5	0.02	0.18	0.04	0.10	0.06	0.02	.06
5 – 6	0.07	0.06	0.02	0.06	–	0.02	.03
6 – 7	0.02	0.02	0.02	0.04	0.06	0.02	.04
7 – 8				0.02	–		
8 – 9					0.02		
Mean daily velocity (km/day^{-1})	1.7 ±1.8	3.8 ±2.1	2.6 ±2.8	4.0 ±4.0	2.7 ±2.5	2.1 ±1.8	